This is to certify that the
thesis entitled

ESTIMATIONS OF HUMAN HIP JOINT CENTER LOCATIONS IN AUTOMOTIVE SEATS: A COMPARISON BETWEEN EXPERIMENTAL DATA AND A PREDICTION MODEL

presented by

VAIBHAV A. EKBOTE

has been accepted towards fulfillment
of the requirements for the

M.S. degree in Mechanical Engineering

Barbara Reed Bush
Major Professor's Signature

August 3, 2004
Date

ESTIMATIONS OF HUMAN HIP JOINT CENTER LOCATIONS IN AUTOMOTIVE SEATS: A COMPARISON BETWEEN EXPERIMENTAL DATA AND A PREDICTION MODEL

By

Vaibhav A. Ekbote

A THESIS

Submitted to
Michigan State University
in partial fulfillment of the requirements
for the degree of

MASTER OF SCIENCE

Department of Mechanical Engineering

2004

ABSTRACT

ESTIMATIONS OF HUMAN HIP JOINT CENTER LOCATIONS IN AUTOMOTIVE SEATS: A COMPARISON BETWEEN EXPERIMENTAL DATA AND A PREDICTION MODEL

By

Vaibhav A. Ekbote

The present study compares experimental data to a prediction model for human hip joint center (HJC) locations in automotive seats. In phase I of the three phase study, seat pan stiffnesses for six different seats were tested using an industry standard manikin and video based motion measurement techniques. For phase II of the study, three of the six seats tested in phase I were selected to represent a range of seat pan stiffnesses varying from soft to stiff. Fifteen male subjects from three anthropometric categories were seated in all three seats and their positional data were recorded. These data were then used to compute the location their HJC locations. In phase III, a prediction of the HJC locations for all test cases in the same three seats was obtained using mathematical modeling techniques developed in previous studies by Radcliffe [6], and Bush and Macklem [3]. Finally the results between the predicted and measured HJC locations were compared. For this comparison two different approaches were used for the computation of the HJC producing slightly different locations. The prediction model successfully predicted the HJC deflections of two of the three subject groups. For the third group a prediction curve was not necessary as it was located using the industry standard manikin.

ACKNOWLEDGEMENTS

I would like to thank Dr. Tamara Reid-Bush for her erudite guidance during last two years. Your positive supervision, mentoring, and support have guided me in the right direction throughout my master's education at Michigan State University. It was only your continuous suggestions on my writing that made it possible for me to complete the seemingly trying task of wording my thesis.

Thank you to my master's committee members. Thank you, Dr. Hubbard for your continuous advice and encouragement and showing the significance of focusing on goals. Thank you, Dr. Liu for helping me settle down and become comfortable in the initial months of my education at Michigan State University.

I would also like to thank my family members for encouraging me to take up the graduate education. Mammi, Pappa, and Bhushan, I thank you for your patience and support.

TABLE OF CONTENTS

LIST OF TABLES

LIST OF FIGURES

NOMENCLATURE

ABT .....ASPECT manikin, butt-thigh segment

ASPECT .....Automotive Seat and Package Evaluation and Comparison Tools

HJC.....Human Hip-Joint Center

MSU ..... Michigan State University

SFS.....Seat Factor Solver Spreadsheet.

Arabic Symbols and Acronyms

F..... generic reaction force under the H-point (could be R_H or F_n)

F_n.....simulation reaction force under the H-pt.

F_H.....simulation input force at the H-pt.

F_K.....simulation input force at the knee

F_T.....simulation input force at the thigh

${}_nK_{f\delta}$ .....n^{th} order reaction force-deflection stiffness coefficient for simulation

${}_nK_{f\theta}$.....n^{th} order reaction force-rotation stiffness coefficient for simulation

${}_nK_{m\delta}$ .....n^{th} order reaction moment-deflection stiffness coefficient for simulation

${}_nK_{m\theta}$ .....n^{th} order reaction moment-rotation stiffness coefficient for simulation

K_H.....spring constant of the seat under the H-pt.

K_K.....spring constant of the seat under the knee (physically non-existent)

R_H.....experimental reaction force under the H-point

Greek Symbols

δ^n .....relative deflection of the H-pt. (same as ΔH)

ϑ^n .....relative rotation of the thigh (referenced to the 2-D template)

ΔH.....relative deflection of the H-pt. (referenced to 2-D template)

ΔK.....relative deflection of the knee (referenced to 2-D template)

Θ_{THIGH} .....thigh angle referenced to horizontal

1. INTRODUCTION

One of the most important aspects of designing a vehicle's interior package is locating the appropriate placement of the seat and the occupant within the vehicle. One identification of occupant placement is a point at or near the hip joint center (HJC). The HJC acts as a reference point in designing the car seat and interior packaging because it is the point on human body with least motion with respect to the car seat during the time interval of an occupant in a car. So placing the occupant's HJC at an intended position in seat is of fundamental importance to meet mandated safety regulations and design and packaging requirements.

Several tools are used to locate or estimate the HJC including Society of Automotive Engineers (SAE) manikins. There are two versions of the SAE manikins, the first is nicknamed OSCAR [1] and the newer one is called ASPECT [2]. Both are representations of average sized male occupants. The point corresponding to human HJC on the manikin is called the H-point and is a representation of Hip Joint Center of an average human occupant (Figure 1).

The focus of this study is to locate the hip joint centers of seated human occupants using experimental techniques and then to compare the measured locations to predicted locations based on the ASPECT manikin and previously developed mathematical techniques [3].

Included as part of the vehicle's Computer Aided Design (CAD) data, the H-point must fall within an envelope in the space that accounts for design variables like cushion deflection and the seat's for- aft and vertical range of motion. The seat designer's goal is to locate the H-point in the most advantageous position within this envelope. A smaller

statured human would have the HJC situated at the envelope's forward end, while the HJC of a larger statured person would be at the rearward part of the envelope. The H-point enables the designer to position the human model within the CAD data of the automobile interior and establishes locations of hand and foot controls, overall packaging and vision requirements.

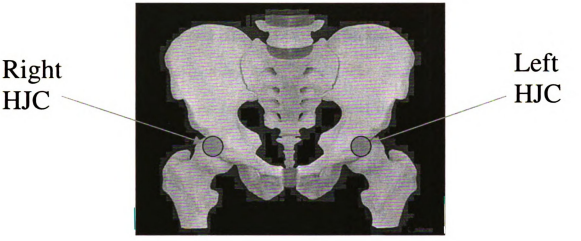

Figure 1: Human Hip Joint Center [8]

Human modeling software such as RAMSIS [4] and JACK [5] simulate various anthropometric sizes, shapes and body positions and movements in the vehicle-seating environment. Once the model is positioned correctly within the CAD environment, these simulations will estimate interior factors such as headroom, legroom, access to controls and interference with hand brake application or other operational movements.

One of the important inputs in the development of these software simulations is a mathematical representation of a wide database of vehicle occupant locations, including the location of occupant's HJC in a deflected seat for a range of seat, package and

anthropometric variables. The present study compares the experimental method of locating the HJC in automotive seats with a mathematical prediction algorithm. The present study was broken into three phases, which are briefly described below.

In phase I of the study, the stiffnesses of the seat pans (seat cushions) of six automotive driver seats were measured using the ASPECT manikin [2] along with video based motion measurement techniques. The experimental data for vertical and horizontal deflection measures of the manikin H-point were obtained and used as input into the mathematical model developed by Radcliffe [6]. The Radcliffe mathematical model estimated the seat pan stiffness based on experimental data for a sequence of manikin loading steps. Based on the Radcliffe model, six seats were categorized according to their seat pan stiffness in comparison to 30 other seats analyzed by Radcliffe.

Three of the six seats were chosen for inclusion in phase II. Seats were selected to represent a wide range of seat pan stiffnesses. During phase II, kinematic data from fifteen male subjects were collected in the three seats selected from phase I. The data represented three-dimensional locations of various anatomical reference points and points on the test seats. In each case the location of the subject's HJC was computed based on the data gathered from the motion measurement system.

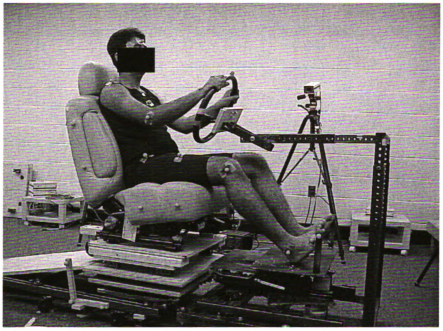

Figure 2: Representative picture of subject testing in Phase II

Lastly in phase III, the data from phase II were used as an input to a previously developed mathematical model by Bush and Macklem [3] to predict the location of HJC. In the previous study by Bush and Macklem it was observed that the Radcliffe model, that was based on industry standard manikins, could only predict the deflection of mid-sized and large male occupants, but offsets to the Radcliffe curve were developed by Bush and Macklem [3] for other anthropometries. These offset curves had a liner trend between male occupants of average height and weight and tall but lightweight male occupants. Also for female occupants the offset curves had parabolic trend. This prediction model was based on the subjects' weights and the seat stiffness curves and had been developed on data from three seats. Data from phase II of the present study was

used to calculate the HJC locations of 15 male occupants in 3 seats .The HJC locations were also estimated using the Bush-Macklem prediction model. The calculated and predicted HJCs were then compared and used to improve the Bush-Macklem model.

2. BACKGROUND

Background for phase I

The primary purpose of phase I was to characterize a set of six automobile seats according to seat stiffness and select three seats to be used in phase II that spanned range of seat pan stiffnesses. In a previous study by Radcliffe [6], a mathematical model was developed to represent experimental data collected for seat pan stiffness (Figure3). The Radcliffe model was used to quantitatively describe and evaluate the mechanical properties of automotive seat pans. In the study by Radcliffe, the deflections of both the ASPECT [2] and SAE J826 [1] manikins into the seat were measured and modeled for 30 production and prototype seats.

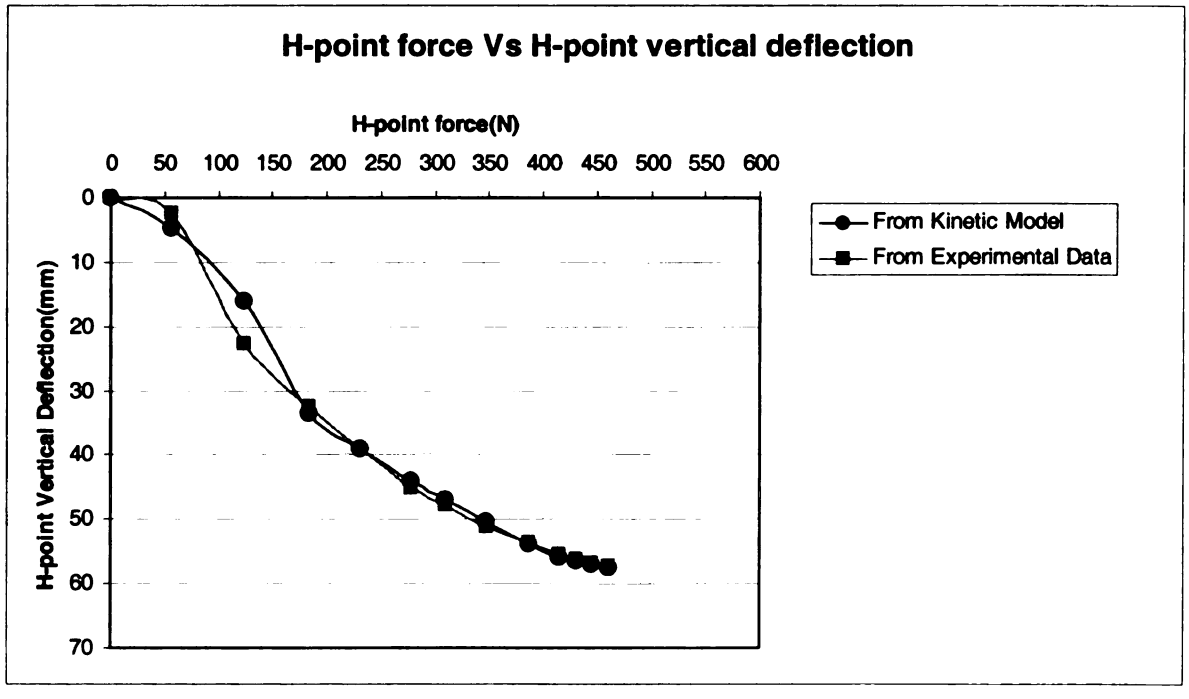

Figure 3: Example of kinetic model by Radcliffe that simulated the seat pan stiffness response of one of the test seats (Audi Leather) for incremental loading of ASPECT butt and thigh region.

Each of the two manikins was loaded incrementally and downward motion of the manikins was measured and recorded. Next, the modified Taylor series based equation

set was found to best fit these experimental parameters thus simulating the experimental behavior of the manikin. All the experimental data for developing this model was collected manually with a scale. The kinetic model developed by Radcliffe was a good predictive tool that described and simulated the buttocks and thigh region of industry standard seating manikins and their interaction with the seat pan.

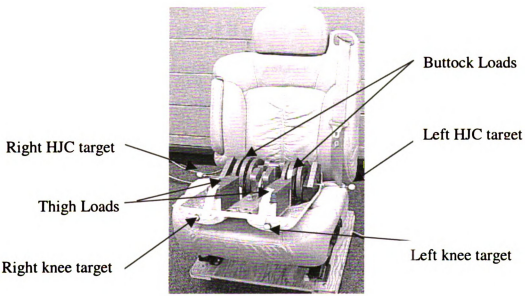

Figure 4: Example of buttock and knee loading of ASPECT manikin

3.1 M
Expe

I

meas

study

was t

meas

meas

locat

[2] m

meas

of m

steps

A.

3.PHASE I

3.1 Methods used in phase I

Experimental data acquisition using ASPECT manikin

In previous work by Hubbard and Gedraitis [7], an experimental technique for measuring seat pan stiffness with the SAE J826 [1] manikin was developed. The present study used a similar technique however a newer manikin, called the ASPECT manikin, was used to record these measures. The horizontal position of H-point, which was not measured in previous studies, was also measured in the present study. These measurements of horizontal shift of H-point were not included in predicting the HJC location however might be useful in future studies. The butt-thigh section of ASPECT [2] manikin was removed and used in testing as briefly described below.

All six seats were mounted on flat wooden bases at a cushion pan angle of 15° measured using OSCAR [1] manikin. OSCAR [1] manikin was used because the method of measuring a cushion pan angle is standardized using that manikin. Following are the steps used in testing all six seats with the ASPECT [2] manikin.

A. Using the butt-thigh segment of ASPECT seating manikin (shown in Figure 4), incremental loads were applied. Targets were attached on left and right H-point axis locations and also on left and right knee locations of the ASPECT Butt Thigh (ABT) section (Figure 4). The vertical and horizontal deflections were measured using Qualisys motion measurement system. The position data were collected for 1 second per load increment with a frequency of 12 Hz.

B. V

m

c

C. H

P

L

f

s

A

c

D. E

r

E. T

0

10

20

30

40

50

60

70

80

H-point Deflection(mm)

Figure
measur

B. Vertical and horizontal positions of the H-point and knee axes were also measured manually using a scale after each applied load. The manual measures were later compared with those from Qualisys motion measurement system.

C. H-point axis measurements were made on the left and right side by measuring the position at the tip of a rod extending out from the H-point axis center (Figure 4). Left and right H-point and knee axis measurements were made at the same distance from the vertical plane of symmetry of the manikin. The variation in level on each side of the manikin was averaged for both horizontal and vertical measurements. Again, the horizontal deflection of H-point into the seat was measured on both sides of H-point axis using recliner pivot of each seat as reference.

D. Between each loading increments (Figures 6-18) a waiting period of 5 minutes was maintained so that the seat pan attains equilibrium with the added load.

E. The load deflection data from Qualisys motion measurement was compared with

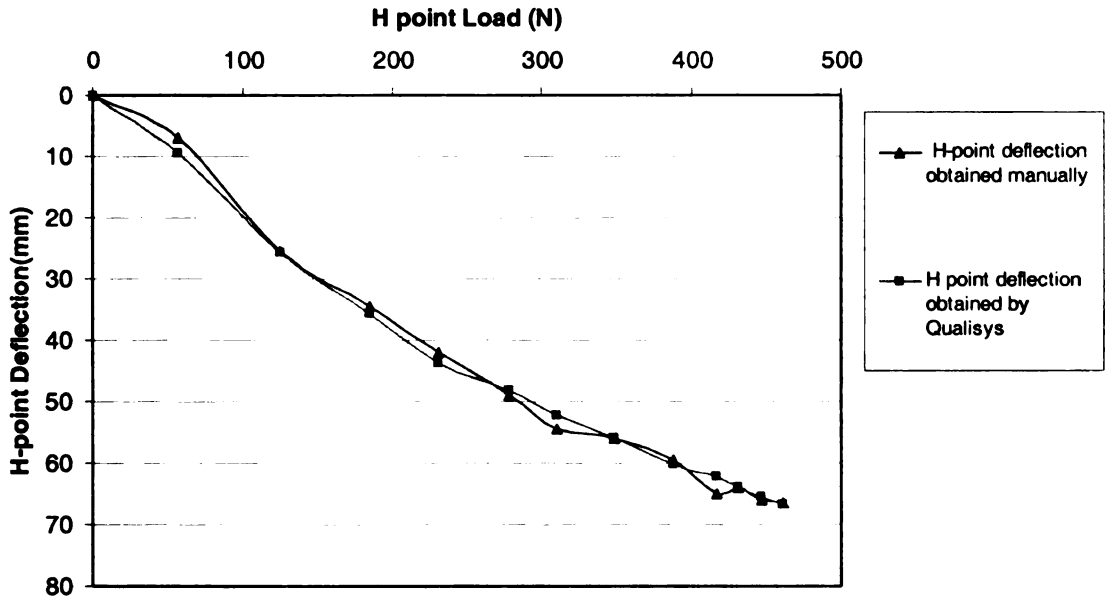

Figure 5: Comparison Between manually measured data and data collected from Qualisys motion measurement system for Tahoe (Cloth) seat.

the manually measured data for four of the six seats tested to verify the consistency between measures from Qualisys system and manual measures. Manual measurements of H-point and knee heights were taken with lab floor as reference using a ruler with a minimum scale of 1mm. Hand measurements taken in earlier studies [6] provided reasonable data. However since the data in phase II was collected with the motion measurement system, the seat protocols were established in phase I and were carried into phase II. Figure 5 shows agreement between the motion data and hand measurements and consistency of the motion measurement data. The average of difference between the two methods for all four seats was 1.8 mm. After comparison of data for 4 seats it was felt that target data were sufficient measures. Manual measurements of horizontal deflection of left H-point were taken for two seats to observe how much the H-pont moves horizontally. Those are tabulated in Appendix B-5.These measurements were not used in any of the calculations in the present study.

F. The data obtained form motion measurements for all six seats was input to Radcliffe model to generate stiffness curves.

3.2 ASPECT butt thigh loading steps

Figures 6-18 show the load steps followed on all of the seats tested.

Figure 6: SAE J826, 2-D template positioned in Tahoe Leather seat for the load step zero with a total weight of 0 N.

The 2-D template of J826 manikin was used as a reference to measure the deflections. The template was placed on the seat so that the template edges fully touched the surface of the seat cushion and seatback near the mid plane of the seat but avoiding any indentations in trim. Targets were attached to left and right ends of a thin solid rod with circular cross-section passing through the H-point axis. This load step represented location of H-point axis in unloaded condition of seat or Zero load step.

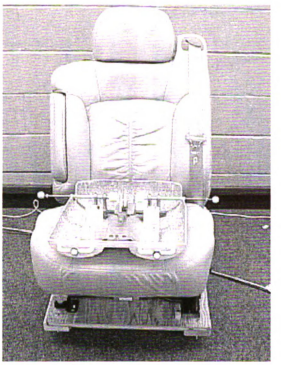

Figure 7: (Load step 1) Aspect Butt Thigh (ABT) segment with no weights added with a total weight 57 N.

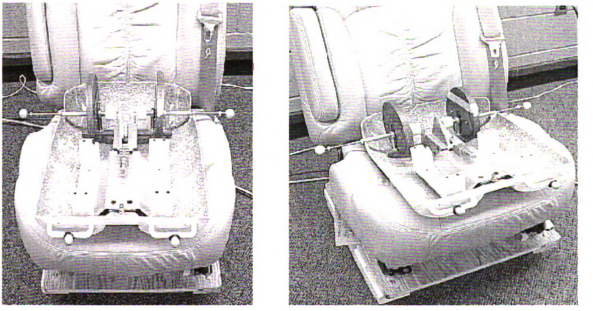

Figure 8: (Load step 2) ABT segment with two 6-plate H-point weights on H-point axes with a total weight 125 N. Front and isometric views.

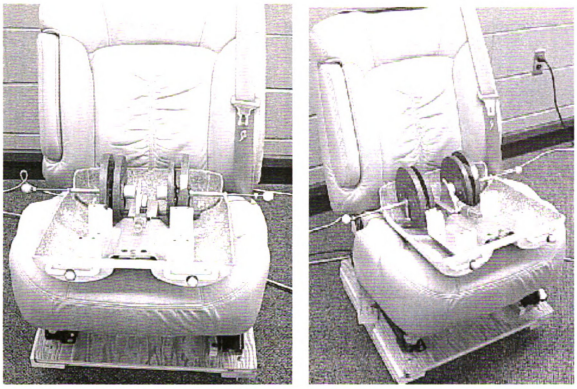

Figure 9: (Load step3) Load step 2 plus 2 five plate H-point weights on H-point axis with a total weight 185 N. Front and Isometric views.

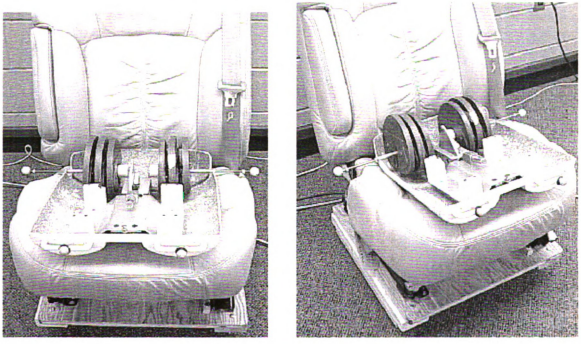

Figure 10: (Load step 4) Load step 3 plus 2 five plate H-point weights on H-point axis with a total weight 231 N. Front and Isometric views.

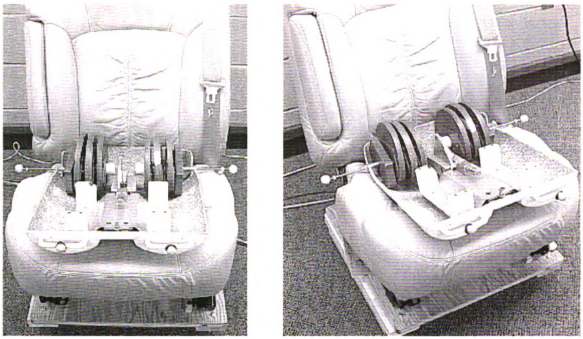

Figure 11: (Load step 5). Load step 4 plus two torso weights on H–pt axis just inside shell of ABT with a total weight 278 N. Front and Isometric views.

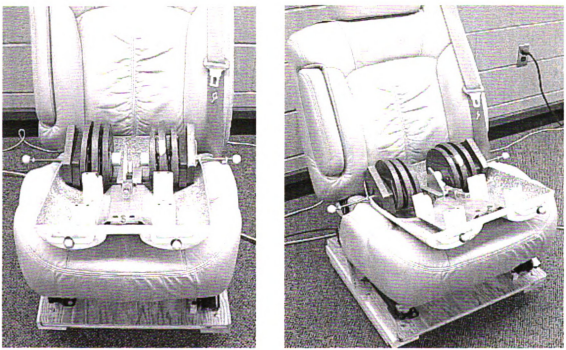

Figure 12: (Load step 6) Load step 5 plus two torso weights on H–pt axis just inside shell of ABT with slots down and back rear edge resting against shell with a total weight 310 N. Front and Isometric views.

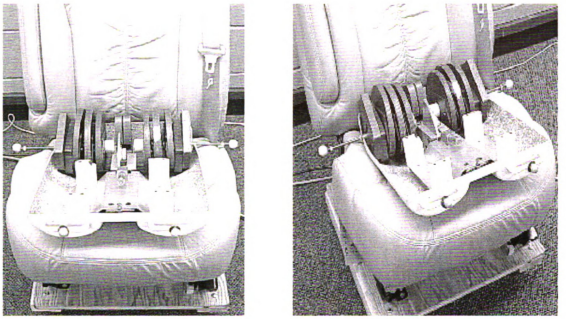

Figure 13: (Load step 7) Load step 6 plus two torso weights behind the center structure with slots forward with a total weight 348 N. Front and Isometric views.

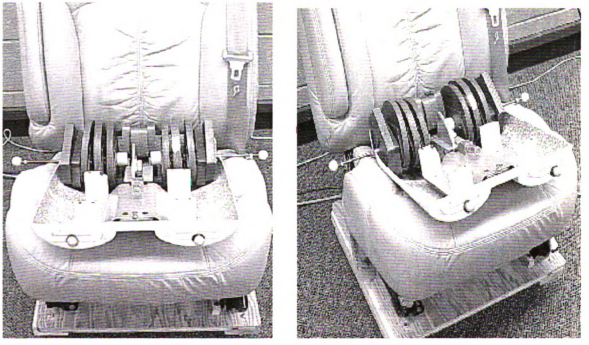

Figure 14: (Load step 8) load step 7 plus two torso weights behind the center structure with slots forward with a total weight 388 N. Front and Isometric views.

Figure 1
ba

Figure 16
Ison

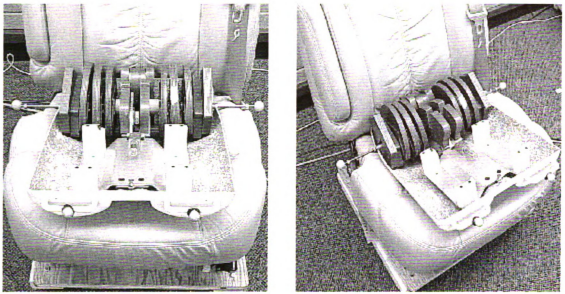

Figure 15: (Load step 9) Load step 8 plus two torso weights on center structure with slots up and back lower edge against nylon bushing with a total weight 416 N. Front and Isometric views.

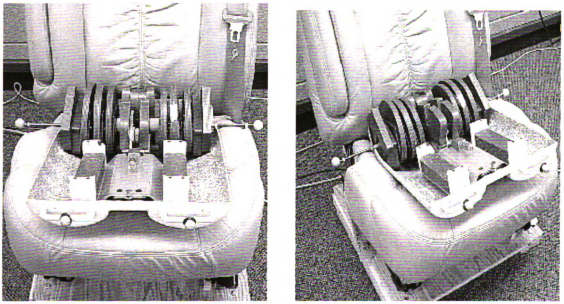

Figure 16: (Load step 10) Load 9 plus two thigh weights with a total weight 431 N. Front and Isometric views.

Figure
Is

Figure 1
Isor

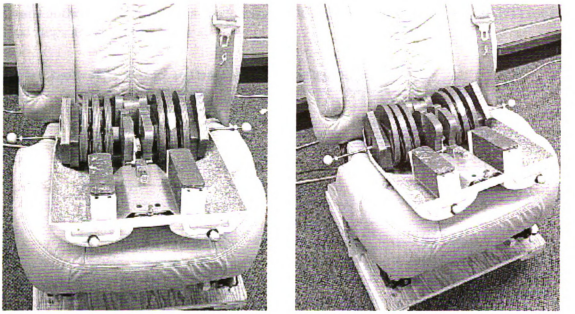

Figure 17: (Load step 11) Load 10 plus two thigh weights with a total weight 446 N. Front and Isometric views.

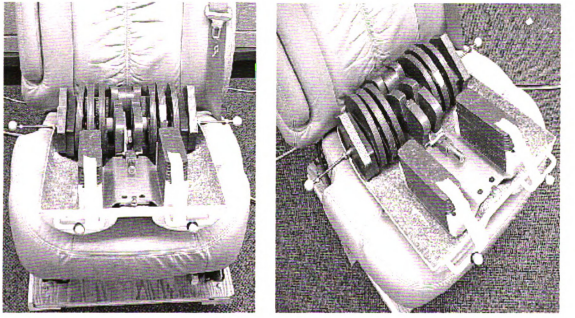

Figure 18: (Load step 12) Load 11 plus two thigh weights with a total load 461 N. Front and Isometric views.

Loads at the H-point and front (knee axis) of ASPECT butt thigh segment (ABT) for all load steps are shown in Table 1.

Table1: Loads at the H-point and front of ABT for all load steps

Load Step	Load on H-point axis (Newtons)	Load on front of ABT. (Knee load) (Newtons)
0	0	0
1	57	29
2	125	29
3	185	29
4	231	29
5	278	29
6	310	32
7	348	26
8	388	21
9	416	28
10	431	56
11	446	83
12	461	111

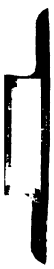

3.3 Co

In

kinetic

Since t

briefly

Th

forces

H-poin

Figu

Know

experimer

automotiv

3.3 Coupled Force and Moment Kinetic model. [6]

In previous work by Radcliffe [6] it was found that a coupled force and moment kinetic model was effective in representing the effects of the seat on manikin position. Since the Radcliffe model was used for seat selection in the phase I of this study, it is briefly explained in the following paragraphs.

The coupled force and moment kinetic model [6] (figure 19) represented two input forces F_H and F_K at the H-point and knee respectively, and two reactions: force, R_H at the H-point axis, and reaction moment M about the H-point axis.

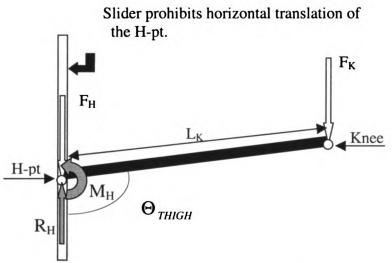

Figure 19: Coupled Force and Moment Kinetic model [6]

Knowing the force–deflection relations of the H-point and knee axes from the experimental data, this model can be used to simulate the static response of the automotive seat to the ASPECT manikin loading.

A static mathematical analysis coupled with the use of Microsoft (MS) Excel solver optimization tool was used to develop the mathematical equations, which represented the manikin response to seat loading. This mathematical modeling used following steps.

A) Developing experimental and simulation equations.

Two sets of equations, a static set and a simulation set were developed and the aim of the procedure was to find the stiffness coefficients that would give minimum Root Mean Square (RMS) error between the simulation and experimental data.

Equations of Statics (figure 19)

The set of static equations (equations 1&2) represented experimental reaction forces and moments based upon experimental, incremental input forces F_H (Force at H-point) and F_K (Force at Knee).

$$R_H = F_H + F_K \quad (1)$$

$$M_H = F_K * L_K * (\cos(\Theta_{THIGH})) \quad (2)$$

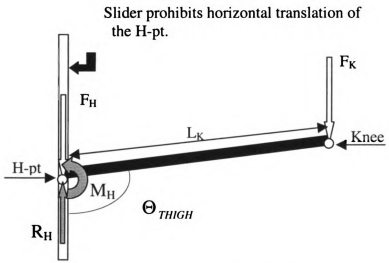

Figure 19: Coupled Force and Moment Kinetic model [6]

Sim

serie

calle

betw

mom

F_n =

M_n =

B) Exp

The

experin

paramet

1

2

3

4

To ca

Radcliffe

Table2, th

spreadshee

Simulation Equations

The set of simulation equations (equations 3 &4) were based on modified Taylor series expansion and included the stiffness coefficient terms (${}_nK_{f\delta}, {}_nK_{f\vartheta}, {}_nK_{m\delta}, {}_nK_{m\vartheta}$) called seat factor parameters, which needed to be optimized, so as the RMS difference between the simulated force and moment (F_n, M_n) and the experimental force and moment was minimum.

$$F_n = \sum_0^n ({}_nK_{f\delta} * \delta^n + {}_nK_{f\vartheta} * \vartheta^n) \quad (3)$$

$$M_n = \sum_0^n ({}_nK_{m\delta} * \delta^n + {}_nK_{m\vartheta} * \vartheta^n) \quad (4)$$

B) Experimental data acquisition.

The experimental data needed for the mathematical analysis was acquired using the experimental data acquisition procedure discussed earlier in section 3.2. The four input parameters needed from the experimental data for the simulations were:

1. Static incremental load at H-point axis (Fh)
2. Static incremental load at knee axis (front of ABT) (Fk)
3. Average vertical displacement of the H-point at that given load.
4. Average vertical displacement of the knee axis of ABT.

To calculate this mathematical model, an Excel spreadsheet was designed by Radcliffe that will be referred to as the seat factor solver (SFS) was used. As shown in Table2, the four input parameters correspond to the first four columns of the analysis spreadsheet. The last four columns are the calculated values.

Table 2: Input data acquired from experimental incremental loading of the manikin is shown in white font within dark cells, along with calculated values based on experimental data shown in dark fonts within gray cells.

Seat C		H-pt	Knee				
Fh(N)	Fk(N)	Avg (z,mm)	Avg (z,mm)	Thigh Ang	Dzh	Dzk	Def Ang
0	0	253.7	311.8	7.29	0.0	0.0	0.00
57	29	251.3	264.7	1.68	2.4	47.0	-5.61
125	29	231.1	279.4	6.06	22.6	32.4	-1.23
185	29	221.1	287.6	8.34	32.6	24.2	1.06
231	29	214.5	292.7	9.82	39.1	19.1	2.54
278	29	208.5	297.5	11.21	45.2	14.2	3.92
310	32	205.8	299.2	11.77	47.9	12.6	4.48
348	26	202.4	305.5	13.01	51.3	6.3	5.72
388	21	200.1	310.3	13.92	53.6	1.5	6.63
416	28	198.2	311.3	14.29	55.4	0.5	7.00
431	56	197.3	304.1	13.49	56.4	7.7	6.20
446	83	196.8	298.1	12.78	56.9	13.7	5.49
461	111	196.3	292.2	12.09	57.4	19.6	4.80

Where,

Fh(N) = Static incremental load at H-point (experimental load data).

Fk (N)= Static incremental load at knee axis (experimental load data).

H-pt Avg z(mm) = Average vertical displacement of left and right side targets on the h-point axis of ABT (experimental data measured from motion measurement system).

Knee Avg z (mm)= Average vertical displacement of left and right side targets on the front of ABT (experimental data measured from motion measurement system).

Thigh Angle (degrees)= Angle of thigh segment of ABT with reference to horizontal obtained from column 3 and 4 and H-point to knee length. (Calculated).

C) Calculation of static reaction force and moment.

Experimental data from the six seats tested were input into the Radcliffe SFS. The static reaction forces and moments, which were based on experimental loadings and

meas

(1) a

comp

Seat

D) O

equa

T

expan

linear

multi

expan

result

expans

RMS d

that the

deflecti

produce

tested. (

reasonab

all six se

measurements, were calculated for each incremental loading step according to equations (1) and (2). These experimental reaction forces and moments were then used as a basis of comparison to optimize the stiffness coefficients (K's) in equations (3) and (4) using the Seat Factor Solver spreadsheet within MS Excel.

D) Optimization of seat factors within modified Taylor Series based simulation equations.

The simulation equations (3) and (4) were based on Modified Taylor Series expansion. These Taylor series expansions were modified in that the 0^{th} order, linearization term was neglected. Also neglected were terms in which the coefficients multiplied by both variable terms ($K*[\delta^n * \vartheta^n]$). With increasing order of Taylor series expansion equations the differences between the experimental data and the simulation results were decreased by each addition of error correcting higher order terms.

First ($_n = 1$), second ($_n = 2$), and third ($_n = 3$) order modified Taylor series expansions were investigated (refer to equations 3 and 4) within the SFS to reduce the RMS differences between the experimental data and simulation results. It was observed that the second order Taylor series expansion equations produced the simulation HJC deflections, with RMS error less than 5.4mm, compared to the third order equations that produced the simulation HJC deflections with RMS error less that 4.1mm for all six seats tested. (Refer to the Appendix.) The second order Taylor series expansion equations that reasonably simulated the experimental and data were used to plot the seat pan stiffness of all six seats.

3.4 S

stiffr

ASPI

repre

the ca

Table

Name
Seat A
Seat B
Seat C
Seat D
Seat E
Seat F

The foll

3.4 Seats tested for Phase I

The goal of phase I was to select 3 seats that would cover a range of seat pan stiffnesses. For this purpose, the following six seats listed in Table 4 were tested with ASPECT manikin for obtaining H-point vertical and horizontal deflections. The seats represented wide range of car segments. Table 3 shows the available information about the car, year of manufacture and name of the manufacturing company for each seat.

Table 3: List showing available information about six seats tested in phase 1.

Name	Car	Year	Seat Manufacturer
Seat A	Audi	1999	Unavailable
Seat B	Ranger (Jeep)	2002	JCI
Seat C	SLK (Mercedes)	1999	Unavailable
Seat D	Tahoe (Cloth trim-Chevy)	2001	Lear Corporation
Seat E	Tahoe (Leather trim-Chevy)	2001	Lear Corporation
Seat F	BMW Sporting	Unavailable	Unavailable

The following is the description of each seat with pictures.

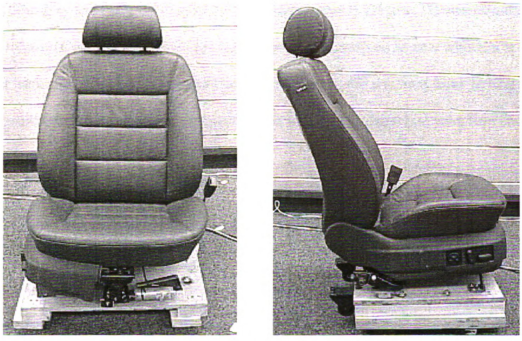

Figure 20: Seat A, the Audi front and side view.

Seat A, a leather covered 1999 Audi (Figure 20) had motorized adjustable mechanical lumbar support, cushion lifter, and back recline operations. The seat back angle for this seat ranged from 9^{o} to 63^{o} rearward from vertical when measured with J826 manikin. The seatback bolsters were soft and prominent whereas the seat pan had soft flat bolsters.

T

by Jol

seat b

meas

The gray and black cloth covered 2002 Ranger seat B, (Figure 21) was manufactured by Johnson Controls Inc. This seat had manual recline with no lumbar adjustment. The seat back angle for this seat ranged from 11° forward to 48° rearward from vertical as measured with J-826 manikin. The bolsters on seat back and seat pan were firm and flat.

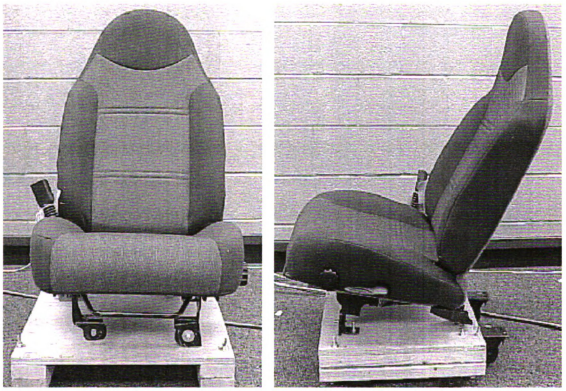

Figure 21: Seat B, the Ranger front and side view.

Seat C, the 1999 SLK as shown in Figure 22, was covered with black leather. This seat had manual recline and with no lumbar support feature. The seat back angle for this seat ranged from 15° forward to 78° rearward from vertical as measured with J-826 manikin. The bolsters on seat back and seat pan were firm and flat.

Figure22: Seat C, the SLK front and side view.

The gray cloth covered 2001 Tahoe seat (seat D), shown in Figure 23, was manufactured by Lear Corp. This seat had manual recline with no lumbar support feature. The seat back angle for this seat ranged from 10^{o} to 47^{o} rearward, from vertical as measured with J-826 manikin. The bolsters on seat back and seat pan were soft and flat.

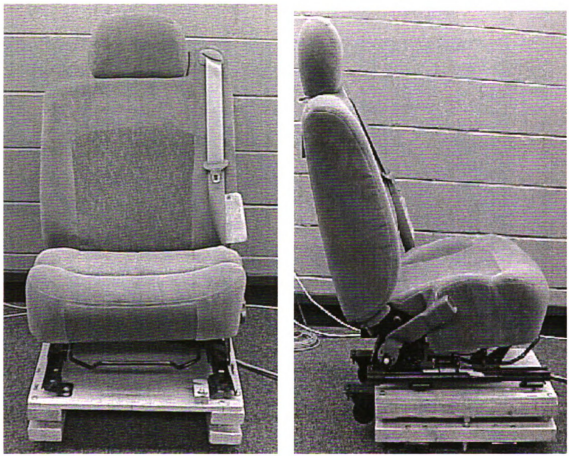

Figure 23: Seat D, the Tahoe-cloth front and side view.

Seat E, leather covered 2001 Tahoe (Figure 24) seat was manufactured by Lear Corporation. This seat had motorized mechanical lumbar support, cushion lifter, and back recline operations. The seat back angle for this seat ranged from 12^{o} to 45^{o} rearward from vertical as measured with J-826 manikin. The bolsters on seat back and seat pan were soft and flat.

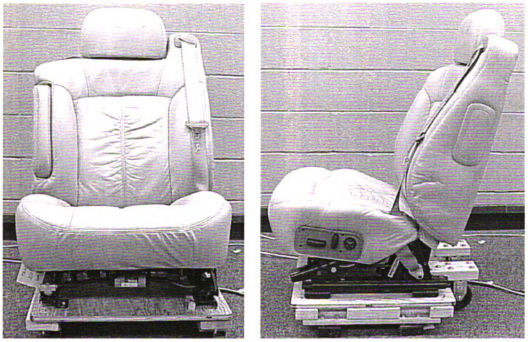

Figure 24: Seat E, the Tahoe-leather front and side view.

Seat F, a cloth covered BMW was manufactured by Lear Corp. This seat had manual recline with no lumbar support feature. This seat ranged from 12° to 75° rearward from vertical as measured with J-826 manikin. This seat had prominent, firm bolsters on seat pan and seat back.

Figure 25: Seat F, the BMW- front and side view.

3.5 Seat Selection for phase II

Based on the coupled force and moment kinematic model with 2nd order Taylor series expansions discussed in section 3.3, the seat pan stiffnesses of all six seats were plotted. These plots of reaction force under h-point versus h-point deflection were compared to examine which seats should be tested for phase II.

Figure 26 shows comparison of H-point load vs. H-point deflection for all six seats tested in phase 1 along with the 22 other seats tested by Radcliffe [6] in his study to develop the SFS and kinematic models.

Displacement (mm) Referenced to Unloaded H-Point Machine

Figure
b
t

T

accom

force c

selecte

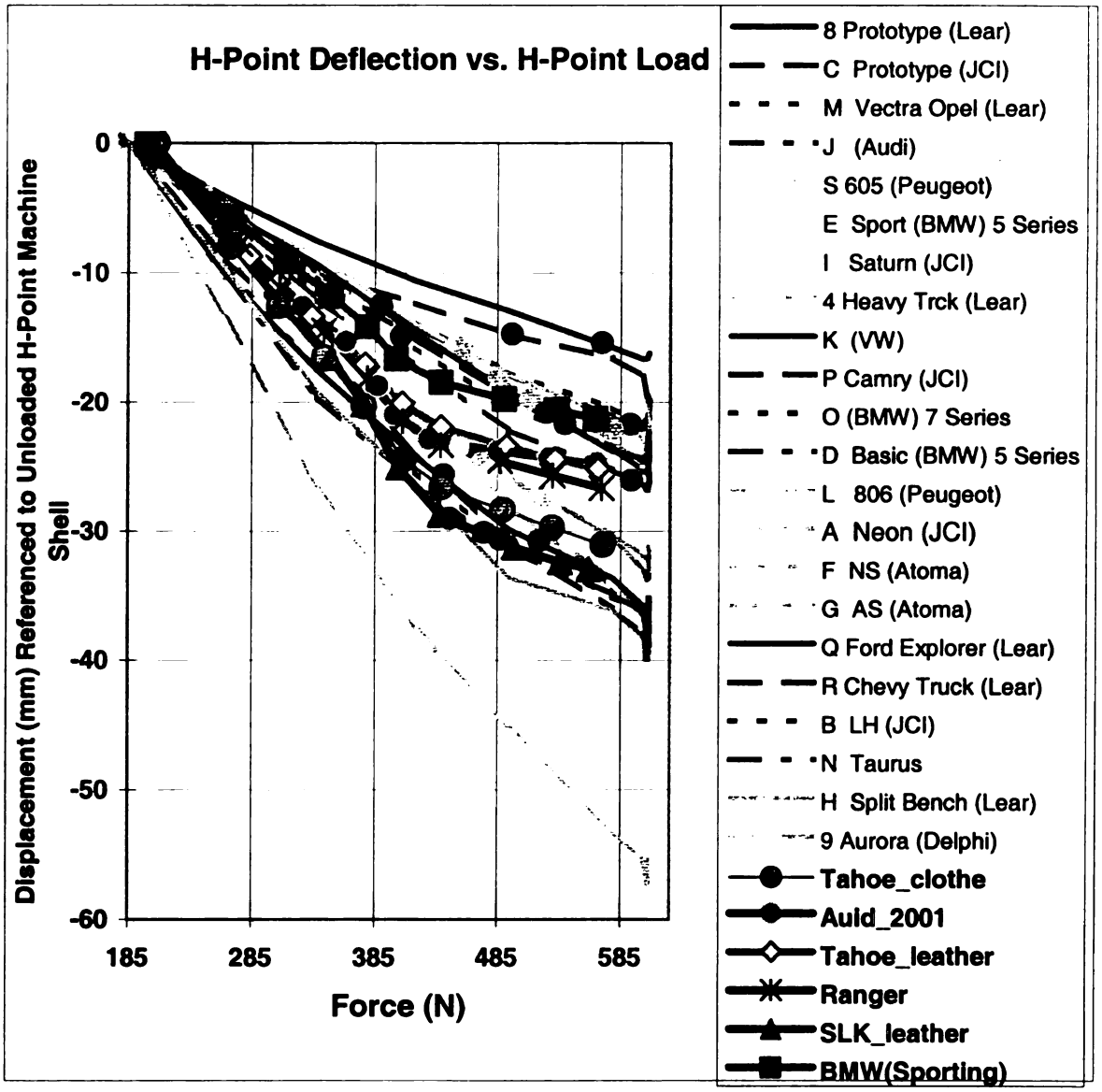

Figure 26: Chart comparing H-point deflection Vs. H-point load for seats tested in phase I (shown in bold legends). Also shown are H-point deflections with increasing H-point load for 22 seats tested by Radcliffe [6].

The six seats were categorized according to their seat pan stiffness. This was accomplished by comparing the H-point deflection corresponding to H-point reaction force of 410 newtons for all six seats. The H-point reaction force of 410 newtons was selected for comparison because it is 54.3% the body weight of an average sized male

occu

the c

Displacement (mm) Referenced to Unloaded

Figur

occupant [171 lb body weight, 69" height] that passes through the buttocks according to the dissertation by Bush [9].

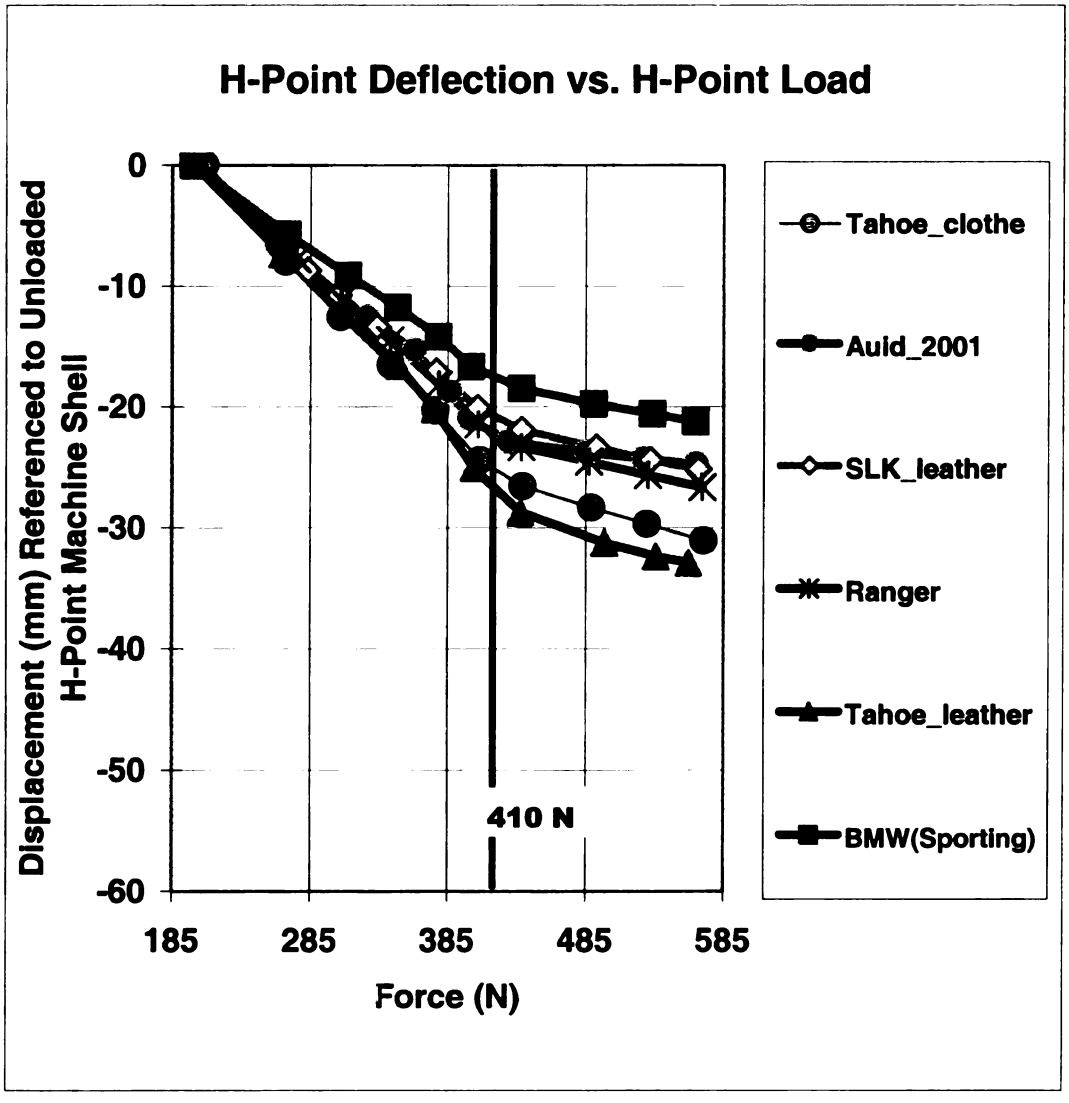

Figure 27: Chart comparing H-point deflection versus H-point load for six seats tested in phase I. The deflections corresponding to a H-point load of 410N were compared.

Three seats from phase I study were selected to represent a wide range of seat pan stiffness. The three seats were,

1. Seat E, the Tahoe (2001 SUV) with leather trim and it had H-point deflection of 50 mm corresponding to 410 N, (figure 28). The seat represented a soft seat pan.
2. Seat F, the BMW (sedan) with H-point deflection of 32 mm corresponding to 410 N, (Figure 29) represented stiff seat pan.
3. Seat C, the SLK (1999 sports) with H-point deflection of 45 mm (figure 30) corresponding to 410 N, represented medium stiff seat pan.

It can be seen from figures 26 and 27 that the three seats selected from phase I covered wide range of cushion pan stiffness.

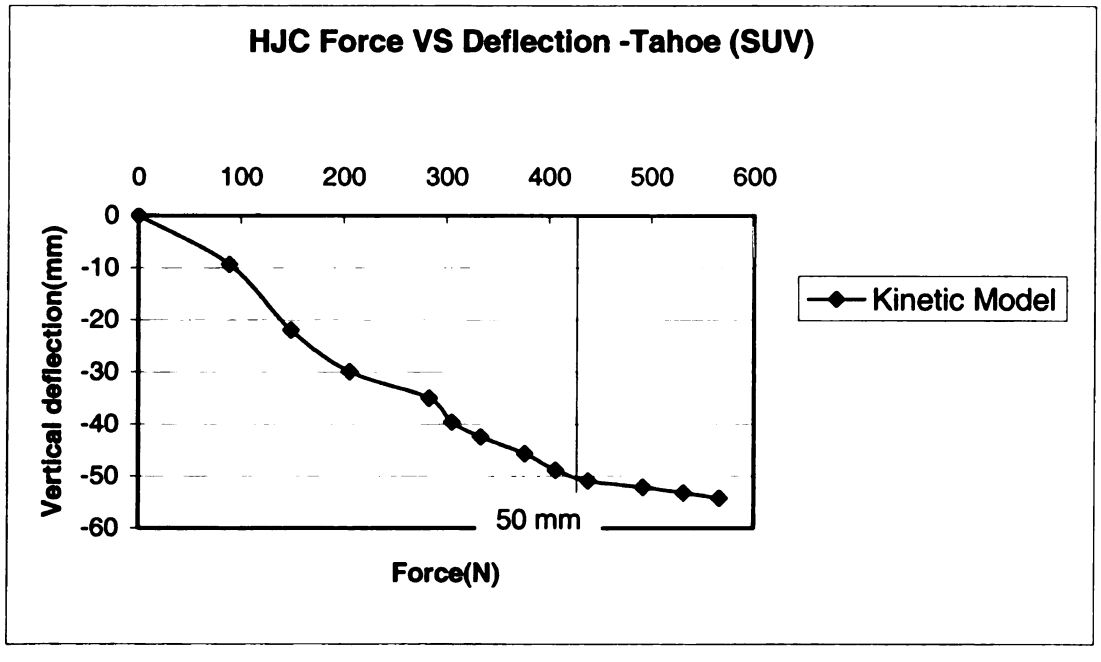

Figure 28: H-point Force Vs H-point deflection for Tahoe (SUV) seat from Radcliff's 2nd order kinetic model [6].

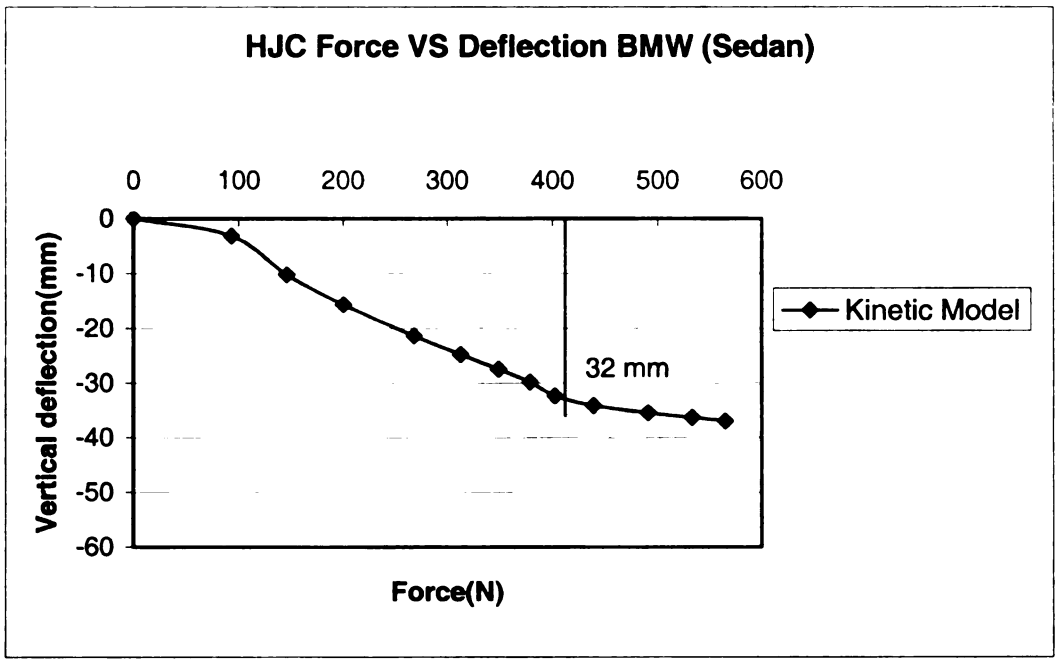

Figure 29: H-point Force Vs H-point deflection for BMW (Sedan) seat from Radcliff's 2nd order kinetic model [6].

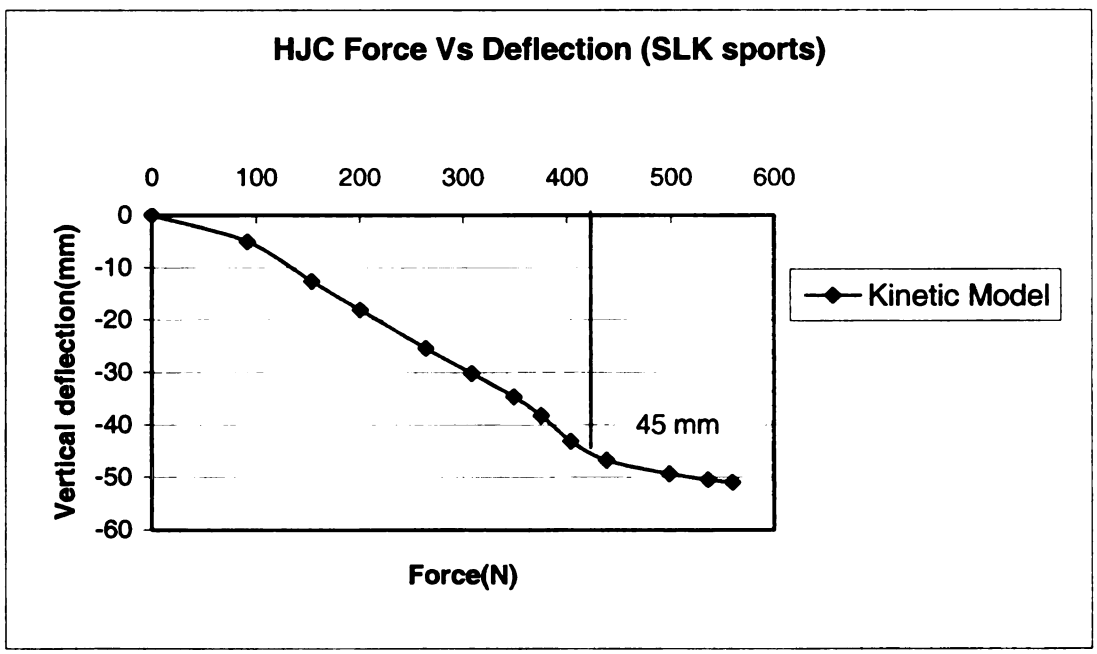

Figure 30: H-point Force Vs H-point deflection SLK (Sports) seat from Radcliff's 2nd order kinetic model [6].

4. PHASE II

The goal of phase II was to collect data to calculate hip joint center (HJC) locations of a sample of male occupants seated in the three seats selected from phase I. The three seats included Seat E-Tahoe, Seat C-SLK and Seat F-BMW and selected because they encompassed a range of seat pan stiffnesses. These three seats were tested with people of various heights and weights. The locations of their HJCs in the seats were computed and compared to the prediction model developed by Bush and Macklem [3] (discussed at the end of section 1.0). The testing protocol, the procedure for data collection, and calculation of HJC deflection are discussed in this section.

4.1 Test Subjects

The purpose of this study was to collect additional data to validate the method of HJC prediction by Bush and Macklem [3]. The scope of this study addressed only the male data. To account for a range of possible HJC locations in the seats, the sample of male occupants covered a wide range of heights and weights. The development of the HJC prediction method was based on a previous study by Gutowski[12] therefore a sample similar to Gutowski's was tested including male occupants of average height and weight, heavy and tall men, and heavy but light men. Thus, data from the present study could be compared to the prediction developed by Bush and Macklem [3] using Gutowski data. The goal was to test five male subjects from each of the anthropometric groups. These groups were based on NATIK [18] data (shown in Table 4). Subjects were recruited on a volunteer basis. They were initially screened to see if they fit in the desired height and weight categories. The actual test subjects varied slightly from their desired height and weight (refer to Table 5).

Table 4: Desired human subjects' anthropometrics as per NATIK [18].

Anthropometric group for Males	Weight	Stature
50% height and 50% weight (50H50W)	171 lb	69 in.
95% height and 5% weight (95H5W)	135 lb	73 in.
95% height and 95% weight (95H95W)	216 lb	73 in.

Table 5: Actual test subjects' anthropometric measurements.

	Weight (lb)	Height (in)	%tile Height	%tile Weight	Age (years)	Pelvic Width (mm)	Pelvic Depth (mm)	Pelvic Height (mm)
Subjects placed in average male category								
Subject1	175	70	65	56	22	284	217	107
Subject2	144	67	25	15	25	263	215	93
Subject7	156	71	85	26	20	268	225	111
Subject8	157	69	50	29	20	242	215	97
Subject10	172	70	70	50	24	272	239	108
Subject12	157	69	50	29	25	247	220	105
Average	**160**	**69**	**68**	**34**				
***STDEV**	**11**	**1**	**21**	**16**				
Subjects placed in tall and light male category								
Subject4	129	71	85	3	27	254	196	88
Subject5	117	71	85	1	29	247	197	100
Subject9	146	71	85	14	26	260	231	101
Subject13	124	71	85	2	25	236	251	87
Average	**129**	**71**	**85**	**5**				
STDEV	**12**	**0**	**0**	**6**				
Subjects placed in tall and heavy male category								
Subject6	189	72	90	76	24	271	238	104
Subject11	198	72	90	85	24	274	252	110
Subject14	213	72	90	94	24	267	258	117
Subject15	236	71	85	99	21	300	272	121
Subject16	202	72	90	89	40	269.5	249	104
Average	**208**	**72**	**89**	**89**				
STDEV	**18**	**0**	**2**	**9**				
Average of all	***168***	***71***	***75***	***45***				
STDEV of all	***35***	***1***	***20***	***36***				

*STDEV : Standard Deviation

The subjects in average height and weight category had average height matched, but were a little light. The subjects in tall and heavy and tall but light groups were one to two inches shorter and little lighter than desired.

Generally speaking, the 50%tile height and 50%tile weight (50H50W) subjects represented male occupants of average height and average weight. The subjects with 95%tile height and 95%tile weight (95H95W) represented tall and heavy male occupants and the subjects with 95%tile height and 5%tile weight (95H5W) represented tall and light male occupants.

Six subjects were tested from tall and heavy (95H95W) group, five from average (50H50W) group and four subjects from tall and light category (95H5W). The anthropometric measurements along with averages and standard deviations for all subjects tested are listed in table 5 including pelvic dimensions (refer to Figure 35) which were necessary for calculating the hip joint centers of the subjects in the reference seat.

4.2 Test Buck setup

All subjects were tested in a reconfigurable test buck. For testing, the H-point to Heel point vertical distance also termed as H30, (Figure 31) was set as per the seat type according to Johnson Controls Incorporation's (JCI) seat testing standards, listed in Table 7 [10]. The J826 manikin and corresponding procedures were used to measure and obtain the dimensions listed in Table 6.

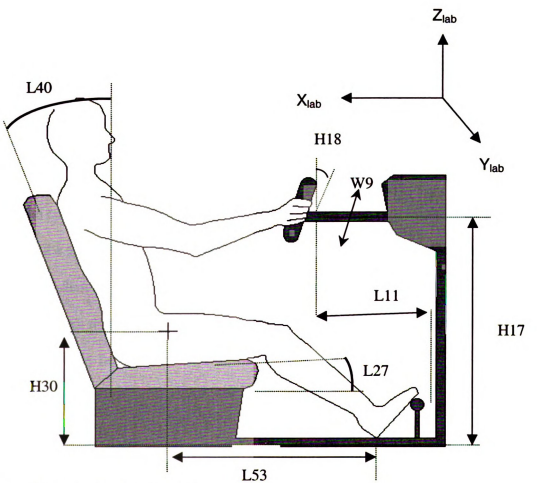

Figure 31: Test buck dimensions. [12]

Table 6: Dimension descriptions for test buck set-up.

SAE #	Dimension Description
H30	Seat (J826 manikin H-point) Height
L27	Cushion Angle with respect to Horizontal
L11	Steering Wheel to Toe bar (X)
H17	Steering Wheel to Heel Point (Z)
H18	Steering Wheel Angle with respect to Vertical
W9	Steering Wheel Diameter (outer)
L53	H-point to Toe bar
L40	Backrest Angle

Table 7: Package dimensions with J826 manikin [1] for the typical car segment-seating environment [10].

Package	1	2	3	4
Typical Segment	Sporty	Passenger Car	SUV	Van
Torso Angle (°)	27	24	21.5	20
Hip Angle (°)	98	95	95.5	95.5
Knee Angle (°)	132	124	121	115
Foot Angle (°)	87	87	87	88
H-point to Heel point-Z (mm)	190.73	239.82	325	360.69

The cushion pan angle of all three seats was fixed at 15 degrees using J826 manikin [1] and the SAE J1100 [11] procedure for measuring the cushion angle. Out of the three seats only Seat E- the Tahoe (SUV) had a lumbar prominence adjustment. To maintain consistency in testing protocol, testing was performed with the lumbar support in the off position for the Tahoe seat.

4.3 Reference Seat

Along with the three production seats, subjects were tested in a reference seat also termed a 'hard seat'. The hard seat was a wooden seat without any padding, and therefore no deflection of the seat pan occurred when loaded. The seat was used to collect positional data on the pelvis and other bony landmarks. The data were later used to calculate the HJC location and the deflection of the buttocks in the hard seat. The seat was set with pan angle of 15° and back angle of 23° (refer to Figure 32). These values corresponded to a cushion pan angle of 11° and a back angle of 24° when measured with the SAE J826 manikin [1].

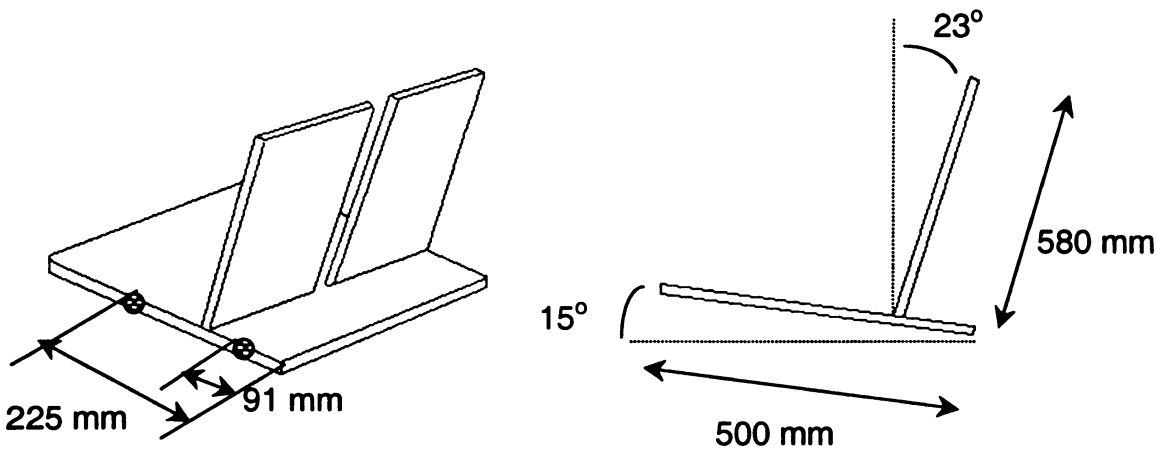

Figure 32: Reference hard seat dimensions. [12]

4.4 Test protocol

From Gutowski's work [12] it was observed that when subjects were not given any instructions about the placement of their buttocks in the seat pan, the positions of their HJC's had an anterior shift as compared to when they were asked to place their buttocks against the seat back. Based on this finding, a test protocol was designed to capture these differences in HJC positions. Each subject was instructed to place his buttocks against the seat back termed 'instructed' position, and then in a preferred position. No instruction about placing his buttocks was given to the subject in the preferred position.

For both the instructed and preferred positions, the steering wheel position could be adjusted vertically and horizontally to achieve the preferred H17 distance (refer to figure 31). Also the toe bar could slide forward and rearward to set subject preferred foot position and thus preferred L11 distance (refer to figure 31).

In the instructed position (figure 33), subjects were asked to sit with their buttocks firmly against the seat back to achieve the most posterior position of their HJC. The seat back recline angle of each seat was set to 24° and cushion pan angle to 15° using J-826 [1] manikin. The subjects were asked to maintain contact with a foot support that represented the gas pedal location. To achieve this, the subjects were allowed to move the seat fore and aft. Subjects were free to choose the position of their hands relative to the wheel and were able to slide the wheel fore and aft to their preferred location.

In the preferred position (figure 34), subjects were asked to sit with their buttocks placed in any preferred position on the seat pan. They were also free to adjust the recline angle, while cushion pan angle was fixed to 15°. As in the instructed position, the fore/aft position of the seat as well as the steering wheel height was adjusted by the subject.

Again subjects were asked to maintain contact with the foot support. Subjects were free to choose the position of their hands relative to the steering wheel.

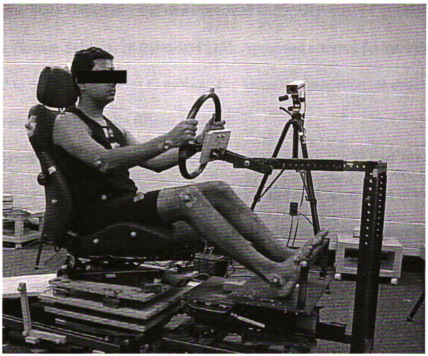

Figure 33: Subject 10 seated in the instructed position in SLK seat.

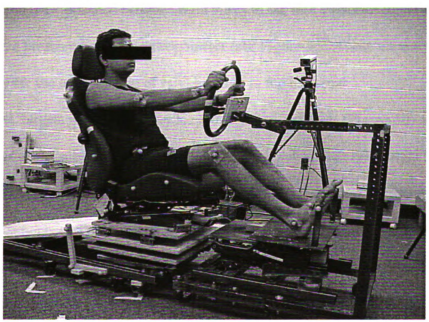

Figure 34: Subject 10 seated in the preferred position in SLK seat. Subject chose more reclined position than the instructed position and a preferred position of his arms.

4.5 Testing Procedure

All testing was performed in the Biomechanical Design and Research Lab (BDRL) of Michigan State University and was approved under University Committee on Research Involving Human Subjects IRB#96-054 [13]. Approved consent forms were fully explained to each subject prior to testing. The same test procedure as described below was followed for each of the fifteen subjects.

Subjects were asked to wear tight fitting clothes (Figures 33 and 34) so as to reduce the movement of the clothing relative to the body and thus the motion of the targets that were attached to the clothing. If the subjects did not have the necessary clothing, it was provided. Once in the appropriate attire, their height (without shoes), weight and age were recorded. Manual measurements of pelvic height (PH: the perpendicular distance from the line joining the right and left Anterior Superior Illiac Spine, ASIS to the top of the pubic symphisys), pelvic width (PW: distance between the right and left ASIS) and pelvic depth (PD: distance between right ASIS to the mid Posterior Superior Illiac Spine, PSIS) were measured with an antropometer (see Figure 35). These measurements were necessary for the computation of HJC location in the hard seat.

Next, targets were put on key locations on the test seats (Figure 36) and on bony landmarks of the subjects (refer to Table 8). For all subjects only the right side of the body was targeted and right HJC was calculated. Since motion measurement system only had five cameras and was limited to 30 targets it was not possible to target both sides of a subject. Also the motion system is able to catch a maximum of only 30 target locations, which does not allow putting targets on both sides of the body of a subject. Wherever

possible targets were affixed directly on the skin while the rest were taped to the clothing at the target locations.

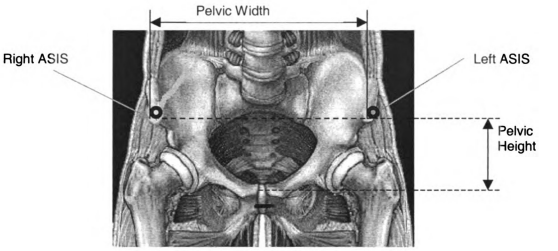

Figure 35: Pelvic width and pelvic height [14]

The target on the right Anterior Superior Illiac Spine (ASIS) and the target on Lateral Femoral Epicondyle of the right knee were the two targets necessary to calculate the HJC in the seated position using the method developed by Bush and Gutowski [15]. The locations of other targets will be useful in further study of various anatomical landmark positions responses of the subject to the seat, however were outside the scope of the present study.

Data files were recorded with instructed and preferred positions as discussed in section 4.4. Two data files for each of the two positions were recorded with 12Hz frequency for 3 seconds using the Qualisys System. Between the two trails of the same position, subjects were asked to move around in the seat and then reposition themselves. To avoid the targets being knocked off during the transition, subjects were not allowed to get out of the seat between the trials. The order in which a subject would sit in each of the three seats was randomized.

Table 8: Target locations for seat testing.

Production Seat	Test Subject
Seat Pan Front and Rear	Sternal Notch
Recline Top and Bottom	Mid-Sternum
Right Toe Bar	Left ASIS and Right ASIS
Buck Front and Rear	Mid-Thigh
Buck Top	Right Knee (Lateral Femoral Epicondyle)
Recliner Pivot	Right Ankle (Lateral Maleolous)
	Right Ball of Foot
	Right Shoulder (Acromion Process)
	Right Elbow (Humeral Lateral Condyle)
	Right Wrist (Ulnar Condyle)
	Right Head (Temple) & Forehead

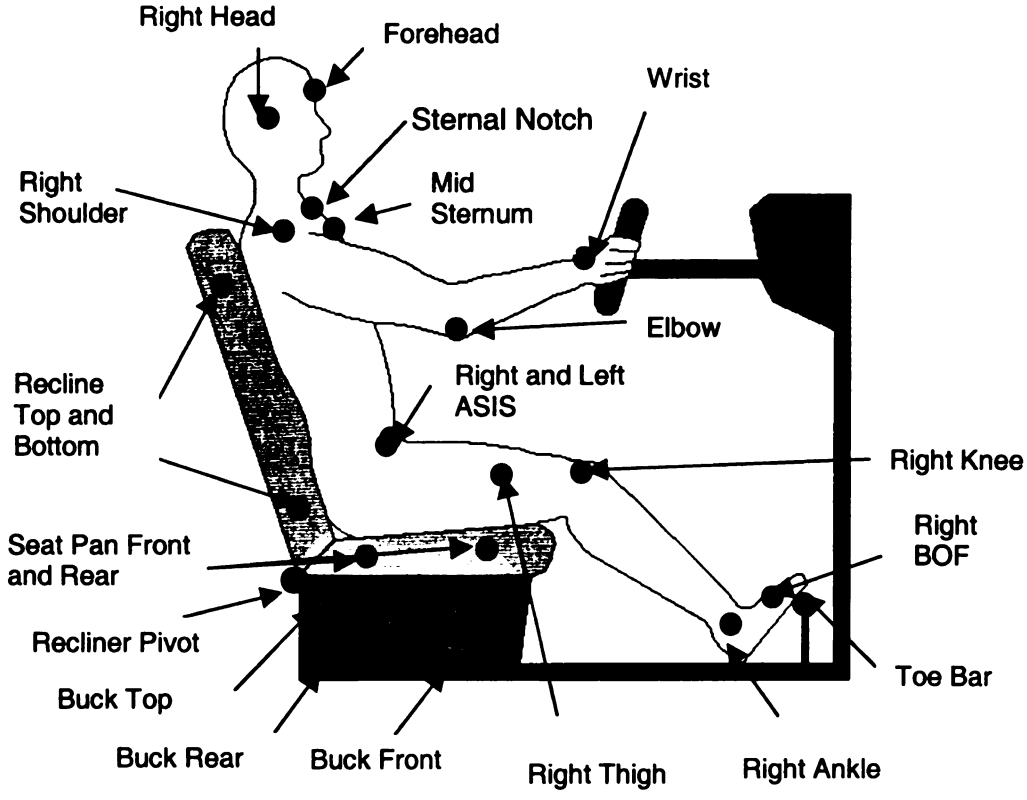

Figure 36: Taget locations on seat and subject for testing in three production seats.

After collecting data files in all three-production seats, the subject was asked to sit in the hard seat with the targets attached to landmarks noted in Table 9 and targets on the reference locations on hard seat. (See Figure 37 and Table 9). For the hard seat trials, five additional targets were placed on the spinous process of C7, T8, T12, L1 and L3.

To find the HJC in hard seat, both right and left Anterior Superior Illiac Spine (ASIS) locations were targeted. Two hard seat trials were recorded for 3 seconds at a frequency of 12Hz. The subjects were asked to reposition themselves in the hard seat between the two test files. Again, they were not allowed to get out of the seat between the two trials.

Table 9: Target locations for hard seat trials.

Reference Seat	Test Subject
Seat Pan Front	Sternal Notch
Seat Pan Rear	Mid-sternum
	C7 (Seventh cervical vertebra)
	T8 (Eighth thoracic vertebra)
	T12 (Twelfth thoracic vertebra)
	L1 (First lumbar vertebra)
	L3 (Third lumbar vertebra)
	Left ASIS and Right ASIS
	Mid-PSIS
	Right Thigh
	Right Knee (Lateral Femoral Epicondyle)
	Right Ankle (Lateral Maleolous)
	Right Ball of Foot
	Right Shoulder (Acromion Process)
	Right Head (Temple)
	Forehead

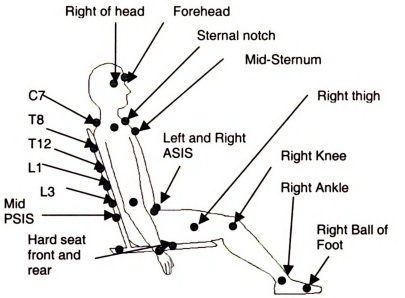

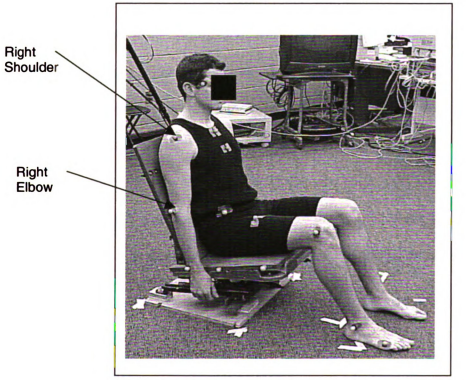

Figure 37: Target locations for testing in hard seat and targeted subject.

5. PHASE III

5.1 Background for phase III

The Radcliffe kinetic model was based on experimental deflections of butt thigh segments of ASPECT and J826 manikins, which represent male occupants of 50th percentile height and 50th percentile weight (50H50W). Because the kinetic model was based on the experimental data obtained by manikins of a single size (50H50W) one task was to determine if the model could be used to predict the HJC deflection people of sizes other than 50H50W along with the 50H50W category.

Bush and Macklem [3] analyzed the applicability of the kinetic model in a previous study. They used the data from a study by Gutowski [12] in which human occupants of various sizes and weights were tested in four different seats and their HJC deflections in each of the seats were calculated directly from the experimental motion data. Bush and Macklem's study [3] began by comparing the HJCs computed from Gutowski's data to the force deflection curve from the kinetic model. To achieve this, the manikin loading data for the seats tested by Gutowski was input to the Radcliffe's kinetic model and the load deflection curves were obtained. Then using Bush's [9] loading estimation (Table 10) the deflection was read corresponding to the loading under the occupants' HJCs (54.3 % of body weight) directly from the load deflection curves obtained from Radcliffe's kinetic model.

Table 10: Loading under the HJC for various anthropometrics as studied by Bush [9]. Body weight for each anthropometric as per the NHANES [16]

Occupant Category	Load under the HJC in newtons (54.3% of body weight)
Small Female (5H5W,F)	271
Medium Male (50H50W,M)	408
Large Male (95H95W,M)	432

It was observed in the study by Bush and Macklem [3] that using Radcliffe's [6] kinetic model, Bush's [9] loading estimation and Gutowski's [12] data, the physical manikins could only predict the HJC deflection of the mid-sized and large male occupants. A notable deviation in the HJC deflection was observed for other anthropometries (Figure 38).

Next, Bush and Macklem [3] developed offset curves for predicting the HJC locations of other sized occupants. These offset equations were based on the HJC computations in Gutowski's study on four seats [12]. It was observed that the deviations in the HJC deflections from the kinetic model had a linear trend between 95H5W males and 50H50W males and parabolic trend for 5H5W females, 5H50W females and 5H95W females (Figure 39 and 40). The HJC deflection for the 95H95W males was found to be on the extended load deflection curve obtained using Radcliffe's kinetic model. These trends in HJC deflection deviations were accounted for by developing mathematical equations termed as offset curves.

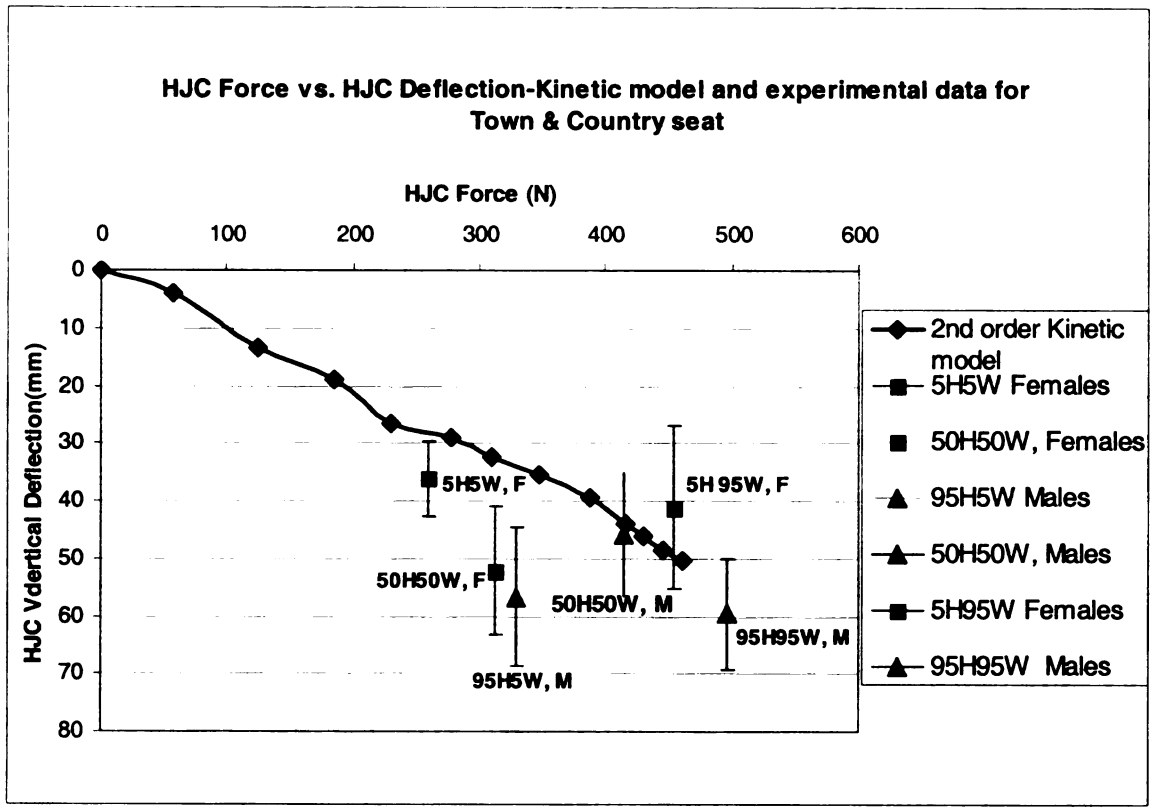

Figure 38: Averages of HJC forces Vs. Deflections with error bars for various anthropometries in Town and Country seat obtained by Bush and Macklem [3] using the data from Gutowski's study. Each point represents the averaged HJC deflection of five subjects. A notable difference in average deflections compared to those predicted by the kinetic model can be observed for anthropometrics other than 50H50W males.

A generalized best-fit linear offset equation was developed between 95H5W and 50H50W male categories relative to the HJC load deflection curve using Radcliffe's kinetic model (Figure 39). A generalized best-fit parabolic equation was developed to predict the HJC deflections relative to the seat deflection curve of 5H5W, 50H50W and 5H95W female categories (Figure 40). Bush and Macklem provided offset curves, based on data from three seats. To refine these curves, (for male occupants' data only) additional data were collected on three additional seats. This portion of the work is considered phase III.

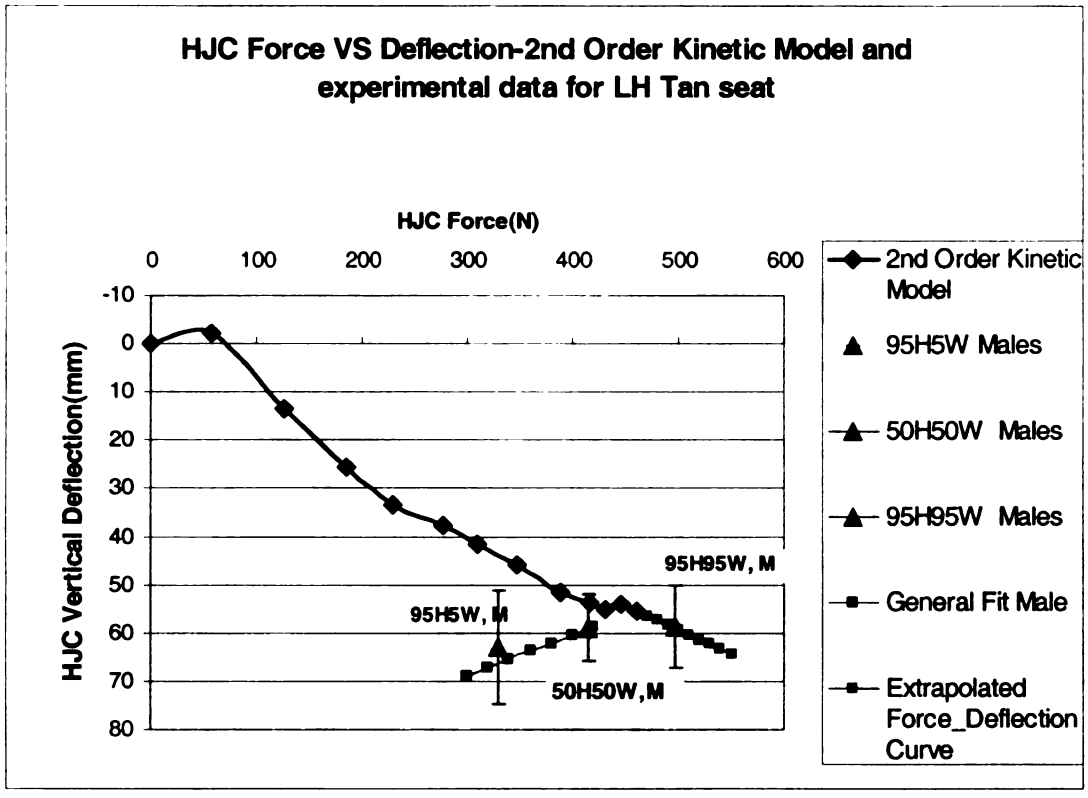

Figure 39: Best fit line for 50H50 W and 95H5W male occupants developed by Bush and Macklem [3]. Each point represents the averaged HJC deflection of five subjects. HJC deflection for 95H95W estimated to be on the linearly extrapolated HJC force deflection curve.

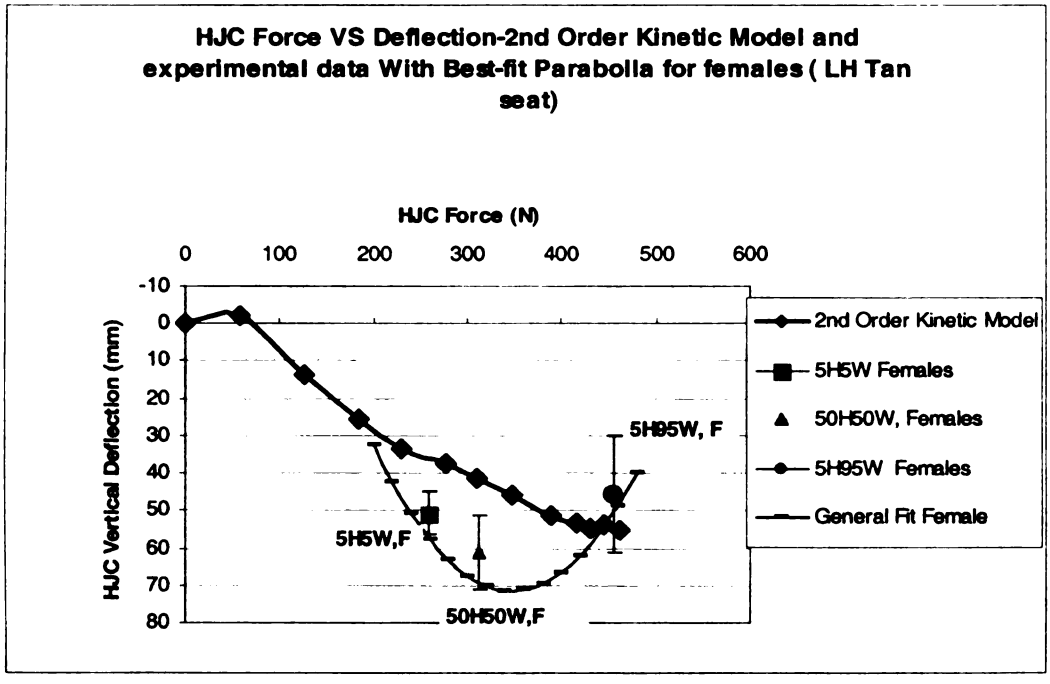

Figure 40: Best fit parabola for female occupants developed by Bush and Macklem [3].

The method used to calculate the deflection of the seat pan under the HJC, the calculation of HJC locations and the results of the comparison are discussed next.

5.2 Calculation of HJC in test seats

After collecting the data for all 15 subjects in phase II, the next task was to calculate their HJC locations in each of the three test seats for both the preferred and the instructed positions (refer section 4.2) and then compute the deflection of the seat pan under the HJC location.

The first step in locating the HJC of the subjects in the production test seats was to locate their HJC in the hard seat. HJC location in the hard seat was calculated using the Seidel [17] method, which used of the manually measured pelvis dimensions (refer section 4.3, figure 35) and the locations of right and left ASIS targets and the mid-PSIS target (Figure 37). The location of HJC in hard seat was necessary to calculate the deflection of subject's buttocks in seated position.

Using the location of HJC in the hard seat and the motion measurement data of the subject seated in the production (deformable) seat, the HJC for that subject in that particular production seat was computed.

Two different methods were used to calculate HJC in the production seats. The first method, used by Gutowski [12] used the coordinates of right ASIS and right lateral epicondyle (right knee) targets in the actual seat along with the coordinates of right HJC in the hard seat. In the method used by Gutowski's [12] three known lengths were used to calculate HJC coordinates in the sagittal plane which were: the length between right knee and right ASIS target in production seat, the length between right HJC and right ASIS in

the hard seat and the length between right HJC and right knee in hard seat. Using these three lengths, and the coordinates of the right ASIS and right knee, the right HJC coordinates were computed. The method used a two-dimensional vector analysis to obtain the HJC coordinates in sagittal plane.

The method, by Bush-Gutowski [15] used the coordinates of right ASIS and right lateral epicondyle (right knee) along with the coordinates of right HJC in the hard seat. In this method, two known lengths were used: the length between right HJC and right ASIS in hard seat (pelvis length) and the length between right HJC and right knee in hard seat (femur length). Bush-Gutowski method assumed that the pelvis length and femur length remained constant irrespective of the subject being in hard seat or a deformable seat. Using the coordinates of right ASIS and right knee in the production seat along with the two known lengths, the HJC coordinates were solved for using an intersection of sphere and circle analysis. Thus, Bush-Gutowski method used a three dimensional approach to solve for HJC coordinates in sagital plane as compared to a two dimensional approach used in Gutowski's method. The Bush method however can only be used in a seated environment.

In previous study by Gutowski [12] the HJC coordinates were calculated only using the one particular method whereas in the present study both the method used in Gutowski's study and Bush-Gutowski method were used to calculate the HJC coordinates. The HJC vertical deflections then were computed using the HJC coordinates obtained from both of the above said methods and those were plotted relative to the deflection predicted by the kinetic model. Both the Bush-Gutowski computations and the

computations used in Gutowski's study were used so data from this study could also be compared to that obtained from the Gutowski study.

5.3 Method to calculate the HJC deflection

The method used to find the deflection of the production seat under the HJC in the study by Bush and Macklem [3] was also used in the present study.

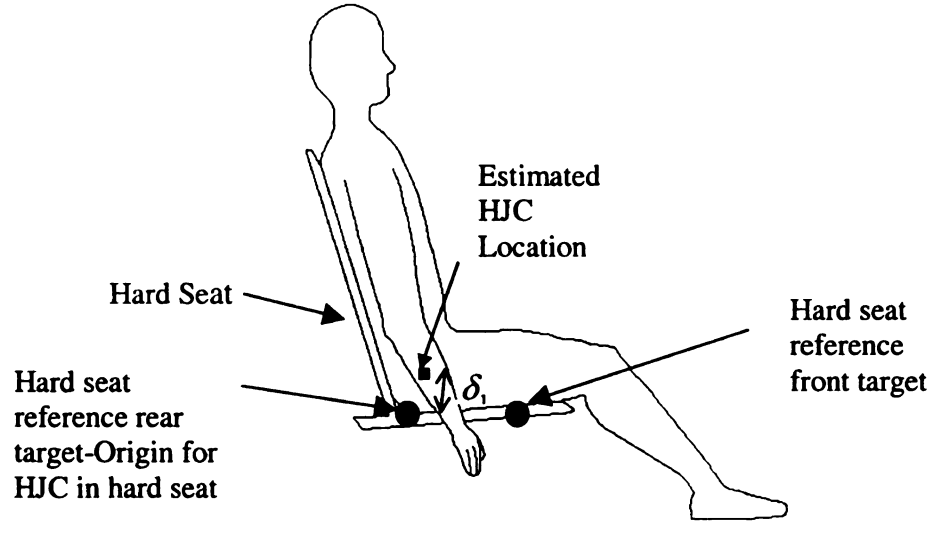

Figure 41: Calculation of δ_1 the vertical deflection of the buttocks [3].

Three measurements were calculated to get the HJC location in production seat. First the vertical distance from HJC to the hard seat pan was calculated and was termed as δ_1 (buttocks' deformation). Next, the distance between a point corresponding to the HJC vertically downward on the undeflected seat contour to a reference point was calculated and was termed as δ_2. The third measurement δ_3 was calculated as the vertical distance between the HJC in the production seat and a reference point on the seat.

Finally, the HJC deflection (Δ) was calculated to be $\Delta = \delta_1 + \delta_2 - \delta_3$. The method is explained in detail as follows.

From the hard seat data and the measurements of pelvic dimensions the 3-dimensional coordinates of the HJC with respect to the rear target (origin) on the reference seat were calculated using Seidel [17] method. The vertical distance between the HJC and the plane of the hard seat pan was estimated as the measurement of buttocks deflection and was identified as δ_1 (Figure 41).

Deflections (both those in the hard seat and in the production seats) are computed vertical rather that perpendicular to the seat pan. This is because the final seat deflection was to be compared to that obtained from the kinetic model, which is based on the vertical deflection of the H-point axis of the manikin.

The vertical distance of the HJC in the production seat was then measured using the recliner pivot as reference on the seat and was defined as δ_3. The recliner pivot target was considered a reference target that did not move during testing. (Refer figure 36).

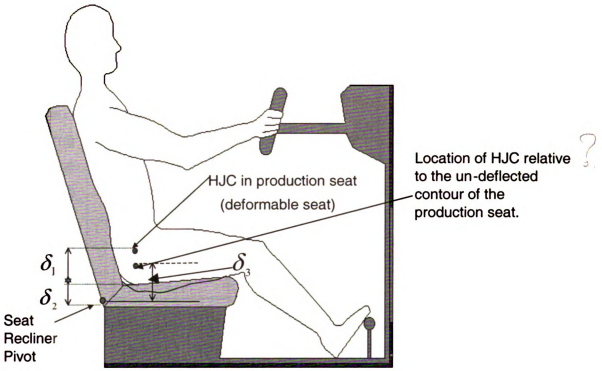

Seat pan deformation under the HJC, $\Delta = \delta_1 + \delta_2 - \delta_3$

Figure 42: Computation of Seat Deflection from human data.

To determine the vertical movement of the HJC in a deformable (production) seat, the location of the HJC relative to the seat pan was needed. So, a point on the undeflected seat pan contour corresponding vertically downward to the HJC was obtained, and the distance between that point and a reference point (recliner pivot) for each trial was calculated as δ_2. To measure δ_2, the seat contour scan was used (refer Figure 43). The HJC coordinates in the sagital plane (X-Z plane) were obtained using two different methods as discussed in section 5.1 and the vertical distance between the point on the seat scan along the Z direction corresponding to the X- coordinate of HJC and the recliner pivot was measured as δ_2.

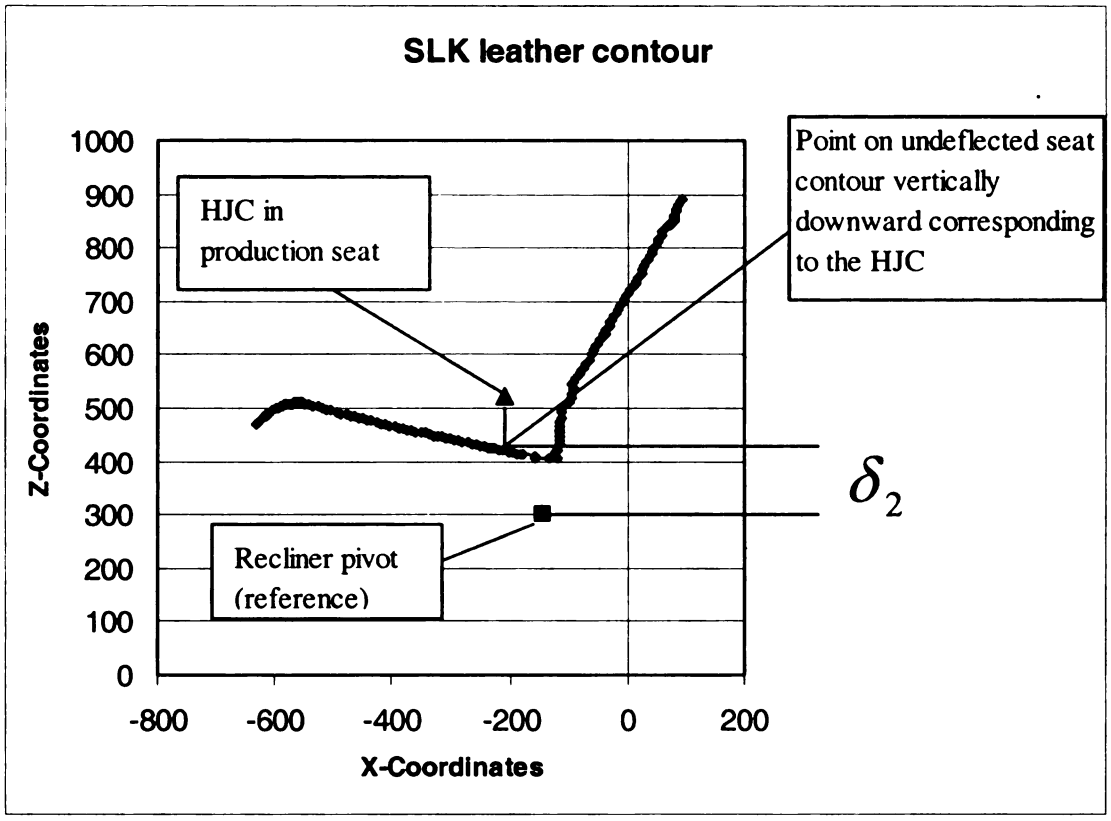

Figure 43: Un-deflected seat contour scan obtained from Qualisys system used to calculate δ_2.

The vertical deflection of the HJC (Δ) was considered as the vertical deflection of the production seat under the HJC, which was equal to (δ_1 + δ_2) - δ_3. Where,

δ_1 = Buttocks vertical deflection in the hard seat.

δ_2 = Vertical distance between the un-deflected seat contour point corresponding to the HJC in production seat and the recliner pivot reference.

δ_3 = Vertical distance between the HJC in production seat and the recliner pivot reference.

The deflections calculated using the above method were then compared with the deflections produced with the kinetic model.

5.4 Results of comparison between the HJC deflections computed experimentally and those predicted using the kinetic model.

The HJC deflection was calculated for each subject in each of the three seats, for both the preferred and instructed positions, for two trials in each position. The HJC deflections were averaged over each category in both instructed and preferred positions to obtain one number per category in each seat and were plotted on the force deflection curves.

Out of the three seats tested it was observed that the HJC deflection pattern for most of the 50H50W subjects in both instructed and preferred positions in the BMW seat had a different behavior with respect to the kinetic model as compared to the other two seats. The HJC deflections were consistently larger than that estimated from the kinetic model (Figures 44 to 46).

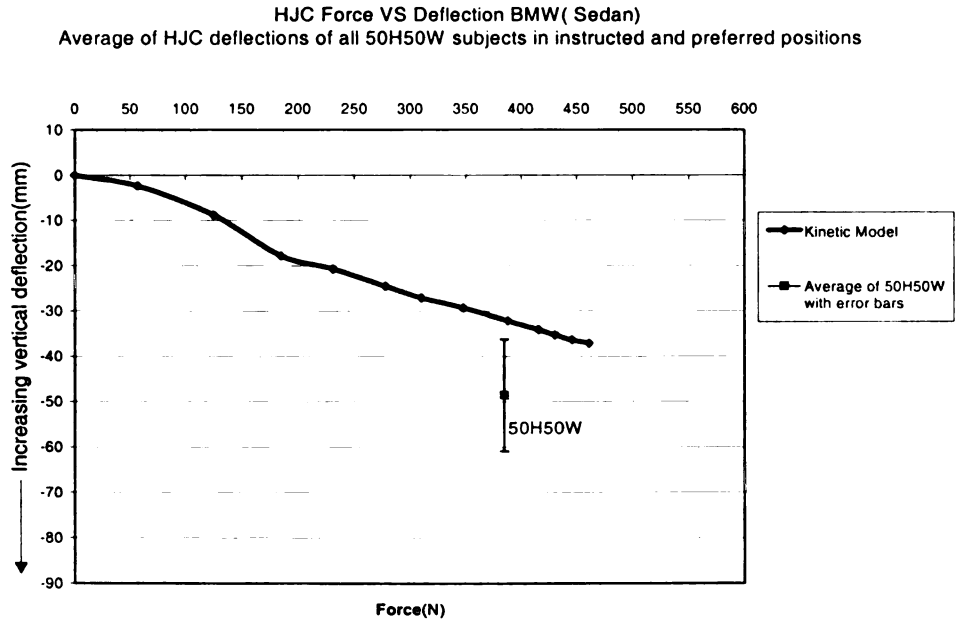

Figure 44: HJC deflections averaged for all 50H50W subjects in BMW seat were found to be higher than that predicted by the kinetic model and was below the force deflection curve.

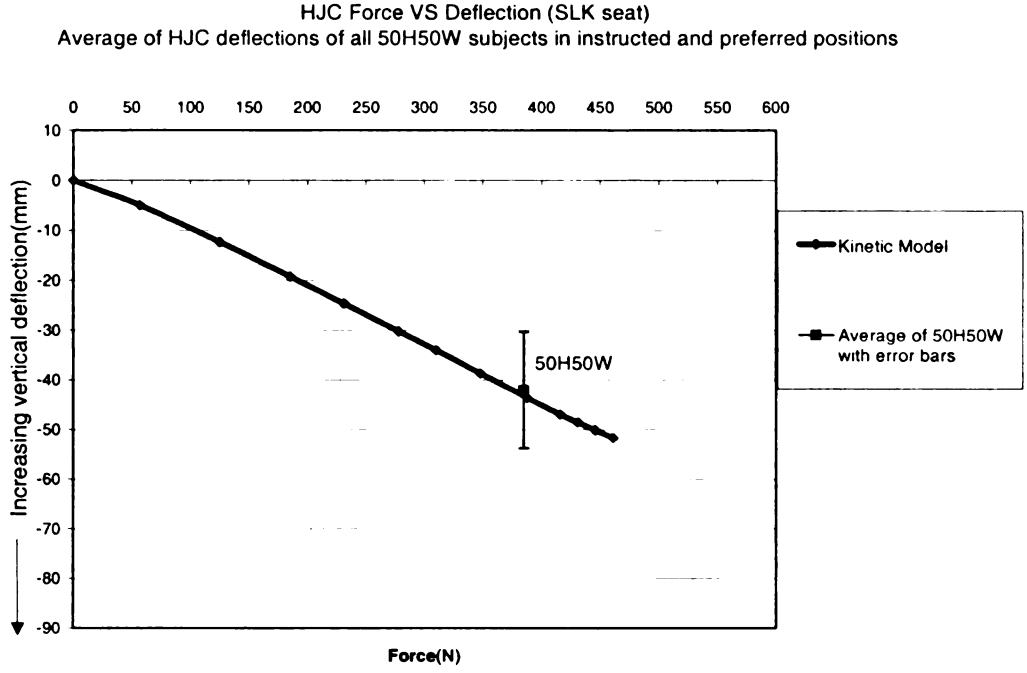

Figure 45: HJC deflections averaged for all 50H50W subjects in SLK seat were close in comparison to the force deflection curve of kinetic model.

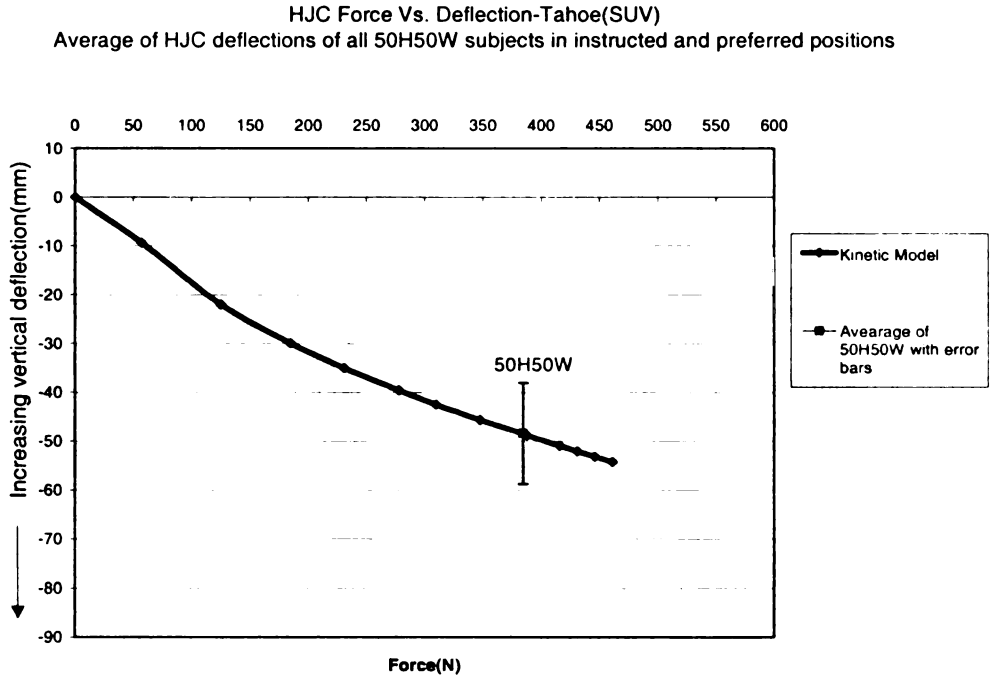

Figure 46: HJC deflections averaged for all 50H50W subjects in Tahoe seat were close in comparison to the force deflection curve of kinetic model.

The BMW seat had prominent, firm seat pan bolsters as compared to the other two seats and this was thought to be the reason for the different behavior. It was suspected that the prominent seat pan bolsters on the BMW seat pan, did not allow full contact of the manikin's butt thigh segment. Investigation with pressure mapping was performed to see how the pressure exerted by the ASPECT Butt Thigh (ABT) segment varied among the seat pans of the three seats (Figures 47 to 49). It can be seen in the figures 47 to 49 that unlike the other two seats, there is a gap in the pressure contours in the elliptically marked region (buttocks region) for the BMW seat representing lack of contact between manikin and seat. It was found that the pressure was evenly distributed on the central and bolster regions of the SLK and Tahoe seat pans while on the BMW seat pan, the pressure was uneven on central and bolster regions and a part of pressure was concentrated on the bolsters. This uneven pressure distribution did not allow the (ABT) segment to come fully in contact with the central portion of the seat pan thereby restricting the vertical motion of the manikin; which resulted in a kinetic model that would produce a deflection curve that may be offset higher (less deflection) than actually would occur with a 50H50W occupant.

Thus the kinetic model for the BMW seat produced a force deflection curve based on the data from the manikin that did not precisely represent a mid-male loading.

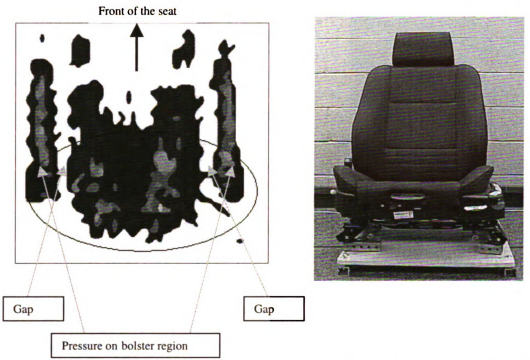

Figure 47: Pressure distribution on BMW seat pan due to ABT loading of 461N (refer section 3.2). A considerable amount of pressure is distributed on the bolsters. The BMW seat with prominent seat pan bolsters is seen in the right.

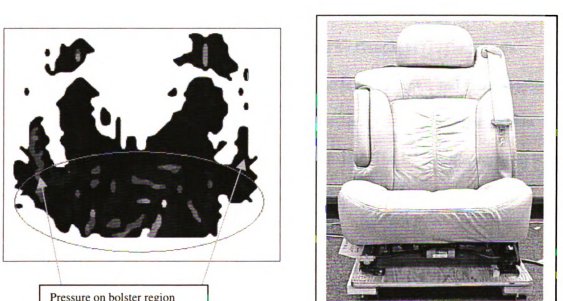

Figure 48: Pressure distribution on Tahoe seat pan due to ABT loading of 461N (refer section 3.2). Amount of pressure distributed on the bolsters is less compared to that in BMW (Figure 47). Tahoe seat is seen on the right.

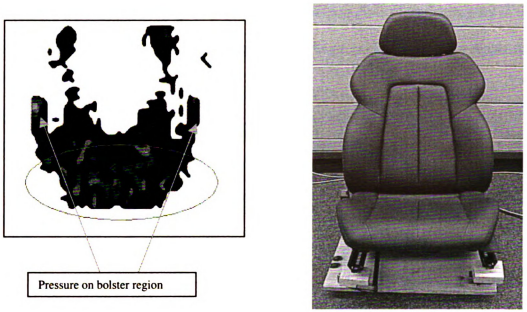

Figure 49: Pressure distribution on SLK seat pan due to ABT loading of 461N (refer section 3.2). Amount of pressure distributed on the bolsters is less compared to that in BMW (Figure 47). SLK seat is seen on the right.

In the process for comparing the calculated HJC deflections to those from the kinetic model, the following aspects were considered. The HJC deflections were calculated using the HJC locations obtained from both the method used by Gutowski [12] and Bush-Gutowski method. Because the Bush-Gutowski method is more recent and is developed for seated environment, all the comparisons for HJC deflections were made using data obtained from Bush-Gutowski's method of calculating HJC. The HJC deflection data was compared with the HJC force-deflection plots obtained using the Radcliffe's kinetic model [6] for each of the three seats.

First, the deflections for each category (50H50W, 95H5W, 95H95W) of subjects in both the instructed and preferred positions were plotted for all three seats and the HJC deflection was compared with that predicted by the kinetic model. The HJC deflection estimated by the kinetic model was read directly from the load deflection curve. As a

representation of all comparison plots, only the comparison plots of each category in one of the three seats are discussed next. The data for all the plots can be found in Appendix.

5.4.1 Comparison of HJC deflections for 50H50W male subjects.

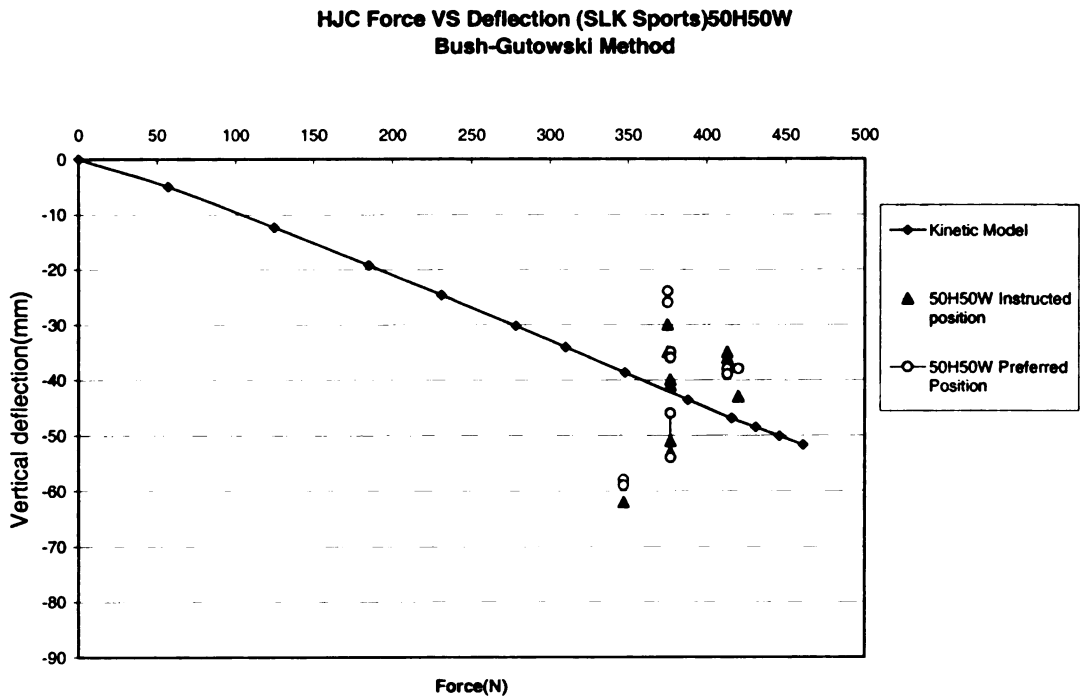

Figure 50: HJC Force vs. Deflection for 50H50W male subjects in SLK seat.

The graph in Figure 50 shows the HJC vertical deflection in preferred and instructed positions for 50H50W male occupants seated in SLK seat. The X- coordinates on the graph represent the 54.3% of body weight (Bush [9]), which is the loading under the buttocks of the occupant. The Y-coordinates are the HJC deflection calculated from the experimental data. It can be seen that the HJC deflection varied to some extent from that predicted by the kinetic model. The HJC deflections calculated were consistent within two trials of the same position for a particular subject in a particular seat (Table 11). Also it was observed that, in most of the trials the HJC deflection in the preferred

position was higher than that in the instructed position. There were no large differences in the HJC deflections between the two positions.

HJC vertical deflection for 50H50W males in SLK				
	Instructed Position	Preferred Position		
Subject No(Trial No)	HJC vertical Deflection	HJC vertical Deflection	HJC vertical Deflection (Kinematic model-Directly from the chart)	HJC force(newtons)(54.3 %of bodyweight)
1(1)	44	50	42	420
2(1)	60	65	35	347
2(2)	59	63	35	347
7(1)	34	44	38	375
7(2)	36	53	38	375
8(1)	51	65	38	377
8(2)	58	63	38	377
10(1)	50	47	41	413
10(2)	45	49	41	413
12(1)	40	44	38	377
12(2)	42	47	38	377
Average	**47**	**54**	**38**	
Standard Deviation	**9**	**9**	**2**	

Table 11: HJC deflection comparison between preferred and instructed position for 50H50W male subjects in SLK seat.

In the preferred position, most of the subjects slid forward in the seat pan with more recline of the seat back. This movement shifted the HJC more anterior and distal (forward and down) with respect to the HJC in the instructed position (Figure 51) and subsequently increased the HJC deflection in the preferred position (Table 11). The HJC deflections for subjects 7 and 8 differed by around 10 to17 mm in preferred position as those subjects choose a comparatively forward position in the seat pan.

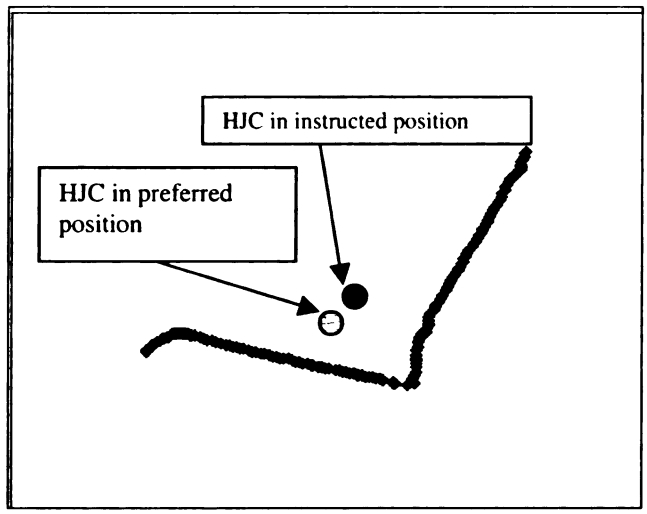

Figure 51: A magnified view of HJC locations in preferred and instructed positions. HJC in preferred position had a trend of being anterior and distal (forward and down) with respect to HJC locations in instructed position.

5.4.2 Comparison of HJC deflections for 95H95W male subjects.

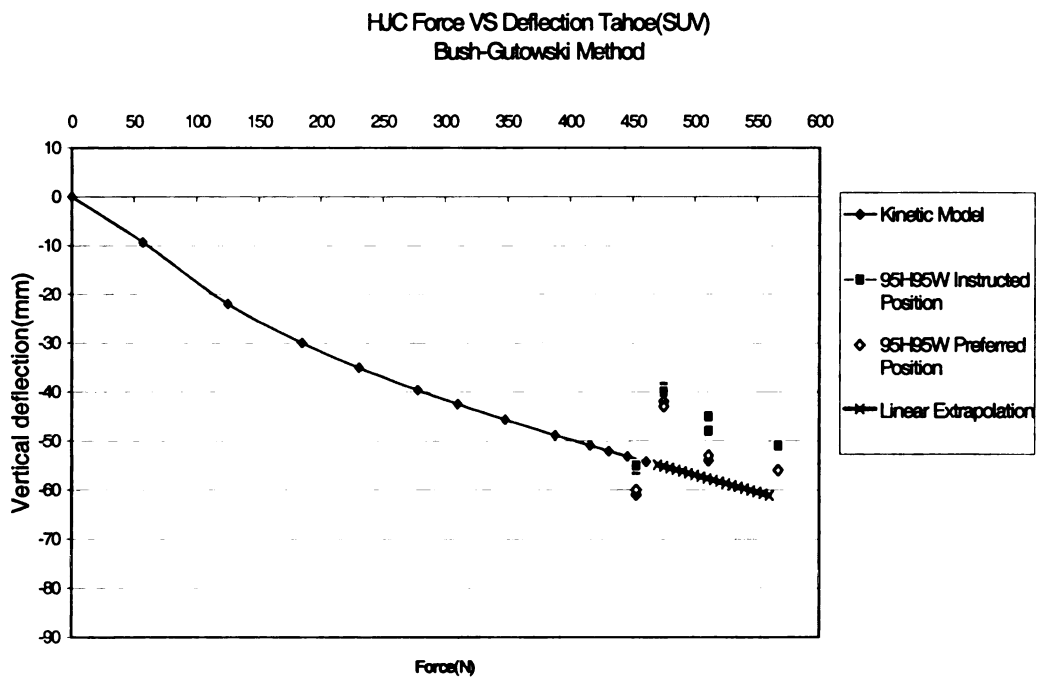

Figure 52: HJC force Vs. Deflection in preferred and instructed position for 95H95W male subjects in Tahoe seat.

The graph in Figure 52 shows the HJC deflection in preferred and instructed positions for tall and heavy males (95H95W) seated in the Tahoe seat. It can be seen that the kinetic model force deflection curve, based on 50th percentile manikin data does not extend to accommodate the HJC force and deflection for 95H95W category. It was proposed in the study by Bush and Macklem [3] that the HJC deflection for 95H95W category could be predicted by extrapolating the force deflection curve to reach loading values for large men. The force deflection curve for each seat was linearly extrapolated from of last two points of the curve till 550 N of HJC force to compare the HJC deflections of 95H95W subjects. The HJC deflection calculations for tall and heavy subjects in the present study were near the extended force deflection curve and supported the proposition by Bush and Macklem [3].

HJC vertical deflection for 95H95W males in Tahoe (SUV)				
	Instructed Position	Preferred Position		
Subject No(Trial No)	HJC vertical Deflection	HJC vertical Deflection	HJC vertical Deflection (Kinematic model)	HJC force(newtons)(54.3 %of bodyweight)
6(1)	56	61	51	453
6(2)	55	60	51	453
11(1)	39	42	52	475
11(2)	40	43	52	475
14(1)	45	54	53	511
14(2)	48	53	53	511
15(1)	51	56	55	567
16(1)	50	54	52	485
16(1)	48	53	52	485
Average	**48**	**53**	**52**	
Standard Deviation	**6**	**7**	**1**	

Table 12: HJC deflection comparison between preferred and instructed position for 95H95W male subjects in Tahoe seat.

The HJC deflections calculated were consistent within two trials of the same position for a particular subject in a particular seat (Table 12). Similar to the 50H50W category subjects, it was observed that, in most of the trials the HJC deflection in the preferred position was higher than that in the instructed position, without any large deviations in the HJC deflections between the two positions.

5.4.3 Comparison of HJC deflections for 95H5W male subjects.

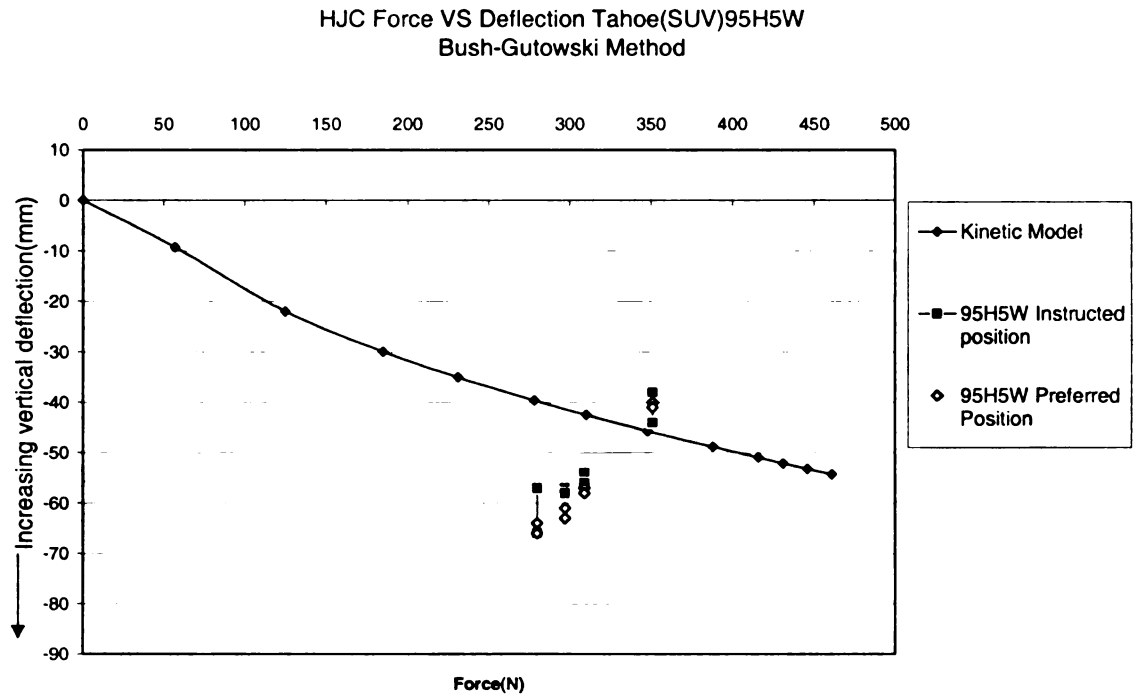

Figure 53: HJC force Vs. Deflection in preferred and instructed position for 95H5W male subjects in Tahoe seat.

The graph in Figure 53 shows the HJC deflection for tall and lightweight males (95H5W) in preferred and instructed positions seated in the Tahoe seat. It was observed that the difference between the HJC deflection in the preferred and instructed positions was small in most of the trials for all three seats (refer Appendix C). Also from the data of HJC deflection in Table 13 and Figure 45 it can be observed that there is large

deviation between the calculated HJC deflection and that predicted using the kinetic model. A large deviation in HJC deflections was observed consistently for the trials of 95H5W category subjects in all three seats. This observation lead to the conclusion that the force deflection curve obtained from the kinetic model needed a correction to reasonably predict the HJC deflections for occupants in 95H5W category.

HJC vertical deflection for 95H5W males in Tahoe (SUV)

	Instructed Position	Preferred Position		
Subject No(Trial No)	HJC vertical Deflection	HJC vertical Deflection	HJC vertical Deflection (Kinematic model- Directly from the chart)	HJC force(newtons)(54.3 %of bodyweight)
4(1)	54	57	36	309
4(2)	56	58	36	309
5(1)	57	64	35	280
5(2)	66	66	35	280
9(1)	44	40	45	351
9(2)	38	41	45	351
13(1)	57	61	46	297
13(2)	58	63	46	297
Average	**54**	**56**	**41**	
Standard Deviation	**9**	**10**	**5**	

Table 13: HJC deflection comparison between preferred and instructed position for 95H5W male subjects in Tahoe seat.

5.5 Comparison with Bush-Macklem [3] offset curves

In previous study by Bush and Macklem [3], an equation of a line offset to the force deflection curve of the Radcliffe kinetic model [6] was developed to reasonably predict the HJC deflection of male occupants of 95H5W group and of groups between the 95H5W and 50H50W. Bush and Macklem also proposed that the HJC deflections for the 95H95W male occupants would lie on the extended force deflection curve produced from the kinetic model.

To verify these propositions, the offset line equations that depended on the seat pan stiffness of each particular seat were developed for all three seats. The generalized offset equation developed by Bush and Macklem [3] was used to get the offset equation for seats in the present study. When using this method, the offset equation for a particular seat depended only on the force deflection data from the kinetic model and was independent of the calculated HJC deflections.

The HJC deflections for each category were averaged over all subjects in all trials and between instructed and preferred positions to get one average HJC deflection corresponding to each anthropometric category. The HJC forces for all subjects in each category were averaged and a single HJC force corresponding to each category was calculated. Deviations from the averaged value were represented by a standard deviation of $\pm$ 1 and were plotted as the error bands for each category. The force deflection curve was linearly extrapolated from last two points of the curve till 550 N of HJC force.

The results for each seat are discussed in the following text.

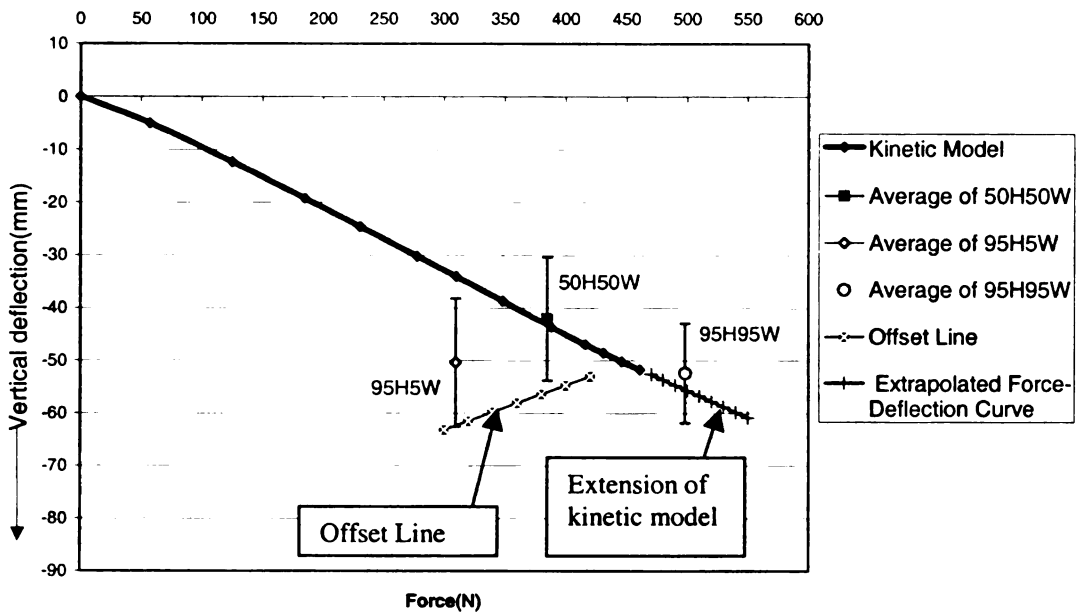

Figure 54: A plot showing offset line for SLK seat along with the extrapolated force deflection curve and averaged HJC deflections for each category with error bars of $\pm$ 1 standard deviation.

It can be observed from the graph in Figure 54 that for the SLK seat the HJC deflection error bands for the 95H5W category intersect with the offset line meaning the offset line predicted the HJC deflections within the error range for the 95H5W category. Also the offset line is just below the error range of HJC deflections for 50H50W category meaning the offset line did not predict the HJC deflection for 50H50W category in this seat. The extrapolated force-deflection line intersects with the error bands of 95H95W category meaning that the extrapolated line predicted the HJC deflection for 95H95W category.

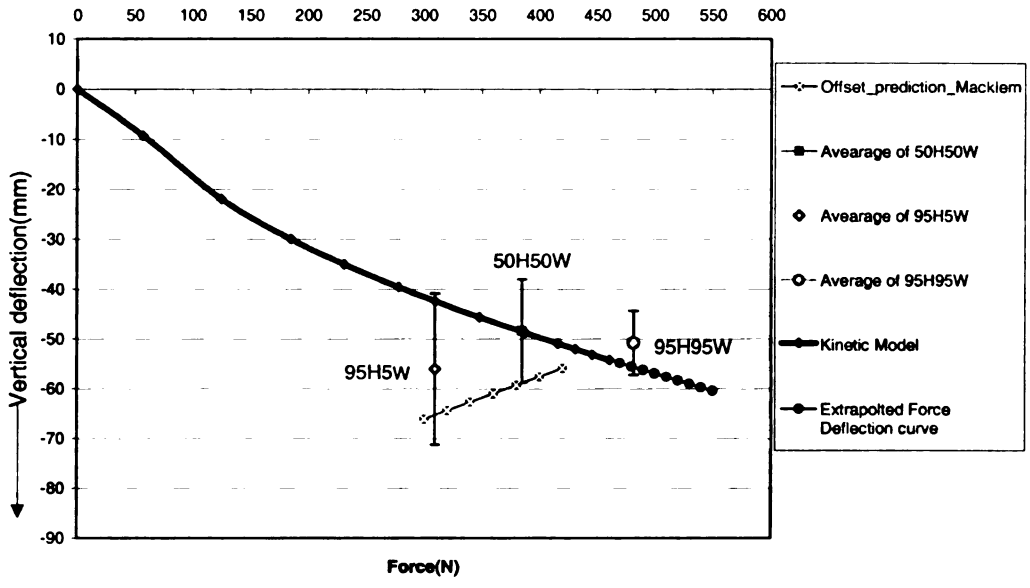

Figure 55: A plot showing offset line for Tahoe seat along with the extrapolated force deflection curve and averaged HJC deflections for each category with error bars of $\pm$ 1 standard deviation.

It can be observed from the graph in Figure 55 that for the Tahoe seat the HJC deflection error bands for the 95H5W and 50H50W categories intersect with the offset line meaning the offset line predicted the HJC deflections within the error range for both the groups. The extrapolated force-deflection line also intersects with the error bands of 95H95W category meaning that the extrapolated line predicted the HJC deflection for 95H95W category.

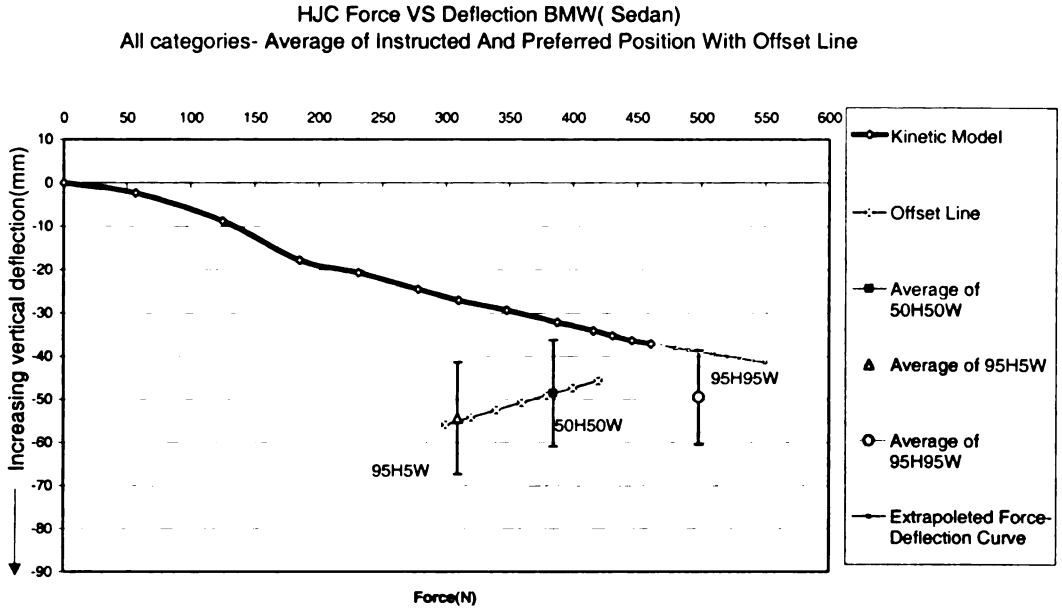

Figure 56: A plot showing offset line for BMW seat along with the extrapolated force deflection curve and averaged HJC deflections for each category with error bars.

As discussed in section 5.3, the BMW seat pan did not fully contacted the ASPECT butt thigh segment and therefore the force deflection curve developed from the kinetic model had a slope less than what it should had been. The offset line, which was based on the force deflection curve, would be shifted downwards than seen in Figure 56, if proper contact between the ABT and BMW seat pan had been established. Because of these facts, the HJC deflections were found much larger than that predicted by the kinetic model.

All the plots presented in this section were calculated based on Bush-Gutowski HJC computation method. Another set of graphs was plotted with HJC deflections obtained based on the method used by Gutowski and the Bush-Gutowski method together to study the difference between HJC obtained using the two methods. The HJC computations with these two methods are discussed below.

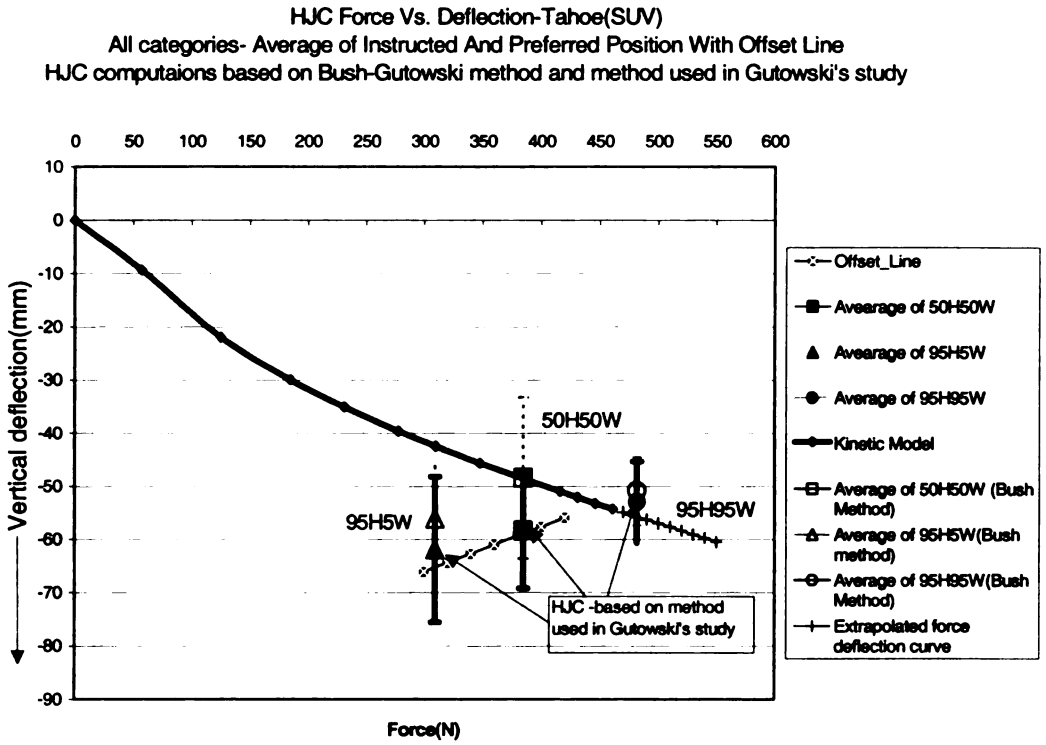

Figure 57:Comparison of HJC computations based on Bush-Gutowski method (legends in hollow) and method used in Gutowski's study (legends in solid) for Tahoe seat.

It can be seen from Figure 57 that the average HJC deflections computed based on the method used in Gutowski's study were larger than those computed based on Bush-Gutowski's method [12] for all three categories in Tahoe seat. A similar trend was observed for all categories in all three seats (Figure 58 and 59). It can also be noticed that the HJC deflections based on the method by Bush-Gutowski were closer to the force deflection curve obtained from the kinetic model than those based on the method used in Gutowski's study. The HJC computations based on Bush-Gutowaski method better represented the HJC location because fewer assumptions were used for computing HJC.

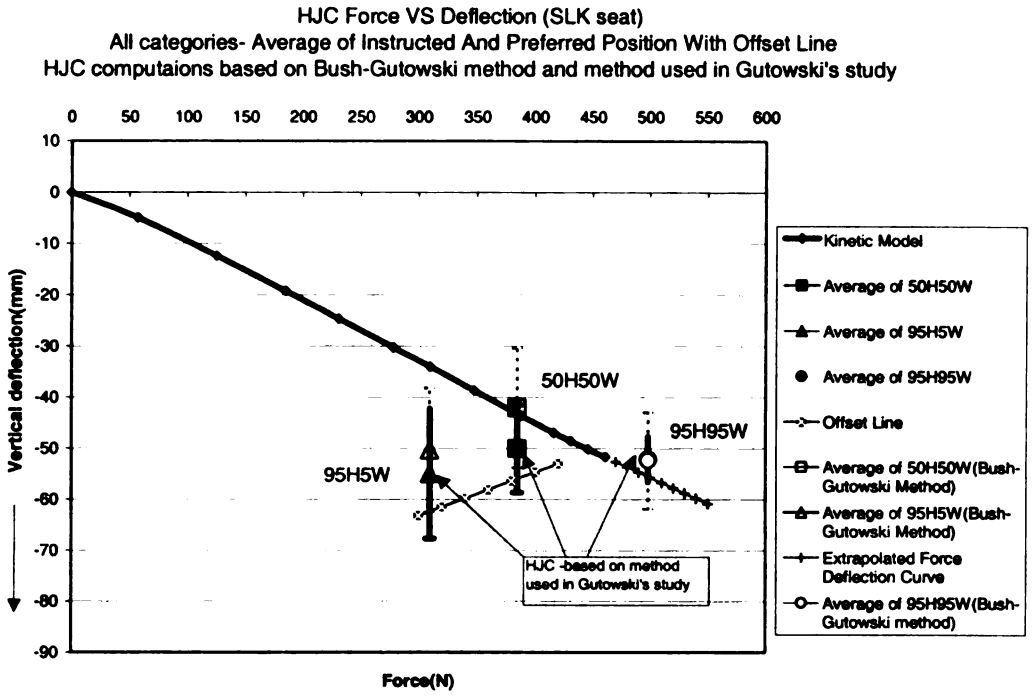

Figure 58:Comparison of HJC computations based on Bush-Gutowski method (legends in hollow) and method used in Gutowski's study (legends in solid) for SLK seat.

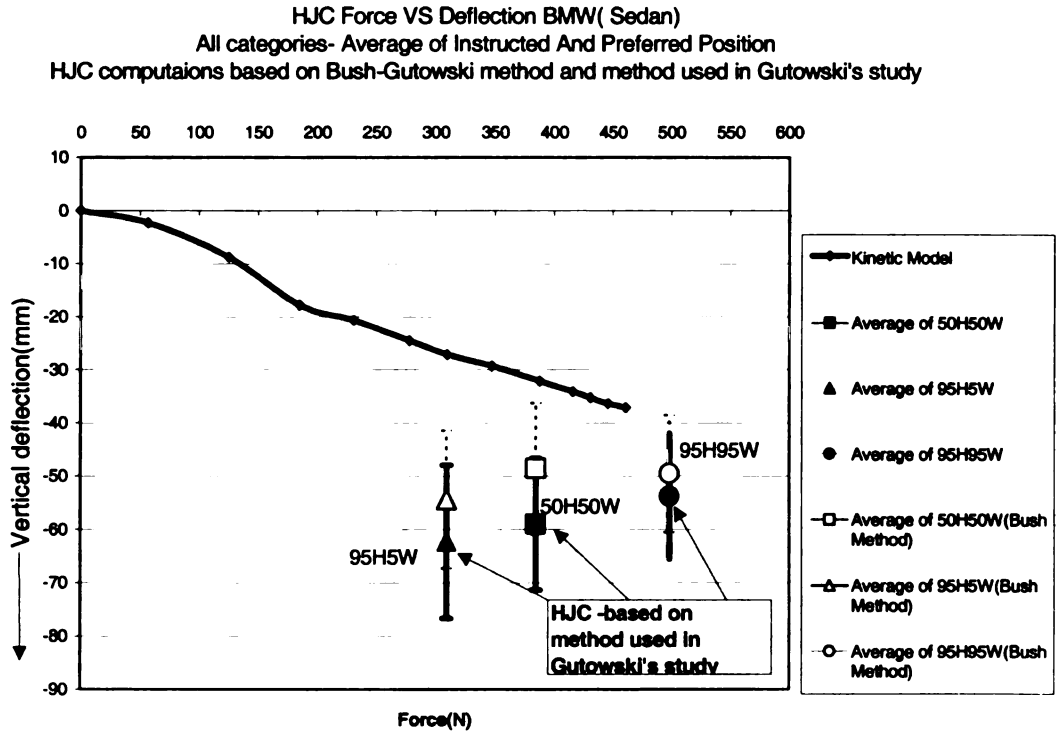

Figure 59:Comparison of HJC computations based on Bush-Gutowski method (legends in hollow) and method used in Gutowski's study (legends in solid) for BMW seat.

6. CONCLUSIONS

If the HJC locations of various anthropometric categories of people in automotive seats with varying stiffness could be predicted and put into mathematical form then it would aid in better ergonomic design of automotive interior packages. The goal of the present study was to verify and refine an existing method of HJC prediction.

In the previous study, Bush and Macklem [3] proposed offset equations dependent upon the kinetic model. This approach was used for reasonably predicting the HJC deflections of groups of males and females other than male occupants of average height and weight. In the present study only the offset equations for males were examined by experimentally calculating the HJC deflections of 15 male subjects and plotting them with the offset equations for comparison.

The HJCs were computed using both the method used in Gutowski's study and Bush-Gutowski method. The first conclusion of the present study was that the HJC calculations based on Bush-Gutowski's[15] method gave a better prediction of HJC location than the HJC calculations based on the method used in Gutowski's study. All the following conclusions made about the HJC location prediction for each of the three male categories were based on the HJC computation using Bush-Gutowski method [15].

The averaged HJC deflections of tall and heavy males (95H95W) in the SLK and Tahoe seats were close to the linearly extrapolated force deflection curve. The second conclusion of this study was that the proposition by Bush and Macklem that the averaged HJC deflection for 95H95W male group can be predicted by extrapolating the force deflection curve obtained from the kinetic model holds good for data in this study.

The averaged HJC deflections for the mid-male (50H50W) subjects were close to that predicted by the kinetic model, which supported the idea that the kinetic model alone can reasonably predict the HJC deflections of mid-male occupants. The third conclusion of this study was that only the force deflection curve from the kinetic model is sufficient enough to predict the HJC deflections of males in the 50H50W category and that the offset line is not needed for predicting HJC deflections of male occupants in this category.

The tall and light male (95H5W) category had significantly larger HJC deflections than those predicted by the force deflection curve. The HJC deflections for 95H5W males were close to or nearly intersected the offset line for that particular seat. Thus it was concluded that the offset equation for males developed by Bush and Macklem is able to predict the averaged HJC deflection for tall and light males for two seats in the present study. However the offset line equation is expected to predict the averaged HJC deflections of male occupants ranging from tall and light (95H5W) to mid-males (50H50W) and further study is necessary to verify this by testing occupants in that range.

In the preferred positions subjects regularly slid forward with more recline of the back making the HJC shift anterior and distal (forward and down) with respect to that in an instructed position where in they seated with their buttocks all the way back in the seat. The shifts in HJC location from instructed to preferred position were only a few millimeters causing the HJC deflection in preferred position to be consistently more by 5 to 15 mm than that in an instructed position.

It was observed from the HJC deflection data for the BMW seat that the 50^{th} percentile manikin does not conform to the seat cushion of stiff seats with prominent seat

pan bolsters and thus does not precisely represent the loading of 50H50W male occupant for such seats.

The offset line equation developed by Bush and Macklem [3] was based on the HJC location data for four seats in Gutowaski's study. Thus the offset line equation was based on HJC computations from the method used in Gutowski's study that is less precise in comparison with the Bush-Gutowski's method and this provided a scope for improvement in the offset line equation.

6.1 Future Work

The offset line for male occupants developed by Bush and Macklem [3] was able to predict the HJC deflections for males in tall and light category but it needs to be verified if the offset line can predict the HJC deflections for males in between the 95H5W(tall and light) and 50H50W(average height and weight) categories.

As discussed in section 5.3 the BMW seat did not make sufficient contact with the butt thigh segments of the ASPECT manikin. The experimental HJC deflection data, which did not correspond with the kinetic model for the BMW seat, initiated a challenge to investigate the applicability of ASPECT manikin to represent mid-male loading for stiff seats with prominent seat pan bolsters.

Bush and Macklem in their study proposed offset curves for male as well as female occupants, but in the present study only male offset equation was verified. The next steps would include the verification of female offset equation by experimental studies for female occupants.

APPENDIX A

SFS analysis –Phase I

Table A-1 SFS analysis to obtain H-point force Vs. H-point deflection for seat-A (Audi).

Seat A- Audi		H-pt	Knee					Models>>>		3rd Order			2nd Order			Linear		
Fh	**Fk**	**Avg (z,mm)**	**Avg (z,mm)**	**Thigh Ang**	**dzh**	**dzk**	**Def Ang**	**Rh(stat.)**	**Mh(stat.)**	**F(3rd)**	**M(3rd)**	**Error^2**	**F(2nd)**	**M(2nd)**	**Error^2**	**F(Lin.)**	**M(Lin.)**	**Error^2**
0	0	253.7	311.8	7.29	0.0	0.0	0.00	0	0	0	0	0.00E+00	0	0	0.00E+00	0	0	0.00E+00
57	29	251.3	264.7	1.68	2.4	47.0	-5.61	86	13276	85	13240	1.77E+00	94	14425	1.26E+02	41	14823	2.16E+03
125	29	231.1	279.4	6.06	22.6	32.4	-1.23	154	13208	161	10361	4.34E+02	138	10704	5.53E+02	195	17448	2.51E+03
185	29	221.1	287.6	8.34	32.6	24.2	1.06	214	13141	206	11005	2.81E+02	202	11605	2.47E+02	270	18423	4.46E+03
231	29	214.5	292.7	9.82	39.1	19.1	2.54	260	13087	253	12709	5.88E+01	261	13404	6.72E+00	320	19130	5.30E+03
278	29	208.5	297.5	11.21	45.2	14.2	3.92	307	13029	312	14975	2.09E+02	326	15555	6.69E+02	365	19727	5.53E+03
310	32	205.8	299.2	11.77	47.9	12.6	4.48	342	14348	348	17058	3.85E+02	361	17516	8.39E+02	386	20149	3.54E+03
348	26	202.4	305.5	13.01	51.3	6.3	5.72	374	11602	381	13193	1.68E+02	387	13090	2.78E+02	410	19395	4.20E+03
388	21	200.1	310.3	13.92	53.6	1.5	6.63	409	9336	404	9036	2.80E+01	401	8291	1.17E+02	426	18681	4.44E+03
416	28	198.2	311.3	14.29	55.4	0.5	7.00	444	12427	440	10899	1.30E+02	429	9854	5.30E+02	440	19008	2.08E+03
431	56	197.3	304.1	13.49	56.4	7.7	6.20	487	24941	492	25742	5.32E+01	486	25420	1.19E+01	451	21519	1.86E+03
446	83	196.8	298.1	12.78	56.9	13.7	5.49	529	37072	530	37124	1.64E+00	527	37300	5.26E+00	458	23535	1.38E+04
461	111	196.3	292.2	12.09	57.4	19.6	4.80	572	49711	567	47555	2.49E+02	565	48108	1.69E+02	464	25472	3.96E+04
												sum[E^2]			sum[E^2]			sum[E^2]
Notes:												2.00E+03			3.55E+03			8.94E+04
positive deflection is downward into the seat												RMS Error			RMS Error			RMS Error
H-point to Knee Length=				458	mm							4.07			5.41			27.19

Significance Magnification on M Calculation	10

Stiffness Matrices (transposed)

	F	M
x	4.22	-785.36
ang	-25.91	-6415.26

	F	M
x^2	0.02	41.29
ang^2	-1.65	-633.55

	F	M
x^3	0.00	0.01
ang^3	0.11	6.69

Stiffness Matrices (transposed)

	F	M
x	-0.02	-785.38
ang	-24.12	-6415.26

	F	M
x^2	0.22	42.10
ang^2	-1.36	-633.52

Stiffness Matrices (transposed)

	F	M
x	8.41	642.42
ang	-3.71	-2371.64

dzh	Def Ang	Error^2	dzh	Def Ang	Error^2	dzh	Def Ang	Error^2
0.0	0.0	1.82E-07	0.0	0.0	7.45E-06	0.0	0.0	1.61E-08
2.6	-5.5	2.52E-06	4.7	-4.5	2.94E-05	8.8	-3.2	1.74E-07
15.5	-5.0	5.09E-05	16.0	-6.5	4.44E-05	18.0	-0.7	1.31E-07
32.6	0.8	1.39E-05	33.4	1.1	1.03E-04	26.1	1.5	9.15E-08
39.9	2.7	1.11E-04	39.1	2.6	1.85E-04	32.4	3.2	1.15E-07
45.2	4.1	1.98E-05	44.1	3.9	5.40E-05	38.7	5.0	1.39E-07
48.1	4.8	2.04E-04	47.0	4.5	6.64E-05	43.2	5.6	1.85E-07
51.1	5.8	6.51E-06	50.6	5.6	9.13E-06	48.1	8.1	1.97E-07
53.8	6.7	1.16E-05	54.0	6.7	2.15E-05	53.3	10.5	2.00E-07
55.5	6.9	4.96E-05	56.0	7.0	2.26E-05	57.4	10.3	2.86E-07
56.2	6.2	4.71E-06	56.6	6.3	1.22E-05	60.5	5.9	6.72E-07
56.8	5.5	1.29E-04	57.1	5.6	1.30E-05	63.6	1.6	1.33E-06
57.3	4.8	3.60E-05	57.5	4.7	1.18E-05	66.8	-2.9	1.89E-06
		sum[E^2]			sum[E^2]			sum[E^2]
		6.40E-04			5.80E-04			5.42E-06
	RMS Error	0			0			0

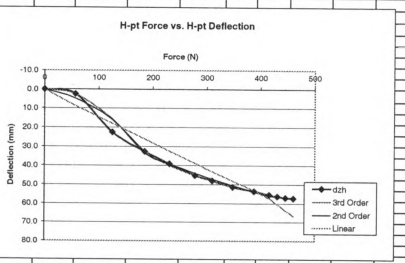

Table A-2 SFS analysis to obtain H-point force Vs. H-point deflection for seat B (Ford Ranger).

Seat B-Ranger		H-pt	Knee					Models>>>		3rd Order		2nd Order			Linear		
Fh	Fk	Avg (z,mm)	Avg (z,mm)	Thigh Ang	dzh	dzk	Def Ang	Rh(stat.)	Mh(stat.)	F(3rd)	M(3rd)	Error^2	F(2nd)	M(2nd)	Error^2	F(Lin.)	M(Lin.)	Error^2
0	0	301.4	376.9	9.49	0.0	0.0	0.00	0	0	0	0	0.00E+00	0	0	0.00E+00	0	0	0.00E+00
57	29	297.3	331.5	4.28	4.1	45.4	-5.21	86	13245	87	13319	1.17E+00	94	14083	1.01E+02	66	13566	3.88E+02
125	29	287.8	338.1	6.30	13.6	38.8	-3.19	154	13202	152	11697	1.12E+02	142	12001	2.23E+02	156	15473	2.48E+02
185	29	279.2	343.6	8.09	22.2	33.3	-1.40	214	13150	211	12156	5.47E+01	205	12315	1.22E+02	237	17306	1.35E+03
231	29	271.4	349.1	9.77	30.0	27.8	0.28	260	13090	273	13735	1.89E+02	275	13864	2.60E+02	309	18807	4.00E+03
278	29	268.0	352.5	10.63	33.4	24.4	1.15	307	13054	302	13603	3.80E+01	308	13728	2.20E+01	341	19196	2.94E+03
310	32	264.7	355.1	11.39	36.7	21.7	1.90	342	14367	336	14303	3.23E+01	343	14414	1.75E+00	372	19745	2.26E+03
348	26	261.0	359.7	12.45	40.4	17.1	2.96	374	11628	374	12500	3.64E+01	379	12677	6.55E+01	405	19895	4.20E+03
388	21	257.7	365.0	13.55	43.7	11.9	4.06	409	9350	409	8347	4.80E+01	407	8351	4.99E+01	434	19732	5.77E+03
416	28	255.8	364.9	13.78	45.6	12.0	4.29	444	12455	444	11807	2.02E+01	439	11762	5.24E+01	453	20485	3.15E+03
431	56	254.6	358.5	13.12	46.8	18.4	3.63	487	24979	489	25899	4.51E+01	487	25842	3.56E+01	468	22650	6.13E+02
446	83	253.5	353.0	12.55	47.9	23.9	3.06	529	37105	531	37803	2.61E+01	530	37720	1.90E+01	482	24553	9.69E+03
461	111	252.5	347.6	11.99	48.9	29.3	2.50	572	49730	570	48845	4.11E+01	570	48730	5.34E+01	495	26383	3.19E+04
												sum[E^2]			sum[E^2]			sum[E^2]
Notes:												6.45E+02			1.01E+03			6.65E+04
positive deflection is downward into the seat												RMS Error			RMS Error			RMS Error
H-point to Knee Length=				458 mm								2.31			2.88			23.44
												Stiffness Matrices (transposed)			**Stiffness Matrices (transposed)**			**Stiffness Matrices (transposed)**
Significance Magnification on M Calculation				10								F	M		F	M		F	M
												x	6.05	-997.02	x	3.68	-994.38	x	10.37	646.97
												ang	-23.34	-7768.80	ang	-22.64	-7772.78	ang	-4.67	-2099.93
													F	M		F	M			
												x^2	0.06	50.76	x^2	0.19	51.09			
												ang^2	-1.45	-868.33	ang^2	-1.54	-855.41			
													F	M						
												x^3	0.00	0.01						
												ang^3	0.15	2.67						

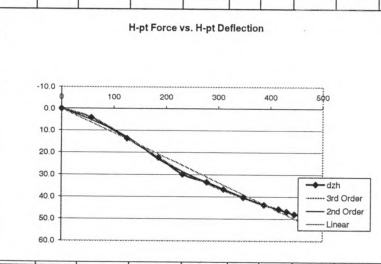

dzh	Def Ang	Error^2	dzh	Def Ang	Error^2	dzh	Def Ang	Error^2
0.0	0.0	6.74E-07	0.0	0.0	1.50E-08	0.0	0.0	1.92E-12
4.0	-5.3	6.62E-07	5.1	-3.7	1.51E-06	6.3	-4.4	3.89E-07
13.0	-4.3	8.56E-01	12.9	-5.0	4.37E-06	14.0	-2.0	1.52E-07
22.1	-1.6	2.37E-06	23.1	-1.3	2.04E-06	20.7	0.1	3.82E-08
28.6	0.0	2.34E-07	28.5	0.0	3.71E-08	25.9	1.7	6.07E-09
34.1	1.4	2.82E-06	33.5	1.2	6.90E-06	31.1	3.4	1.74E-08
37.2	2.0	4.12E-06	36.6	1.9	4.84E-06	34.7	3.9	2.54E-08
40.5	3.1	7.46E-06	40.1	3.0	3.29E-06	39.0	6.5	1.61E-07
43.5	4.0	1.29E-06	43.6	4.0	2.72E-06	43.5	8.9	6.46E-07
45.5	4.2	3.72E-06	45.9	4.3	3.44E-06	46.6	8.4	4.02E-07
46.8	3.7	2.80E-06	46.9	3.7	5.34E-06	48.3	3.0	5.43E-09
47.9	3.1	3.11E-06	47.9	3.1	5.85E-06	50.0	-2.3	2.74E-07
48.9	2.4	5.99E-06	48.9	2.4	1.05E-05	51.7	-7.8	3.09E-07
		sum[E^2]			sum[E^2]			sum[E^2]
		8.56E-01			5.08E-05			2.43E-06
	RMS Error	0.08			0			0

Table A-3 SFS analysis to obtain H-point force Vs. H-point deflection for seat-C (Mercedes-SLK).

Seat C- SLK		*H-pt*	*Knee*					*Models>>>*		*3rd Order*			*2nd Order*			*Linear*		
Fh	**Fk**	**Avg (z,mm)**	**Avg (z,mm)**	**Thigh Ang**	**dzh**	**dzk**	**Def Ang**	**Rh(*stat.*)**	**Mh(*stat.*)**	**F(*3rd*)**	**M(*3rd*)**	**Error^2**	**F(*2nd*)**	**M(*2nd*)**	**Error^2**	**F(*Lin.*)**	**M(*Lin.*)**	**Error^2**
0	0	166 6	266 8	12 64	0 0	0 0	0 00	0	0	0	0	0 00E+00	0	0	0 00E+00	0	0	0 00E+00
57	29	161 6	227 4	8 27	5 0	39 4	-4 37	86	13144	87	14035	3 83E+01	92	14586	1 31E+02	88	12646	1 77E+01
125	29	153 9	230 5	9 63	12 7	36 3	-3 01	154	13095	156	11929	7 06E+01	154	12177	4 02E+01	160	14956	1 96E+02
185	29	148 5	233 2	10 65	18 1	33 6	-1 99	214	13053	205	11709	1 70E+02	201	11895	2 45E+02	210	16473	5 76E+02
231	29	141 2	238 9	12 32	25 4	27 9	-0 32	260	12976	267	11903	9 78E+01	264	12141	5 19E+01	276	17951	1 43E+03
278	29	136 3	242 3	13 38	30 3	24 5	0 74	307	12921	308	13156	4 23E+00	309	13465	1 70E+01	319	19011	1 92E+03
310	32	131 9	245 9	14 41	34 7	20 9	1 77	342	14195	346	14599	2 73E+01	349	14941	8 04E+01	359	19848	1 81E+03
348	26	128 3	251 7	15 63	38 3	15 1	2 99	374	11468	371	13211	1 57E+02	375	13471	1 93E+02	388	19700	3 42E+03
388	21	123 4	261 6	17 55	43 1	5 2	4 91	409	9170	402	8806	5 74E+01	404	8552	4 54E+01	425	18959	4 83E+03
416	28	119 8	264 5	18 42	46 8	2 3	5 78	444	12167	442	10779	9 81E+01	438	10094	2 44E+02	458	19619	2 83E+03
431	56	117 3	255 2	17 53	49 3	11 6	4 89	487	24457	499	26784	4 10E+02	498	26584	3 45E+02	492	23217	9 65E+01
446	83	116 1	247 4	16 66	50 5	19 4	4 02	529	36419	536	38080	1 79E+02	536	38205	2 00E+02	511	25827	5 68E+03
461	111	115 6	241 3	15 94	51 0	25 5	3 30	572	48884	560	45756	6 16E+02	559	46062	5 39E+02	522	27703	2 39E+04
												sum[E^2]			sum[E^2]			sum[E^2]
Notes:												1 93E+03			2 13E+03			4 67E+04
positive deflection is downward into the seat												RMS Error			RMS Error			RMS Error
H-point to Knee Length=				458	mm							3 99			4 20			19 64
										Stiffness Matrices (transposed)			**Stiffness Matrices (transposed)**			**Stiffness Matrices (transposed)**		
Significance Magnification on M Calculation				10							F	M		F	M		F	M
										x	8 51	-523 98	x	8 33	-524 76	x	10 74	679 75
										ang	-17 55	-5545 26	ang	-14 75	-5544 78	ang	-7 84	-2110 91
											F	M		F	M			
										x^2	0 06	36 19	x^2	0 07	36 77			
										ang^2	-1 23	-416 01	ang^2	-0 88	-415 12			
											F	M						
										x^3	0.00	0.01					0	
										ang^3	0.13	6.33						
										dzh	Def Ang	**Error^2**	dzh	Def Ang	**Error^2**	dzh	Def Ang	**Error^2**
										0 0	0 0	7 25E-07	0 0	0 0	3 96E-07	0 0	0 0	8 37E-12
										9 6	-7 9	6 56E-05	5 0	-3 7	3 43E-04	4 5	-4 8	2 22E-07
										12 1	-3 5	8 48E-05	12 4	-3 4	2 34E-04	12 8	-2 1	2 26E-07
										18 7	-2 2	2 45E-06	19 2	-2 0	3 15E-05	20 1	0 3	3 12E-07
										24 2	-0 8	3 11E-06	24 7	-0 7	4 88E-05	25 8	2 2	4 16E-07
										30 2	0 8	1 48E-05	30 2	0 8	1 12E-04	31 5	4 0	5 04E-07
										34 3	1 7	5 11E-06	34 0	1 7	8 90E-05	35 2	4 6	7 08E-07
										39 3	3 5	1 33E-06	38 7	3 4	1 91E-05	40 3	7 6	5 00E-07
										43 8	5 1	7 17E-06	43 6	5 0	1 20E-05	45 6	10 3	4 92E-07
										46 8	5 6	1 29E-05	47 0	5 6	8 28E-06	48 5	9 9	6 00E-07
										48 6	4 9	3 66E-05	48 6	4 9	1 94E-05	48 2	3 9	1 35E-06
										50 2	4 1	1 05E-05	50 2	4 1	1 20E-04	47 9	-1 8	3 74E-07
										51 5	3 1	2 83E-06	51 7	3 2	1 69E-04	47 5	-7 9	2 01E-06
												sum[E^2]			sum[E^2]			sum[E^2]
												2 48E-04			1 21E-03			7 72E-06
											RMS Error	0			0 01			0

H-pt Force vs. H-pt Deflection

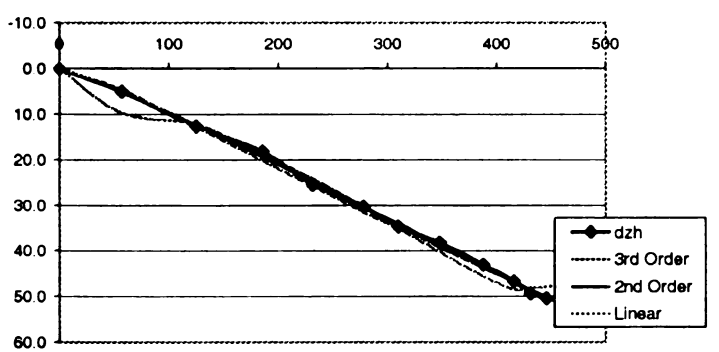

Table A-4 SFS analysis to obtain H-point force Vs. H-point deflection for seat-D (Chevy-Tahoe-cloth trim).

Seat D- Tahoe(Cloth)		*H-pt*	*Knee*					*Models>>>*		*3rd Order*			*2nd Order*			*Linear*		
Fh	**Fk**	**Avg (z,mm)**	**Avg (z,mm)**	**Thigh Ang**	**dzh**	**dzk**	**Def Ang**	**Rh(stat.)**	**Mh(stat.)**	**F(3rd)**	**M(3rd)**	**Error^2**	**F(2nd)**	**M(2nd)**	**Error^2**	**F(Lin.)**	**M(Lin.)**	**Error^2**
0	0	256.2	301.4	5.67	0.0	0.0	0.00	0	0	0	0	0.00E+00	0	0	0.00E+00	0	0	0.00E+00
57	29	246.7	277.3	3.83	9.5	24.1	-1.84	86	13252	85	14312	5.44E+01	88	14313	5.67E+01	89	20476	2.56E+03
125	29	230.4	286.6	7.05	25.8	14.8	1.39	154	13182	156	12925	5.51E+00	151	12918	1.43E+01	199	20103	4.28E+03
165	29	220.5	293.0	9.11	35.7	8.4	3.45	214	13114	210	12556	2.79E+01	208	12551	4.68E+01	264	19259	4.32E+03
231	29	212.5	298.2	10.78	43.7	3.2	5.11	260	13048	266	12789	3.88E+01	267	12779	5.50E+01	317	18574	4.71E+03
278	29	207.9	300.7	11.69	48.3	0.7	6.02	307	13007	305	13587	2.18E+01	307	13572	1.52E+01	348	18442	3.07E+03
310	32	203.9	303.1	12.50	52.2	-1.7	6.84	342	14308	341	14153	2.61E+00	344	14127	3.82E+00	374	18162	1.75E+03
348	26	200.2	307.0	13.50	56.0	-5.6	7.83	374	11579	374	12578	4.76E+01	376	12524	4.65E+01	398	16718	1.82E+03
388	21	196.0	312.9	14.78	60.1	-11.5	9.11	409	9300	410	8361	4.32E+01	409	8241	5.36E+01	422	13993	1.22E+03
416	28	193.9	311.9	14.93	62.3	-10.5	9.27	444	12391	442	12055	9.20E+00	440	11947	2.95E+01	438	15448	4.78E+02
431	56	192.1	303.9	14.13	64.1	-2.5	8.46	487	24872	489	25910	5.71E+01	489	25902	5.49E+01	458	21881	1.25E+03
446	83	190.8	296.9	13.40	65.4	4.5	7.74	529	36979	529	37371	7.38E+00	529	37439	1.03E+01	474	27366	7.41E+03
461	111	189.4	289.8	12.67	66.8	11.6	7.00	572	49601	571	48764	3.42E+01	571	48901	2.54E+01	490	32953	1.99E+04
												sum[E^2]			sum[E^2]			sum[E^2]
Notes:												3.50E+02			4.14E+02			5.27E+04
positive deflection is downward into the seat												RMS Error			RMS Error			RMS Error
H-point to Knee Length=				458	mm							1.70			1.85			20.86
Significance Magnification on M Calculation=				10														

Stiffness Matrices (transposed)

	F	M
x	4.41	363.24
ang	-20.96	-5635.37

	F	M
x^2	0.11	18.03
ang^2	-1.39	-328.18

	F	M
x^3	0.00	0.00
ang^3	0.10	0.42

Stiffness Matrices (transposed)

	F	M
x	4.49	363.24
ang	-20.60	-5635.37

	F	M
x^2	0.10	17.97
ang^2	-0.23	-327.94

Stiffness Matrices (transposed)

	F	M
x	8.07	1078.08
ang	-6.84	-5577.88

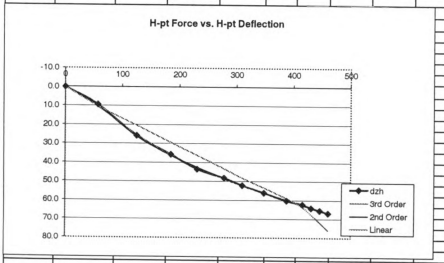

dzh	Def Ang	Error^2	dzh	Def Ang	Error^2	dzh	Def Ang	Error^2	dzh	Def Ang	Error^2
0.0	0.0	4.41E-07	0.0	0.0	6.02E-08	0.0	0.0	2.13E-11			
10.6	-1.4	2.01E-07	10.2	-1.5	2.92E-04	10.3	-0.4	3.30E-07			
25.3	1.2	1.37E-04	26.3	1.4	2.71E-04	20.4	1.6	7.56E-08			
36.0	3.4	7.31E-05	36.3	3.5	9.32E-04	29.4	3.3	1.15E-07			
42.8	4.9	9.05E-05	42.7	4.9	4.06E-04	36.2	4.7	3.64E-07			
48.7	6.2	1.30E-04	48.4	6.1	1.07E-04	43.2	6.0	8.02E-07			
52.3	6.8	2.76E-05	52.0	6.8	2.10E-04	48.2	6.7	1.08E-06			
56.3	8.0	3.65E-05	56.0	7.9	1.79E-05	53.4	8.3	1.74E-06			
59.9	9.0	3.14E-05	60.0	9.0	7.74E-05	59.1	9.7	2.12E-06			
62.4	9.3	3.73E-06	62.6	9.3	1.10E-04	63.7	10.1	2.64E-06			
64.0	8.5	7.26E-05	64.1	8.6	1.09E-04	67.8	8.6	2.30E-06			
65.5	7.8	8.32E-06	65.5	7.8	2.20E-04	71.8	7.2	1.35E-06			
66.7	6.9	2.90E-05	66.8	6.9	7.38E-05	75.8	5.8	4.65E-07			
		sum[E^2]			sum[E^2]			sum[E^2]			
		6.41E-04			2.83E-03			1.34E-05			
	RMS Error	0			0.02			0			

Table A-5 SFS analysis to obtain H-point force Vs. H-point deflection for seat-E (Chevy-Tahoe-leather trim).

Seat E-Tahoe(Leather)		*H-pt*	*Knee*					*Models>>>*		*3rd Order*			*2nd Order*			*Linear*		
Fh	**Fk**	**Avg (z,mm)**	**Avg (z,mm)**	**Thigh Ang**	**dzh**	**dzk**	**Def Ang**	**Rh(stat.)**	**Mh(stat.)**	**F(3rd)**	**M(3rd)**	**Error^2**	**F(2nd)**	**M(2nd)**	**Error^2**	**F(Lin.)**	**M(Lin.)**	**Error^2**
0	0	272.9	340.1	8.44	0.0	0.0	0.00	0	0	0	0	0.00E+00	0	0	0.00E+00	0	0	0.00E+00
57	29	265.1	300.7	4.45	7.8	39.4	-3.98	86	13242	87	13663	1.05E+01	89	14725	1.12E+02	70	17106	9.80E+02
125	29	252.1	308.7	7.10	20.9	31.4	-1.34	154	13180	152	13908	2.94E+01	149	13761	4.52E+01	185	18208	2.14E+03
185	29	244.1	313.9	8.77	28.8	26.2	0.33	214	13127	212	14074	4.87E+01	206	13794	8.63E+01	254	18690	3.09E+03
231	29	235.4	321.2	10.79	37.5	18.9	2.36	260	13047	277	12651	3.06E+02	283	12419	5.48E+02	331	18642	6.49E+03
278	29	233.4	322.3	11.20	39.5	17.8	2.76	307	13029	302	13039	2.50E+01	306	12817	4.22E+00	349	18842	3.35E+03
310	32	230.8	324.5	11.80	42.2	15.6	3.37	342	14346	329	12610	3.15E+02	334	12363	2.59E+02	372	18832	1.83E+03
348	26	227.1	327.3	12.64	45.9	12.8	4.20	374	11620	374	12341	2.51E+01	377	11999	1.51E+01	404	18897	3.43E+03
388	21	224.0	331.6	13.58	48.9	8.5	5.14	409	9349	413	8695	3.35E+01	407	7997	9.14E+01	431	18186	4.19E+03
416	28	222.2	330.9	13.73	50.7	9.2	5.29	444	12458	445	12167	5.08E+00	439	11538	6.70E+01	447	18990	2.04E+03
431	56	220.7	323.5	12.97	52.2	16.6	4.54	487	24993	485	26919	1.81E+02	493	27028	2.29E+02	460	22232	1.10E+03
446	83	219.7	317.8	12.37	53.2	22.3	3.93	529	37132	526	37862	3.62E+01	532	38427	8.90E+01	469	24723	1.09E+04
461	111	219.0	311.8	11.69	54.0	28.3	3.25	572	49784	576	48343	1.14E+02	567	49260	4.13E+01	476	27239	3.35E+04
												sum[E^2]			sum[E^2]			sum[E^2]
Notes:												1.13E+03			1.59E+03			7.30E+04
positive deflection is downward into the seat												RMS Error			RMS Error			RMS Error
H-point to Knee Length=				458	mm							3.06			3.62			24.57
										Stiffness Matrices (transposed)			**Stiffness Matrices (transposed)**			**Stiffness Matrices (transposed)**		
Significance Magnification on M Calculation=				10							F	M		F	M		F	M
										x	-21.89	-494.91	x	2.21	-484.23	x	8.83	683.35
										ang	-85.80	-6987.71	ang	-19.67	-6992.49	ang	-0.23	-2959.67
											F	M		F	M			
										x^2	1.45	38.12	x^2	0.18	36.36			
										ang^2	-4.45	-745.27	ang^2	-1.12	-728.73			
											F	M						
										x^3	-0.01	-0.04					0	
										ang^3	1.50	12.43						
										dzh	Def Ang	**Error^2**	dzh	Def Ang	**Error^2**	dzh	Def Ang	**Error^2**
										0.0	0.0	6.15E-06	0.0	0.0	2.42E-06	0.0	0.0	3.63E-13
										7.3	-4.1	8.60E-01	9.3	-3.1	1.37E-03	9.7	-2.2	2.36E-07
										22.5	-0.9	9.49E-03	22.0	-1.0	6.71E-05	17.4	-0.4	2.21E-07
										30.4	0.8	6.64E-04	30.0	0.7	1.59E-04	24.3	1.2	2.33E-07
										35.5	1.9	3.06E-05	35.1	1.8	2.72E-04	29.5	2.4	2.60E-07
										40.0	2.9	5.08E-04	39.6	2.8	1.51E-04	34.9	3.6	2.99E-07
										42.4	3.3	5.64E-04	42.5	3.3	1.25E-04	38.8	4.1	3.73E-07
										46.0	4.3	2.75E-04	45.7	4.2	8.35E-05	42.5	5.9	2.98E-07
										48.6	5.0	5.99E-05	48.8	5.0	1.02E-04	46.5	7.6	2.12E-07
										50.6	5.3	2.06E-04	50.9	5.3	1.50E-04	50.5	7.4	3.25E-07
										53.0	4.9	1.74E-04	52.1	4.7	1.07E-04	55.2	4.3	8.97E-07
										57.1	5.0	4.48E-04	53.2	4.0	1.03E-04	59.9	1.3	7.50E-08
										55.7	3.6	1.46E-03	54.3	3.3	2.50E-04	64.7	-1.9	1.08E-06
												sum[E^2]			sum[E^2]			sum[E^2]
												8.73E-01			2.95E-03			4.51E-06
											RMS Error	0.08			0.02			0

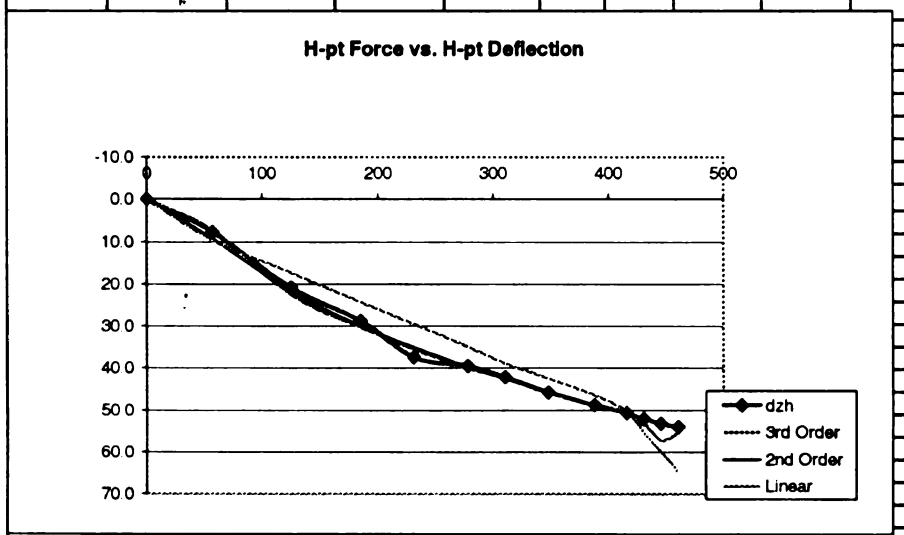

Table A-6 SFS analysis to obtain H-point force Vs. H-point deflection for seat F (BMW).

Seat F- BMW | H-pt | Proj.Knee | Models>>> | 3rd Order | 2nd Order | Linear

Fh	Fk	Avg (z,mm)	(z,mm)	Thigh Ang	dzh	dzk	Def Ang	Rh(stat.)	Mh(stat.)	F(3rd)	M(3rd)	Error^2	F(2nd)	M(2nd)	Error^2	F(Lin.)	M(Lin.)	Error^2
0	0	259.8	242.1	-2.21	0.0	0.0	0.00	0	0	0	0	0.00E+00	0	0	0.00E+00	0	0	0.00E+00
57	29	256.7	294.7	4.77	3.2	-52.6	6.98	86	11097	86	11845	2.27E-02	93	11845	4.90E+01	36	1112	2.48E+03
125	29	249.6	296.4	6.12	10.2	-56.2	8.33	154	11073	156	10018	5.03E+00	146	10047	6.22E+01	134	5554	4.01E+02
185	29	244.1	302.2	7.28	15.7	-60.0	9.49	214	11046	208	10025	4.15E+01	200	10081	1.92E+02	209	8958	2.38E+01
231	29	238.4	306.6	8.56	21.4	-64.5	10.78	260	11012	267	11237	4.82E+01	268	11310	6.92E+01	288	12518	7.75E+02
278	29	235.0	309.7	9.40	24.8	-67.6	11.61	307	10987	307	11952	1.95E-02	313	12021	3.31E+01	334	14623	7.56E+02
310	32	232.3	312.6	10.09	27.5	-70.4	12.30	342	12098	341	12217	4.55E-01	349	12273	4.51E+01	371	16262	8.37E+02
348	26	229.9	316.0	10.84	29.9	-73.9	13.05	374	9806	373	11006	1.28E+00	379	11040	2.11E+01	404	17721	8.74E+02
386	21	227.4	321.3	11.82	32.4	-79.2	14.04	409	7893	404	6492	2.83E+01	402	6488	4.52E+01	437	19215	8.07E+02
416	28	225.5	321.5	12.08	34.2	-79.3	14.29	444	10514	444	10010	2.72E-02	439	9981	2.73E+01	462	20358	3.38E+02
431	56	224.3	316.9	11.66	35.5	-74.8	13.87	487	21060	494	21781	4.83E+01	491	21740	1.53E+01	481	21261	3.54E+01
446	83	223.5	312.2	11.17	36.3	-70.1	13.38	529	31269	534	32557	2.51E+01	533	32511	1.81E+01	493	21871	1.28E+03
461	111	222.9	308.7	10.80	37.0	-66.6	13.02	572	41868	565	40406	5.20E+01	565	40354	5.09E+01	503	22344	4.79E+03
												sum[E^2]			sum[E^2]			sum[E^2]
												2.50E+02			6.29E+02			1.34E+04
												RMS Error			RMS Error			RMS Error
												4.39			6.95			32.10

Notes: SFS and Contents © 2001 Nathan Radcliffe

positive deflection is downward into the seat

H-point to ASPECT front = 384

H-point to Knee Length= 458

H-point to Thigh L.C. Length= 235

Stiffness Matrices (transposed)

	F	M
x	13.31	-179.57
ang	26.88	7195.45

	F	M
x^2	-0.13	63.20
ang^2	-3.34	-789.33

	F	M
x^3	0.01	0.01
ang^3	0.06	0.04

Stiffness Matrices (transposed)

	F	M
x	5.13	-179.55
ang	27.58	7195.46

	F	M
x^2	0.31	63.72
ang^2	-2.44	-789.15

Stiffness Matrices (transposed)

	F	M
x	14.01	652.24
ang	-1.14	-135.24

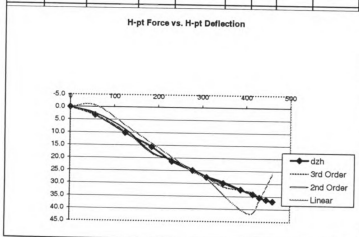

dzh	Def Ang	Error^2
0.0	0.0	3.20E-07
3.3	7.2	5.42E-08
9.7	8.0	1.07E-06
18.2	-0.9	5.64E-07
20.8	10.6	7.16E-07
25.0	11.7	1.03E-06
27.6	12.3	9.64E-07
31.2	-6.3	4.40E+04
32.5	14.0	1.10E-06
33.4	-7.7	1.17E+05
35.2	13.8	2.90E-06
36.2	13.4	2.40E-06
37.1	13.0	3.74E-06
		sum[E^2]
		1.61E+05

dzh	Def Ang	Error^2
0.0	0.0	2.75E-09
4.7	2.3	1.43E+02
8.8	5.7	3.29E+02
17.8	0.5	5.14E+02
20.7	10.6	1.02E+00
24.5	11.6	1.05E+00
27.1	12.2	1.30E+00
29.4	-6.3	5.62E+04
32.2	13.8	1.47E+01
34.1	-6.9	4.80E+04
35.3	13.8	1.14E+00
36.4	13.5	2.61E+00
37.1	13.0	1.38E-01
		sum[E^2]
		1.05E+05

dzh	Def Ang	Error^2
0.0	0.0	5.32E-10
-0.9	-86.2	1.39E-07
7.1	-47.4	2.62E-07
14.2	-13.1	5.00E-07
19.6	13.3	9.20E-07
25.2	40.2	1.74E-06
28.2	46.5	2.19E-06
34.2	92.5	6.63E-07
40.2	135.5	9.67E-07
41.7	123.5	3.28E-06
39.4	19.7	5.58E-06
31.2	-80.6	9.51E-06
25.8	-185.1	1.74E-05
		sum[E^2]
		4.32E-05

APPENDIX-B

Manual measurements of H-point vertical and horizontal deflection -Phase I.

Table B1: Seat A-Audi, manual measurements of H-point vertical deflection.

H-point Load	Distance from lab floor(mm)	Verical Deflection(mm)
0	306	0
57	305	2
125	287	20
185	277	30
231	271	36
278	265	41
310	262	44
348	260	46
388	260	47
416	257	49
431	256	51
446	250	56
461	248	58

Table B2: Seat B-Ranger, manual measurements of H-point vertical deflection.

H-point Load	Distance from lab floor(mm)	Verical Deflection(mm)
0	481	0
57	478	3
125	467	15
185	460	22
231	452	30
278	448	33
310	446	35
348	444	38
388	440	41
416	439	42
431	439	42
446	438	43
461	438	44

Table B3: Seat C-SLK, manual measurements of H-point vertical deflection.

H-point Load	Distance from lab floor(mm)	Verical Deflection(mm)
0	342	0
57	336	6
125	329	13
185	324	18
231	319	23
278	314	28
310	309	33
348	306	36
388	301	41
416	296	46
431	295	47
446	294	48
461	293	49

Table B4: Seat D-Tahoe (Cloth), manual measurements of H-point vertical deflection.

H-point Load	Distance from lab floor(mm)	Verical Deflection(mm)
0	355	0
57	348	7
125	329	26
185	320	35
231	313	42
278	306	49
310	300	55
348	299	56
388	295	60
416	290	65
431	291	64
446	289	66
461	288	67

Table B5: Seat A-Audi, manual measurements of H-point horizontal deflection.

H-point Load	Distance from seat referece(mm)	Horizontal Deflection(mm)
0	87	0
57	70	17
125	62	25
185	68	19
231	66	21
278	66	21
310	64	23
348	61	26
388	61	26
416	59	28
431	59	28
446	60	27
461	61	26

Table B 6: Seat C-SLK, manual measurements of H-point horizontal deflection.

H-point Load	Distance from seat reference (mm)	Horizontal Deflection(mm)
0	105	0
57	93	12
125	90	15
185	90	15
231	90	15
278	89	16
310	87	18
348	87	18
388	85	20
416	85	20
431	84	21
446	83	22
461	82	23

Table B 7: Seat D-Tahoe (Cloth), manual measurements of H-point horizontal deflection.

H-point load	Distance from seat reference(mm)	Horizontal deflection(mm)
0	132	0
57	103	29
125	98	34
185	96	36
231	94	38
278	91	41
310	91	41
348	91	41
388	91	41
416	89	43
431	89	43
446	89	43
461	89	43

Table B 8: Seat E-Tahoe (Leather), manual measurements of H-point horizontal deflection.

H-point Load	Distance from seat referece(mm)	Horizontal Deflection(mm)
0	102	0
57	81	21
125	78	24
185	78	24
231	76	26
278	74	28
310	71	31
348	70	32
388	68	34
416	66	36
431	66	36
446	67	35
461	67	35

APPENDIX –C
Experimental data-Phase III

Table C1: HJC experimental data for 50H50W category in BMW seat with HJC calculated using method used by Gutowski.

HJC vertical deflection for 50H50W in BMW sedan								
					Instructed Position	Preferred Position		
Subject No(Trial No)	Seat Back angle wrt buck rear(Instructed Position)(°)	Seat Back angle wrt buck rear(Preferred Position)(°)	X_HJC Instructed position(Gutowski method)(mm)	X_HJC Preferred position(Gutowski method)(mm)	HJC vertical Deflection (Gutowski method)(mm)	HJC vertical Deflection (Gutowski method)(mm)	HJC vertical Deflection (Kinematic model-Directly from chart)(mm)	HJC force(N)(54.3%of bodyweight)
1(1)	60	53	-265	-248	40	47	35	420
1(2)	60	53	-258	-260	41	46	35	420
2(1)	60	50	-267	-239	58	80	27	347
2(2)	60	50	-255	-244	63	82	27	347
7(1)	62	58	-253	-251	50	60	29	375
7(2)	62	58	-248	-253	49	58	29	375
8(1)	62	58	-292	-299	63	67	30	377
8(2)	62	57	-295	-307	64	75	30	377
10(1)	58	56	-243	-268	51	65	35	413
12(1)	61	53	-311	-246	53	68	30	377
				Average	53	65	31	
				Standard Deviation	9	12	3	

Table C 2: HJC experimental data for 50H50W category in BMW seat with HJC calculated using Bush-Gutowski method.

HJC vertical deflection for 50H50W in BMW sedan								
					Instructed Position	Preferred Position		
Subject No(Trial No)	Seat Back angle wrt buck rear(Instructed Position)(°)	Seat Back angle wrt buck rear(Preferred Position)(°)	X_HJC Instructed position(Bush-Gutowski method)(mm)	X_HJC Preferred position(Bush-Gutowski method)(mm)	HJC vertical Deflection (Bush-Gutowski method)(mm)	HJC vertical Deflection (Bush-Gutowski method)(mm)	HJC vertical Deflection (Kinematic model-Directly from chart)(mm)	HJC force(N)(54.3%of bodyweight)(N)
1(1)	60	53	-266	-271	33	37	35	420
1(2)	60	53	-258	-267	33	39	35	420
2(1)	60	50	-267	-266	56	75	27	347
2(2)	60	50	-256	-276	60	75	27	347
7(1)	62	58	-277	-291	40	42	29	375
7(2)	62	58	-271	-284	41	43	29	375
8(1)	62	58	-306	-331	59	56	30	377
8(2)	62	57	-305	-336	60	65	30	377
10(1)	58	56	-224	-244	39	43	35	413
12(1)	61	53	-284	-277	45	49	30	377
				Average	47	52	31	
				Standard Deviation	11	15	3	

Table C3: HJC experimental data for 50H50W category in SLK seat with HJC calculated using method used by Gutowski.

HJC vertical deflection for 50H50W in SLK (sports)								
					Instructed Positio	Preferred Position		
Subject No(Trial No)	Seat Back angle wrt buck rear(Instructed Position)(°)	Seat Back angle wrt buck rear (preferred position)(°)	X_HJC Instructed position(mm)	X_HJC Preferred position(mm)	HJC vertical Deflection(mm)	HJC vertical Deflection(mm)	HJC vertical Deflection (Kinematic model- Directly from chart)(mm)	HJC force(N)(54.3%of bodyweight)
1(1)	65	63	-280	-287	44	50	42	420
2(1)	66	63	-216	-230	60	65	35	347
2(2)	66	63	-214	-224	59	63	35	347
7(1)	66	64	-217	-227	34	44	38	375
7(2)	66	64	-212	-224	36	53	38	375
8(1)	66	65	-245	-276	51	65	38	377
8(2)	66	65	-255	-275	58	63	38	377
10(1)	65	60	-258	-262	50	47	41	413
10(2)	65	60	-246	-268	45	49	41	413
12(1)	66	62	-230	-236	40	44	38	377
12(2)	66	62	-234	-247	42	47	38	377
				Average	47	54	38	
				Standard Deviation	9	9	2	

Table C 4: HJC experimental data for 50H50W category in SLK seat with HJC calculated using Bush-Gutowski method.

HJC vertical deflection for 50H50W in SLK (sports)								
					Instructed Positio	Preferred Position		
Subject No(Trial No)	Seat Back angle wrt buck rear(Instructed Position)(°)	Seat Back angle wrt buck rear(Preferred Position)(°)	X_HJC Instructed position(Bush-Gutowski method)(mm)	X_HJC Preferred position(Bush-Gutowski method)(mm)	HJC vertical Deflection (Bush-Gutowski method)(mm)	HJC vertical Deflection (Bush-Gutowski method)(mm)	HJC vertical Deflection (Kinematic model- Directly from chart)(mm)	HJC force(N)(54.3%of bodyweight)
1(1)	65	63	-274	-290	38	43	42	420
2(1)	66	63	-220	-252	58	62	35	347
2(2)	66	63	-229	-248	59	62	35	347
7(1)	66	64	-244	-264	26	35	38	375
7(2)	66	64	-246	-266	24	30	38	375
8(1)	66	65	-266	-308	54	51	38	377
8(2)	66	65	-260	-309	46	53	38	377
10(1)	65	60	-224	-225	38	35	41	413
10(2)	65	60	-228	-226	39	36	41	413
12(1)	66	62	-219	-223	35	40	38	377
12(2)	66	62	-224	-230	36	41	38	377
				Average	41	44	38	
				Standard Deviation	12	11	2	

Table C5: HJC experimental data for 50H50W category in Tahoe seat with HJC calculated using method used by Gutowski.

HJC vertical deflection for 50H50W in Tahoe (SUV)								
					Instructed Positio	Preferred Position		
Subject No(Trial No)	Seat Back angle wrt buck rear(Instructed Position)(°)	Seat Back angle wrt buck rear(Preferred Position)(°)	X_HJC Instructed position(Gutowski method)(mm)	X_HJC Preferred position(Gutowski method)(mm)	HJC vertical Deflection (Gutowski method)(mm)	HJC vertical Deflection (Gutowski method)(mm)	HJC vertical Deflection (Kinematic model-Directly from chart)(mm)	HJC force(N)(54.3%of bodyweight)
1(1)	72	66	-251	-243	49	55	50	420
1(2)	72	66	-248	-244	46	57	50	420
2(1)	72	68	-258	-300	73	85	42	347
2(2)	72	68	-256	-300	75	88	42	347
7(1)	72	71	-227	-237	32	50	45	375
7(2)	72	70	-230	-241	35	45	45	375
8(1)	72	66	-270	-273	58	70	45	377
8(2)	72	67	-259	-284	60	68	45	377
10(1)	72	67	-261	-264	60	61	49	413
10(2)	72	67	-257	-271	59	64	49	
12(1)	73	67	-277	-286	50	55	45	377
				Average	54	63	46	
				Standard Deviation	14	14	3	

Table C 6: HJC experimental data for 50H50W category in Tahoe seat with HJC calculated using Bush-Gutowski method.

HJC vertical deflection for 50H50W in Tahoe (SUV)								
					Instructed Positio	Preferred Position		
Subject No(Trial No)	Seat Back angle wrt buck rear(Instructed Position)(°)	Seat Back angle wrt buck rear(Preferred Position)(°)	X_HJC Instructed position(Bush-Gutowski method)(mm)	X_HJC Preferred position(Bush-Gutowski method)(mm)	HJC vertical Deflection (Bush-Gutowski method)(mm)	HJC vertical Deflection (Bush-Gutowski method)(mm)	HJC vertical Deflection (Kinematic model-Directly from chart)(mm)	HJC force(N)(54.3%of bodyweight)
1(1)	72	66	-268	-272	42	45	50	420
1(2)	72	66	-263	-271	40	47	50	420
2(1)	72	68	-240	-299	69	80	42	347
2(2)	72	68	-232	-274	70	82	42	347
7(1)	72	71	-248	-251	28	27	45	375
7(2)	72	70	-268	-279	33	37	45	375
8(1)	72	66	-283	-316	55	54	45	377
8(2)	72	67	-289	-311	54	53	45	377
10(1)	72	67	-262	-291	39	44	49	413
10(2)								
12(1)	73	67	-272	-298	48	53	45	377
				Average	48	52	46	
				Standard Deviation	14	17	3	

Table C7: HJC experimental data for 95H5W category in BMW seat with HJC calculated using method used by Gutowski.

HJC vertical deflection for 95H5W in BMW sedan								
					Instructed Position	Preferred Position		
Subject No(Trial No)	Seat Back angle wrt buck rear(Instructed Position)(°)	Seat Back angle wrt buck rear(Preferred Position)(°)	X_HJC Instructed position(Gutowski method)	X_HJC Preferred position(Gutowski method)(mm)	HJC vertical Deflection (Gutowski method)(mm)	HJC vertical Deflection (Gutowski method)(mm)	HJC vertical Deflection (Kinematic model)(mm)	HJC force(N)(54.3%of bodyweight)
4(1)	60	51	-254	-248	77	78	24	309
4(2)	59	51	-256	-254	78	78	24	309
5(1)	59	64	-245	-271	61	65	22	280
5(2)	60	63	-251	-270	63	67	22	280
9(1)	60	54	-280	-279	44	44	27	351
13(1)	63	60	-255	-300	55	70	23	297
13(2)	63	61	-261	-289	59	68	23	297
				Average	62	67	24	
				Standard Deviation	12	11	2	

Table C 8: HJC experimental data for 95H5W category in BMW seat with HJC calculated using Bush-Gutowski method.

HJC vertical deflection for 95H5W in BMW sedan								
					Instructed Position	Preferred Position		
Subject No(Trial No)	Seat Back angle wrt buck rear(Instructed Position)(°)	Seat Back angle wrt buck rear(Preferred Position)(°)	X_HJC Instructed position(Bush-Gutowski method)(mm)	X_HJC Preferred position(Bush-Gutowski method)(mm)	HJC vertical Deflection (Bush-Gutowski method)(mm)	HJC vertical Deflection (Bush-Gutowski method)(mm)	HJC vertical Deflection (Kinematic model)(mm)	HJC force(N)(54.3%of bodyweight)
4(1)	60	51	-233	-258	72	75	24	309
4(2)	59	51	-235	-264	70	73	24	309
5(1)	59	64	-273	-287	46	55	22	280
5(2)	60	63	-280	-305	49	58	22	280
9(1)	60	54	-279	-296	44	44	27	351
13(1)	63	60	-220	-327	41	60	23	297
13(2)	63	61	-241	-284	42	49	23	297
				Average	52	59	24	
				Standard Deviation	13	12	2	

Table C9: HJC experimental data for 95H5W category in SLK seat with HJC calculated using method used by Gutowski.

HJC vertical deflection for 95H5W in SLK (sports)								
					Instructed Positio	Preferred Position		
Subject No(Trial No)	Seat Back angle wrt buck rear(Instructed Position)(°)	Seat Back angle wrt buck rear(Preferred Position)(°)	X_HJC Instructed position(Gutowski method)(mm)	X_HJC Preferred position(Gutowski method)(mm)	HJC vertical Deflection (Gutowski method)(mm)	HJC vertical Deflection (Gutowski method)(mm)	HJC vertical Deflection (Kinematic model-Directly from chart)(mm)	HJC force(N)(54.3%of bodyweight)
4(1)	65	62	-227	-262	68	76	30	309
4(2)	65	62	-228	-257	67	75	30	309
5(1)	66	73	-217	-221	57	58	27	280
5(2)	66	73	-219	-222	58	60	27	280
9(1)	65	63	-245	-285	40	48	34	351
9(2)	65	63	-237	-275	41	47	34	351
13(1)	67	63	-230	-237	44	47	38	297
13(2)	67	63	-237	-250	43	50	38	297
				Average	52	58	32	
				Standard Deviation	12	12	4	

Table C 10: HJC experimental data for 95H5W category in SLK seat with HJC calculated using Bush-Gutowski method.

HJC vertical deflection for 95H5W in SLK (sports)								
					Instructed Position	Preferred Position		
Subject No(Trial No)	Seat Back angle wrt buck rear(Instructed Position)(°)	Seat Back angle wrt buck rear(Preferred Position)(°)	X_HJC Instructed position(Bush-Gutowski method)(mm)	X_HJC Preferred position(Bush-Gutowski method)(mm)	HJC vertical Deflection (Bush-Gutowski method)(mm)	HJC vertical Deflection (Bush-Gutowski method)(mm)	HJC vertical Deflection (Kinematic model-Directly from chart)(mm)	HJC force(N)(54.3%of bodyweight)
4(1)	65	62	-211	-270	64	67	30	309
4(2)	65	62	-225	-280	65	69	30	309
5(1)	66	73	-253	-252	52	58	27	280
5(2)	66	73	-234	-241	54	54	27	280
9(1)	65	63	-234	-305	38	39	34	351
9(2)	65	63	-257	-315	42	45	34	351
13(1)	67	63	-219	-265	39	38	38	297
13(2)	67	63	-246	-297	41	43	38	297
				Average	49	52	32	
				Standard Deviation	11	12	4	

Table C 11: HJC experimental data for 95H5W category in Tahoe seat with HJC calculated using method used by Gutowski.

HJC vertical deflection for 95H5W in Tahoe (SUV)								
					Instructed Position	Preferred Position		
Subject No(Trial No)	Seat Back angle wrt buck rear(Instructed Position)(°)	Seat Back angle wrt buck rear(Preferred Position)(°)	X_HJC instructed position(Gutowski method)(mm)	X_HJC Preferred position(Bush-Gutowski method)(mm)	HJC vertical Deflection (Gutowski method)(mm)	HJC vertical Deflection (Gutowski method)(mm)	HJC vertical Deflection (Kinematic model-Directly from chart)(mm)	HJC force(N)(54.3%of bodyweight)
4(1)	71	67	-195	-207	58	62	36	309
4(2)	71	67	-200	-215	57	65	36	309
5(1)	72	80	-278	-301	63	75	35	280
5(2)	72	80	-272	-298	69	73	35	280
9(1)	72	66	-250	-252	47	52	45	351
9(2)	73	66	-251	-275	47	51	45	351
13(1)	72	71	-268	-284	60	66	46	297
13(2)	72	71	-260	-279	59	67	46	297
				Average	58	64	41	
				Standard Deviation	7	9	5	

Table C 12: HJC experimental data for 95H5W category in Tahoe seat with HJC calculated using Bush-Gutowski method.

HJC vertical deflection for 95H5W in Tahoe (SUV)								
					Instructed Position	Preferred Position		
Subject No(Trial No)	Seat Back angle wrt buck rear(Instructed Position)(°)	Seat Back angle wrt buck rear(Preferred Position)(°)	X_HJC instructed position(Bush-Gutowski method)(mm)	X_HJC Preferred position(Bush-Gutowski method)(mm)	HJC vertical Deflection (Bush-Gutowski method)(mm)	HJC vertical Deflection (Bush-Gutowski method)(mm)	HJC vertical Deflection (Kinematic model-Directly from chart)(mm)	HJC force(N)(54.3%of bodyweight)
4(1)	71	67	-174	-204	54	57	36	309
4(2)	71	67	-181	-220	56	58	36	309
5(1)	72	80	-307	-324	57	64	35	280
5(2)	72	80	-303	-326	66	66	35	280
9(1)	72	66	-250	-290	44	40	45	351
9(2)	73	66	-248	-316	38	41	45	351
13(1)	72	71	-235	-284	57	61	46	297
13(2)	72	71	-241	-293	58	63	46	297
				Average	54	56	41	
				Standard Deviation	9	10	5	

Table C 13: HJC experimental data for 95H95W category in BMW seat with HJC calculated using method used by Gutowski.

HJC vertical deflection for 95H95W in BMW sedan								
					Instructed Position	Preferred Position		
Subject No(Trial No)	Seat Back angle wrt buck rear(Instructed Position)(°)	Seat Back angle wrt buck rear(Preferred Position)(°)	X_HJC Instructed position(Bush-Gutowski method)(mm)	X_HJC Preferred position(Bush-Gutowski method)(mm)	HJC vertical Deflection (Bush-Gutowski method)(mm)	HJC vertical Deflection (Bush-Gutowski method)(mm)	HJC vertical Deflection (Kinematic model)(mm)	HJC force(N)(54.3%of bodyweight)
6(1)	61	60	-321	-319	64	68	35	453
6(2)	61	59	-325	-320	64	70	35	453
11(1)	60	56	-308	-290	43	37	37	475
11(2)	60	56	-307	-298	45	40	37	475
14(1)	70	80	-247	-219	37	48	38	511
14(2)	70	80	-239	-228	38	48	38	511
15(1)	63	58	-324	-321	57	57	38	567
16(1)	61	60	-304	-312	64	59	37	485
				Average	52	53	37	
				Standard Deviation	12	12	1	

Table C 14: HJC experimental data for 95H95W category in BMW seat with HJC calculated using Bush-Gutowski method.

HJC vertical deflection for 95H95W in BMW sedan								
					Instructed Position	Preferred Position		
Subject No(Trial No)	Seat Back angle wrt buck rear(Instructed Position)(°)	Seat Back angle wrt buck rear(Preferred Position)(°)	X_HJC Instructed position(Bush-Gutowski method)(mm)	X_HJC Preferred position(Bush-Gutowski method)(mm)	HJC vertical Deflection (Bush-Gutowski method)(mm)	HJC vertical Deflection (Bush-Gutowski method)(mm)	HJC vertical Deflection (Kinematic model)(mm)	HJC force(N)(54.3%of bodyweight)
6(1)	61	60	-334	-319	57	63	35	453
6(2)	61	59	-331	-325	51	54	35	453
11(1)	60	56	-312	-305	40	41	37	475
11(2)	60	56	-320	-311	42	43	37	475
14(1)	70	80	-250	-259	36	32	38	511
14(2)	70	80	-263	-270	37	34	38	511
15(1)	63	58	-315	-318	51	52	38	567
16(1)	61	60	-288	-297	59	63	37	485
				Average	47	48	37	
				Standard Deviation	9	12	1	

Table C 15: HJC experimental data for 95H95W category in SLK seat with HJC calculated using method used by Gutowski.

HJC vertical deflection for 95H95W in SLK (sports)								
					Instructed Position	Preferred Position		
Subject No(Trial No)	Seat Back angle wrt buck rear(Instructed Position)(°)	Seat Back angle wrt buck rear(Preferred Position)(°)	X_HJC instructed position(Gutowski method)(mm)	X_HJC Preferred position(Gutowski method)(mm)	HJC vertical Deflection (Gutowski method)(mm)	HJC vertical Deflection (Gutowski method)(mm)	HJC vertical Deflection (Kinematic model-Directly from chart)(mm)	HJC force(N)(54.3%of bodyweight)
6(1)	67	66	-249	-247	49	45	47	453
6(2)	67	66	-243	-250	47	47	47	453
11(1)	67	65	-245	-270	52	56	48	475
11(2)	67	65	-257	-275	54	60	48	475
14(1)	67	60	-252	-262	47	51	50	511
14(2)	67	60	-249	-267	47	54	50	511
15(1)	66	61	-324	-322	57	57	51	567
16(1)	67	63	-247	-202	49	31	48	485
				Average	50	50	49	
				Standard Deviation	4	9	2	

Table C 16: HJC experimental data for 95H95W category in SLK seat with HJC calculated using Bush-Gutowski method.

HJC vertical deflection for 95H95W in SLK (sports)								
					Instructed Position	Preferred Position		
Subject No(Trial No)	Seat Back angle wrt buck rear(Instructed Position)(°)	Seat Back angle wrt buck rear(Preferred Position)(°)	X_HJC instructed position(Bush Gutowski method)(mm)	X_HJC Preferred position(Bush-Gutowski method)(mm)	HJC vertical Deflection (Bush-Gutowski method)(mm)	HJC vertical Deflection (Bush-Gutowski method)(mm)	HJC vertical Deflection (Kinematic model-Directly from chart)(mm)	HJC force(N)(54.3%of bodyweight)
6(1)	67	66	-262	-267	42	36	47	453
6(2)	67	66	-257	-274	39	41	47	453
11(1)	67	65	-271	-302	49	52	48	475
11(2)	67	65	-264	-294	47	55	48	475
14(1)	67	60	-251	-268	44	47	50	511
14(2)	67	60	-249	-264	44	48	50	511
15(1)	66	61	-248	-267	48	54	51	567
16(1)	67	63	-269	-280	65	68	48	485
				Average	47	50	49	
				Standard Deviation	8	10	2	

Table C 17: HJC experimental data for 95H95W category in Tahoe seat with HJC calculated using method used by Gutowski.

HJC vertical deflection for 95H95W in Tahoe (SUV)								
					Instructed Position	Preferred Position		
Subject No(Trial No)	Seat Back angle wrt buck rear(Instructed Position)(°)	Seat Back angle wrt buck rear(Preferred Position)(°)	X_HJC Instructed position(Gutowski method)(mm)	X_HJC Preferred position(Gutowski method)(mm)	HJC vertical Deflection (Gutowski method)(mm)	HJC vertical Deflection (Gutowski method)(mm)	HJC vertical Deflection (Kinematic model)(mm)	HJC force(N)(54.3%of bodyweight)
6(1)	72	70	-277	-281	49	50	51	453
6(2)	72	70	-271	-303	58	48	51	453
11(1)	71	67	-303	-307	59	61	52	475
11(2)	71	67	-309	-315	58	64	52	475
14(1)	72	67	-258	-247	39	39	53	511
14(2)	72	67	-261	-276	45	49	53	511
15(1)	72	66	-303	-318	57	63	55	567
16(1)	72	67	-283	-283	48	53	52	485
16(1)	72	67	-287	-290	50	52	52	485
				Average	51	53	52	
				Standard Deviation	7	8	1	

Table C 18: HJC experimental data for 95H95W category in Tahoe seat with HJC calculated using Bush-Gutowski method.

HJC vertical deflection for 95H95W in Tahoe (SUV)								
					Instructed Position	Preferred Position		
Subject No(Trial No)	Seat Back angle wrt buck rear(Instructed Position)(°)	Seat Back angle wrt buck rear(Preferred Position)(°)	X_HJC Instructed position(Bush-Gutowski method)(mm)	X_HJC Preferred position(Bush-Gutowski method)(mm)	HJC vertical Deflection (Bush-Gutowski method)(mm)	HJC vertical Deflection (Bush-Gutowski method)(mm)	HJC vertical Deflection (Kinematic model)(mm)	HJC force(N)(54.3%of bodyweight)
6(1)	72	70	-307	-342	56	61	51	453
6(2)	72	70	-297	-307	55	60	51	453
11(1)	71	67	-312	-328	39	42	52	475
11(2)	71	67	-315	-335	40	43	52	475
14(1)	72	67	-257	-266	45	54	53	511
14(2)	72	67	-269	-288	48	53	53	511
15(1)	72	66	-298	-315	51	56	55	567
16(1)	72	67	-310	-324	50	54	52	485
16(1)	72	67	-308	-328	48	53	52	485
				Average	48	53	52	
				Standard Deviation	6	7	1	

REFERENCES

1. "Devices for Use in Defining and Measuring Vehicle Seating Accommodation", Society of Automotive Engineers Recommended Practice J826.

2. Schneider, L., M. Reed, R. Roe, M. Manary, C. Flannagan, R. Hubbard, and G. Rupp, "ASPECT: The Next Generation H-point Machine and Related Seat Design and Measurement Tools", Soc. of Auto. Engin. (SAE) Paper Number 1999-01-0962, presented at the 1999 SAE International Congress, March 1999.

3. Bush, T.R., Macklem, W., "Methodology for the Development of Female and Male Seat Functions for the Kinetic Model A Supplement to an Excel Spreadsheets", April 2002.

4. RAMSIS: 3D-CAD-ergonomics tool by Human Solutions. http://www.human-solutions.com/produkte_ramsis_e.php

5. JACK: 3D interactive software environment for controlling articulated figures. Center for Human Modeling and Simulation at the University of Pennsylvania, available from Unigraphics Inc. http://www.cis.upenn.edu/~hms/jack.html

6. Radcliffe, N.J,"Kinetic Modeling And Seat Factors Relating To Manikin-Seat Interaction In Automobiles" dissertation for the degree of M.S., Department of Mechanical Engineering, Michigan State University, 2000.

7. Hubbard, R., and C. Gedraitis, "Initial Measurements and Interpretations of Seat Factors for the ASPECT Program," Society of Automotive Engineers (SAE) Paper Number 1999-01-0958, presented at the 1999 SAE International Congress, March, 1999.

8. Human Pelvis [Online Image]: Available www.peteresser.de/skizzen/skiz_02.html

9. Bush, T. R., "Posture and Force Measures of Mid-Sized Men in Seated Positions," Thesis for Doctoral Degree, Michigan State University, 2000.

10. Package dimensions with J826 manikin [ref] for the typical car segment-seating environment. Johnson Controls Inc. December, 2003.

11. Devices for use in defining and measuring vehicle seating accommodation, SAE Surface Vehicle Standard, SAE J1100, revised May 1995.

12. Gutowski, P. E, "Influence of Automotive Seat Factors on Posture and Applicability to Design Models", Thesis for Masters Degree, Michigan State University, 2000.

13. University Committee on Research Involving Human Subjects (UCRIHS), Michigan State University, IRB # 96-054, August 2003.

14. Human Pelvis [Online Image]: Available http://www.hkin.educ.ubc.ca/361/anatgifs/pubics.GIF

15. Bush, T.R., Gotowski, P. E., "An approach for hip joint center calculation for use in seated postures", Journal of Biomechanics 36 (2003) 1739-1743, March 2003.

16. National Health and Nutrition Examination Survey.

17. Seidel, G. K., Marchinda, D. M., Dijkers, M., Soutas-Little, R. W., "Hip Joint Center Location from Palpable Bony Landmarks – A Cadaver Study," *Journal of Biomechanics*, Vol. 28, No. 8, pp. 995-998, 1995.

18. NATIK 1988 Anthropometric survey of U.S. army personnel: Summary statistics interim report, NATICK/TR-89/027, March 1989.